UNIVERSITY OF NAPLES FEDERICO II

DEPARTMENT OF PHARMACY

PhD programme in Pharmaceutical Sciences

PHARMACOLOGICAL AND NUTRITIONAL CONTROL OF DYSBIOSIS RELATED TO CNS DISORDERS: GUT-BRAIN AXIS

PhD student
ADRIANO LAMA

Coordinator
Prof.
MARIA VALERIA D'AURIA

Tutor
Prof.
GIUSEPPINA MATTACE RASO

XXXI CYCLE (2016-2018)

Summary

Abstract

'Leaky gut' syndrome has attracted much attention in recent years, and represents now a complementary/alternative target for several complex diseases characterized by this pathological condition. It is often described as an increase in the permeability of the intestinal mucosa, allowing bacteria, toxic digestive metabolites, bacterial toxins, and small detrimental molecules to 'leak' into the bloodstream. The microbiota-gut is an integral component of the gut–brain neuroendocrine metabolic axis and any microbiota-gut disruption that can occur, could distressed homeostasis and share an inflammatory response, affecting distal organs including the brain. It has been shown, indeed, that the gut can influence the blood brain barrier (BBB) through gastrointestinal-derived hormones, small molecule and metabolic co-factor production, or through cytokine synthesis and other inflammatory mechanisms. Therefore, the CNS is under constant attack or, conversely, advantage from a wide variety of neuro-psychotropic-modulating microbes, and their metabolites. So, the proper neurodevelopment and functioning of the CNS depends from an integrated, rather than opposing, cross-talk between gut-gut microbiota and brain. Several CNS disturbances were related to gastrointestinal dysfunction and 'leaky brain', underlining the need of identifying new integrative and multi-

targeted approaches. These complex diseases, being multifactorial, could result, in fact, less responsive to targeted standard drugs, since poorly fits ‘one-disease one-target’ and ‘one-target one-compound’ paradigms in this context.

Here, we focused on autism spectrum disorders (ASDs) and major depressive disorder (MDD), two brain disorders linked to a dysfunction of BBB and impacted by immune and inflammatory peripheral stimuli. Our aim has been to evaluate the possible therapeutic potential of modulating several aspects of these multifactorial disorders, in order to benefit of peripheral and central contributions, converging on an improvement of overall health.

To this aim we used BTBR T+tf/J (BTBR) mice model of ASDs and high fat diet-induced MDD in young mice, and the possible pharmacological modulation by palmitoylethanolamide (PEA) was investigated.

PEA, is an endogenous N-acyl-ethanolamine, biosynthesized to maintain cellular homeostasis when this is challenged by external stressors provoking inflammation, neuronal damage and pain. The interaction and activation of PPARα has been recognized as the main mechanism of the effects evoked by this acylethanolamide. In particular, the analgesic and anti-inflammatory effects of PEA were demonstrated to be mediated by PPARα activation, since it has no effect in PPARα null mice.

Indeed, the discovery of PPARα in distinct areas of the brain, opened a new scenario to explore the possible activity of this acylethanolamide in the CNS. Recently it has been demonstrated that genetic inactivation of PPARα, particularly abundant in the CNS, leads to a behavioral and cognitive phenotype reminiscent of that of preclinical models of ASDs, i.e. mouse model BTBR T+tf/J (BTBR), which displays an improved repetitive behavior when autistic mice are treated with a synthetic PPARα agonist. These results, not only indicated a central role for this receptor in neurological functions associated with the behavior, but more interestingly highlighted PPARα as a potential pharmacological target to lessen ASDs symptoms. On the other side PEA activity at intestinal level has suggested a possible role of this acylethanolamide in modulating not only gut function, such as intestinal transit and permeability, but also gut-brain axis.

Before evaluating the effect of PEA on BTBR mice, in the first part of this PhD programme, we performed a study, also evaluating sex influence, on gut microbiota composition, behavioral features, and intestinal integrity, inflammatory status and architecture of adult male and female BTBR mice. These gender characterizations arise from the well-known different clinical features of male and female autistic patients and the need to identify them in a mouse model of ASD.

Consistently with gut-brain axis hypothesis, we showed that BTBR mice presented a profound intestinal dysbiosis compared to control strain, more marked in female than in male mice, indicating *Bacteroides*, *Parabacteroides*, *Sutterella*, *Dehalobacterium* and *Oscillospira* genera as key drivers of sex-specific gut microbiota profiles associated with altered behavior. Interestingly, we also showed that the dysbiosis was accompanied in BTBR mice by increased gut permeability and colon inflammation. Therefore, we have considered BTBR mice, as an idiopathic model of autism useful to investigate not only the correction of the autistic behavior, but also a starting point to investigate whether the reduction of intestinal inflammation and integrity, and possibly the restoration of gut microbiota balance may ameliorate pathological traits.

Based on this background, the aim of this study was to investigate the pharmacological effects of PEA on autistic-like behaviour of BTBR T+tf/J mice and to shed light on the contributing mechanisms. PEA was able to revert the altered behavior of autistic mice. This effect was contingent to PPARα activation, since was blunted by PPARα blocking or deletion. At mechanistic level, PEA restored hippocampal BDNF signaling, improved mitochondrial dysfunction and reduced serum, hippocampal and colonic inflammation. These beneficial effects were related to the reduction of leaky

gut in PEA-treated BTBR mice mediated by increased expression of colonic tight junctions. In addition, PEA modulated gut microbiota composition, underlining the strong link between gut and brain.

In last years, the connection between modification in gut microbiota induced by obesity and the development of MDD has become more evident. High fat feeding causes the production of several inflammatory mediators that can compromise colonic epithelial barrier function, with the translocation of bacterial metabolites in CNS, evoking deleterious events. The modulation of PPARα, mostly expressed in hippocampus, has demonstrated to improve synaptic dysfunction and HFD-related pathological events in MDD.

Here, we have addressed the effects of PEA in a mouse model of HFD-induced depression, focusing on converging mechanisms involved in its activity. In particular, we assessed PEA capability in modulating the gut-brain axis and ameliorating depressive behavior. The treatment with PEA improved the depressive-like behavior and memory deficit, shown by HFD animals, impacting on BDNF signaling pathway and reducing neuroinflammation, both in hypothalamus, hippocampus and prefrontal cortex. These beneficial effects of PEA, as PPARα agonist, were correlated to an increased expression of PPARα, its coactivator PGC1α, and the downstream gene FGF21. As in BTBR model, here PEA also modulated gut

microbiota composition, reducing the amount of endotoxin-producer *Desulfovibrio* and increasing *Clostridiales* genus relative abundance, and consistently Clostridiales-producing metabolites, including short-chain fatty acids.

In conclusion, PEA, a multifunctional compound, can represent a novel therapeutic approach for multifactorial disorders, such as ASDs and MDD, able to counteract the alteration of central and peripheral pathways involved in their onset and progression.

Introduction

Autism is a multifactorial disorder, where many genes converge, through multiple molecular mechanisms, onto common processes involved in the development and function of neural circuits, whose alteration leads and sustains the core symptoms of ASDs (1). Evidence based on environmental factors, such as infection, gut microbiome alteration, and immunological features are also growing, suggesting the involvement of many scenarios overlapping in this complex neurodevelopmental pathology. Obviously, even if targeted specific treatments would clarify the relevance of the altered pathways in ASDs, on the other hand the complex heterogeneity in ASDs children population could require a multi-targeted approach. Here, we analysed the modulatory effect of PEA on many of the pathways and factors, starting from the idea that the abnormalities reported to be at the onset and progression of this neurodevelopmental pathology are responsible of brain dysfunction and consistently associated in core symptoms of ASDs.

Depression, as well, has a multifactorial nature, resembling that of other complex disorders. Very recently, it has been shown that obesity, in critical periods for neurodevelopment and neuronal plasticity, may contribute to mood and cognitive disorders, therefore constituting a risk factor for developing depression and anxiety. In this case, westernized dietary patterns

and dysbiosis seem to contribute to obesity-related CNS complications involving gut microbiota, as a mediating factor between peripheral signals and the brain. It is conceivable to hypothesise that alteration of gut microbiota may contribute to the endocrine, neurochemical and inflammatory alterations underlying to gut-brain axis interplay. These include dysregulation of the HPA-axis with overproduction of glucocorticoids, alterations in levels of neuroactive metabolites (e.g., neurotransmitters, short-chain fatty acids) and activation of a pro-inflammatory milieu that can cause neuroinflammation. Up to date, PEA has proven to be a multi-targeted compound: the main pharmacological effects of PEA are mediated by the activation of PPARα (2, 3), a transcription factor involved in the regulation of gene networks, which control pain and inflammation (4). This mechanism is supported by the inhibition of neuronal firing (5) and by the stimulation of neurosteroid synthesis, indicating that multiple mechanisms contribute to the central effect of PEA (6).

On the other side, PEA has demonstrated to have a peripheral anti-inflammatory effect shown both on BTBR mice, reducing cytokine production, decreasing the inflammatory state at colonic and systemic levels, and in rodent models of obesity where it was able to reduce the overall low-grade inflammation (7), also impacting on the modulation of gut microbiota.

1. Palmitoylethanolamide

1.1. PEA: origin, structure, and activity

The acylethanolamides (AEs) are bioactive fatty molecules, synthetized "on demand" from membrane phospholipids (8). The recovery of AEs in several tissues and their pharmacological effects on multiple biological pathways, have suggested a regulator role of these endogenous molecules in paracrine or autocrine functions (9). Known their beneficial effects on nociception, lipid metabolism, and inflammation, AEs were initially considered Autacoid Local Injury Antagonism Amides (ALIAmides) (10). In last years, several research groups supported their possible role as neuromodulators, since AEs are produced in various areas of brain, both in physiological and pathological conditions (11). Indeed, both AEs are produced during neuronal damage, carrying out their neuroprotective activity through both receptor and non-receptor specific mechanisms (12).

Among all AEs, PEA is abundant in central nervous system and only recently its biological functions have been clarified (13). As shown by **Figure 1.1**, PEA is biosynthesized from phosphatidylethanolamine (PE) by two sequential enzymatic reactions (14, 15). The first reaction is the transfer of an acyl-group (palmitic acid) from sn-1 position of phosphatidylcholine

(PC) to PE by an N-acyltransferase (NAT), generating N-acyl- PE (NAPE) (16). Afterwards, PEA is released from NAPE by a phosphodiesterase of phospholipase D (NAPE-PLD) (17). PEA is rapidly catabolized by fatty acid amide hydrolase (FAAH) to palmitic acid and ethanolamine (18, 19) or N-acylethanolamine-hydrolyzing acid amidase (NAAA) in inflammatory status (20). Considering that NAAA preferentially hydrolyzes PEA rather than other AEs, the use of selective NAAA inhibitors could increase local levels of endogenous PEA, resulting anti-inflammatory and analgesic molecule (20). From the phospholipid bilayer of the plasma membrane, PEA is transported by fatty acid binding proteins or heat shock proteins (21) to degrading enzymes or target receptors, such as peroxisome PPARα (22) and transient receptor potential vanilloid (TRPV)1 (23).

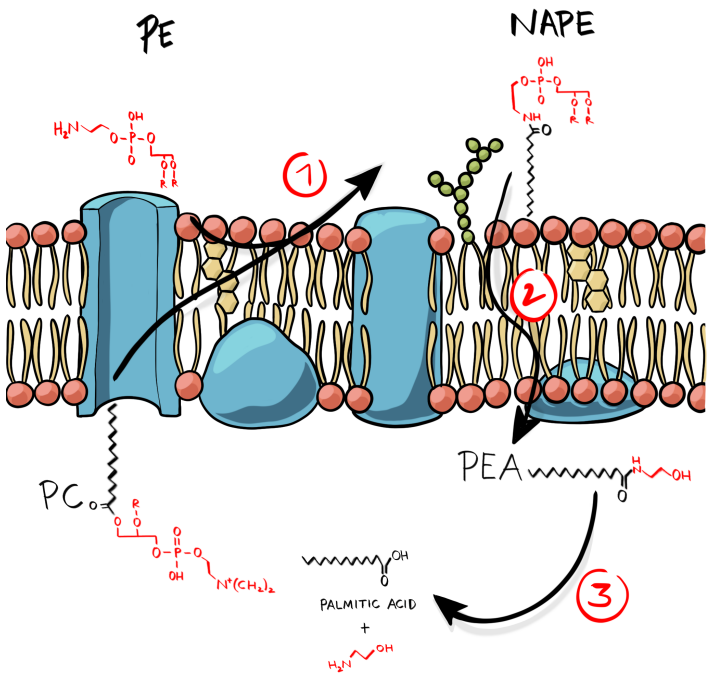

Figure 1.1. The metabolic conversion of PEA.

1.2. Peroxisome proliferator-activated receptors (PPARs): PPARα functions in the brain

PPARs are ligand-activated transcription factors called lipid "sensors", owning the key role in lipid and lipoprotein metabolism, energy homeostasis, cell proliferation death and differentiation. As shown by **Figure 1.2**, these nuclear receptors include three isotypes: PPARα (NR1C1), PPARβ/δ (NR1C2), and PPARγ (NR1C3). PPARs, as other members of the nuclear receptor superfamily, have four domains: (i) a N-

terminal A/B domain, important mediator of PPAR subtype-specificity, determining PPAR subtype-specificity and containing a weak ligand-independent transactivation function called AF-1; (ii) a C domain, highly conserved, that binds DNA via a two zinc-finger motif (hallmark of the NR superfamily); (iii) a D domain, which is a hinge region; (iv) an E/F domain, which is the ligand binding domain (LBD) (24).

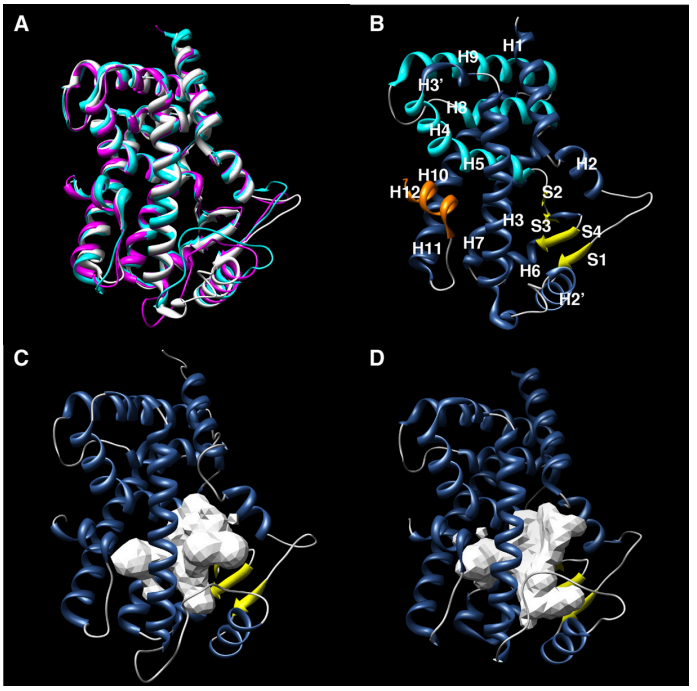

Figure 1.2 (A) Structural superposition of PPARα (white), PPARδ (magenta) and PPARγ (cyan). 3D structure of **(B)** PPARα, **(C)** PPARδ and **(D)** PPARγ.

The conformational change of PPARs is induced by different type of fatty acids, triggering the transcription of specific genes that encode for several metabolic and cellular processes, such as fatty acid β-oxidation and

adipogenesis (25). To this purpose, molecules that target PPARs can modulate lipid and glucose metabolism, representing excellent therapeutic tools for metabolic disorders (26, 27).

The activity of PPARs is based on the bond with specific DNA sequence elements (named PPAR response elements, PPREs), and on regulation of gene expression like heterodimers with retinoid X receptors (RXRs) (28-30). Indeed, the dimerization between specific RXR isotypes (α, β, γ) and PPARs seems to influence the recognition of target gene promoters (31) (**Figure 1.3**)

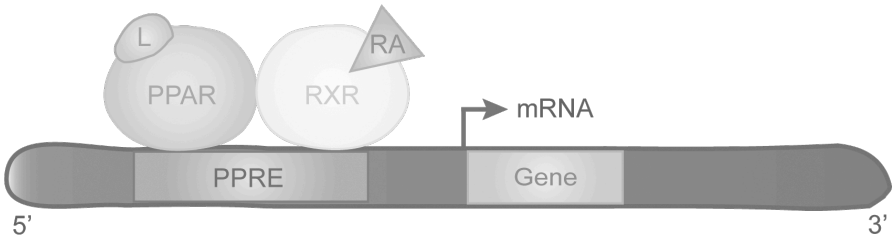

Figure 1.3. PPARs bind RXR to constitute PPRE. Ligands can modulate the transcription of target genes. L, ligand; RA. 9-cis-retinoic acid.

It is well known that PPAR-mediated effects are modulated by the interaction with several factors, including corepressors and coactivators (32). The steroid receptor coactivator 1 and the cAMP response element-binding (CREB) protein are two pivotal coactivators of PPARs and they own histone acetyl transferase activity that induces chromatin decondensation

and target gene activation. Beyond the clear interaction with PPARγ, PPARγ coactivator 1α (PGC-1α) binds PPARα in ligand-dependent manner, carrying out cellular functions, such as reactive oxygen species (ROS) and fatty acids (FAs) metabolism associated with mitochondrial and peroxisomal biogenesis (33-36). These functions are pivotal in counteracting CNS disorders, where redox unbalance and lipid dysmetabolism play a detrimental role in neurodegeneration. The distribution of PPARα varies in different tissues, it is generally expressed at high extent in metabolically active ones (liver, heart, skeletal muscle, intestinal mucosa and brown adipose tissue) (37), even if studies demonstrated their occurrence in brain (38, 39). In particular, Moreno et al. (40) described deeply the distribution of PPARs and RXRs in rodent brain. PPARα shows several functions in the brain: regulation of lipid metabolism (shortening of VLCFAs, use of FAs as metabolic fuel, biosynthesis of PUFAs) (41, 42); management of ROS metabolism (increase of antioxidant systems and induction of H_2O_2-producing enzymes) (43-45); neural cell proliferation, differentiation and apoptosis (46-49); modulation of dopaminergic, glutamatergic and cholinergic neurotransmission (50-52); cognitive and memory function, spatial learning, emotionality (53-55); modulation of pain pathways (4, 56-

59); modulation of fasting and satiety responses via hypothalamus-pituitary axis and peripheral glucose homeostasis (60-63).

Despite the hippocampus does not produce energy from fat metabolism, PPARα has been identified in different subfields of this tissue in rodents (64, 65). Interestingly, PPARα knockdown mice showed a reduction of several plasticity-associated molecules (NR2A, NR2B, GluR1 and Arc), but not voltage-gated ion channel ones, suggesting a crucial role of PPARα in hippocampal plasticity (64). In the same study, the authors demonstrated that PPARα agonists induced the activation of CREB (pivotal in synaptic plasticity) promoter in hippocampal neurons from wild type mice and not from PPARα knockout ones (64). All these findings highlight PPARα involvement in brain functions.

1.3. PPARα activation as mechanism of action of PEA

The anti-inflammatory, analgesic and neuroprotective effects of PEA are related to the involvement of both central and peripheral nervous system targets (2-4). In particular, different cell types involved in resolving chronic pain and inflammation (immune cells, microglia and neurons) synthetize and metabolize PEA (66).

PEA is an endocannabinoid-like molecule and, as such, was originally considered a CB2 agonist (67). Furthermore, PEA activity has been also associated to its capability in increasing half-life and therefore its effects on CB or TRPV1 (68-70), the so-called “entourage effects” due to PEA competitive inhibition of AEA hydrolysis on FAAH (71) and/or direct allosteric effect on TRPV1 (72, 73). Therefore, PEA is not a merely “classical” endocannabinoid because its pharmacological effects reside outside of a strict interaction with CB receptors. Beyond the interactions of PEA with orphan receptors, such as G protein-coupled receptor (GPR) 55 and GPR119 (74-77), the main role of pharmacological activity of PEA is related to PPARα activation (13). Indeed, PEA increases properties of calcium-activated intermediate (IKCa) and big-conductance potassium (BKCa) potassium channels via a PPARα dependent non-genomic mechanism, leading to a fast reduction of neuronal firing (3). In addition, as demonstrated by Sasso et al. (78) in acute or persistent pain mice model, the activation of PPARα, through a genomic mechanism, increases the expression of steroidogenic acute regulatory protein (StAR) and cytochrome P450 side-chain cleavage (CYP450scc), leading to the transport of cholesterol into mitochondria and its metabolic conversion into pregnanolone. The subsequent increase of allopregnanolone production

induce a positive allosteric activation of aminobutyric acid (GABA)-A receptors, an increase in Cl^- fluxes and a reinforcing effect on the reduction of neuronal firing. Furthermore, the anti-inflammatory effects of PEA seem to be correlated with PPARα capability in preventing the nuclear translocation of NF-kB and repressing the expression of pro-inflammatory proteins (i.e. TNF-α, IL-1β), limiting the recruitment of immune cells (79) (**Figure 1.4**)

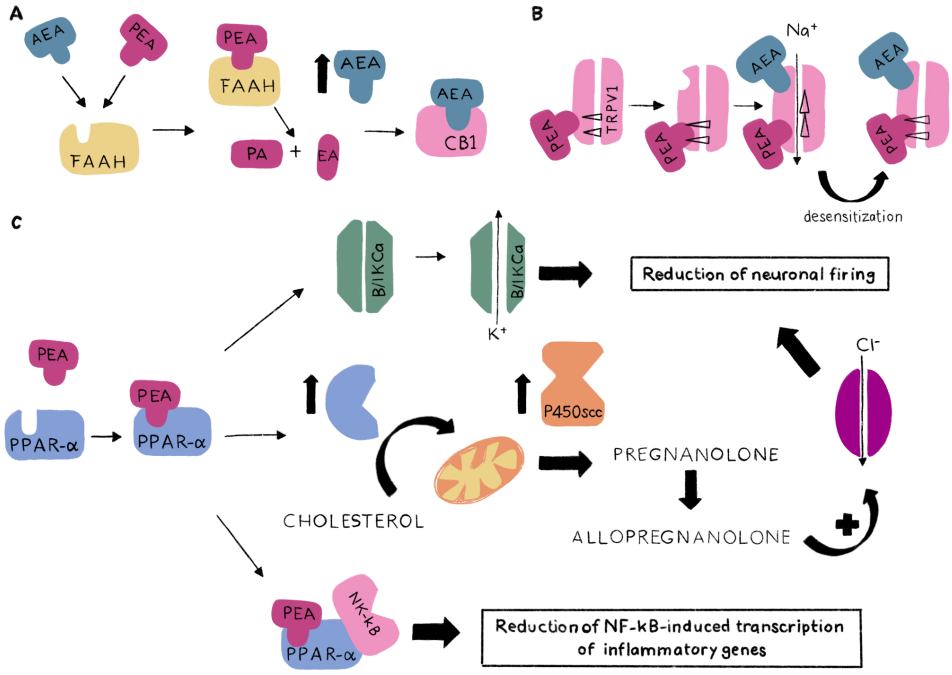

Figure 1.4. **Direct and indirect mechanisms of action of PEA. (A)** the competitive inhibition of AEA metabolism by FAAH; **(B)** allosteric activity on TRPV1 and its desensitization; **(C)** genomic and non-genomic mechanisms dependent on PPARα.

1.4. Pharmacological effects of PPARα agonists: focus on PEA in CNS disorders

On the basis of these observations, it is conceivable that targeting PPARα can represent the basis for novel therapies in the treatment of acute and chronic CNS pathologies. Indeed, several studies highlighted the beneficial effects of different PPARα agonists in improving neuroinflammation, underlying neurodegenerative disease and neuropsychiatric disorders (80). Among endogenous ligands of PPARα, OEA and PEA own several neuroprotective functions (81-83). In rat model of transient focal cerebral ischemia, PEA achieved a significant neuroprotective effect by reducing infarcted tissue size (84). Moreover, this molecule was able to protect neuronal cells from oxidative stress and alter the expression levels of kinases involved in neuroprotection (85). Koch et al (86) demonstrated also that PEA protected dentate gyrus granule cells from excitotoxically-induced neuronal damage, activating PPARα and not PPARγ in microglial cells and hippocampal neurons. Consistently, our research group demonstrated that PEA reduced oxidative stress in astroglial cells through PPARα-triggered biosynthesis of allopregnanolone (87). The role of PEA in regulating the complex systems involved in inflammatory and adaptive immune response, acute and chronic pain is now well understood (13). Concerning pathogenic

mechanisms of pain, PPARα has been shown to be overexpressed in rat spinal cord after peripheral noxious stimulation (56). Furthermore, D'Agostino et al. (4) demonstrated that intracerebroventricular administration of PEA significantly reduced the expression of the pro-inflammatory mediators, such as COX-2 and iNOS, in dorsal root ganglia following carrageenan-induced intraplantar oedema. The obligatory role of PPARα was confirmed by the loss of anti-nociceptive effects in PPARα knockout mice.

In neurodegenerative disorders, such as Parkinson's Disease (PD) and Alzheimer Disease (AD), PPARα agonists, and in particular PEA, seem to have a therapeutic effect. In MPTP-treated mice, an animal model of PD, PEA reversed MTPT-induced motor deficits in PPARα-dependent manner, reducing microglial activation, astrocyte number and S100β overexpression (88). Avagliano et al. (89) demonstrated that PEA levels are drastically reduced in post-mortem brain samples from AD patients. Consistently, both in *in vitro* and *in vivo* AD model, PEA was able to improve pathological features (90, 91).

The beneficial effects of PEA in mood disorders, especially in depression, are still overlooked. To date, only two preclinical studies and double-blind, randomized and placebo-controlled trial suggested the hypothesis that PEA

can reduce a depressive-like behavior (92-94). In particular, in a mouse model of anxiety/depression induced by corticosterone administration, a formulation of PEA and luteolin improved hippocampal neurogenesis and neuroplasticity. Yu et al. (92) demonstrated that oral PEA produced a significant reduction in immobility time in both tail suspension test (TST) and forced swimming test (FST). Only in a clinical study, recently published, the association of PEA with citalopram effectively improves symptoms of patients (predominantly male gender) with major depressive disorder, even if further investigations are needed (94).

Among neurodevelopmental disorders, autism spectrum disorder (ASD) is characterized by alterations in the brain's endocannabinoid system as demonstrated by Kerr et al. (95). In particular, these authors showed that in rat valproic acid model of autism there was a reduction of PPARα and GPR55 expression in the frontal cortex and PPARγ and GPR55 expression in the hippocampus while CB1 or CB2 receptor expression was not altered in all any brain regions. In another recent study, Bertolino et al (96) showed the beneficial effects of an association of PEA and luteolin in VPA mouse model and in an autistic child, even if the mechanisms of action keep still unclear.

1.5. New formulation of PEA: ultra-micronized PEA

Although the excellent pharmacological activity, PEA drawbacks are based on its poor solubility and bioavailability, due to its lipophilic nature. Moreover, apart from dissolution-rate-limited PEA absorption, another limit is particle size, inversely related to PEA bioavailability. All these drawbacks have prompt to improve PEA pharmacokinetic features. The micronization has been an excellent strategy to this aim, producing microparticles <10 μm (97, 98), in order to increase surface area and rate of dissolution (99), together with a reduction of absorption variability (100). Indeed, ultra-micronized PEA (PEA-um) has demonstrated an improved efficacy when administered per os compared to standard PEA powder administration. Recently, Petrosino et al. (101) have published an article focused not only on the absorbability of PEA-um and naïve PEA, but, interestingly, also on their distribution in peripheral and central tissues in physiological and inflammatory conditions. Notably, the authors demonstrated an increased plasma concentration by ultramicronization of PEA, in fact, differently from naïve PEA administration, PEA-um (30 mg/kg per os) to healthy animals resulted detectable in the bloodstream already after 5 min, with a peak plasma concentration of 5.4 ± 1.87 pmol/ml. This pharmacokinetic profile was even more favorable in inflamed animals, showing an increase of PEA-um concentration in plasma and inflamed tissues (including spinal cord).

Ultra-micronized PEA, provided by Epitech Group, is produced by the air-jet milling technique, where powder is slowly inserted into a jet-mill apparatus endowed with a chamber of 300 mm in diameter that operates with "spiral technology" driven by compressed air. The high number of collisions that occur between particles as a result of the high level of kinetic-not mechanical-energy produces sub-micron-sized crystals.

2. Autism spectrum disorders

2.1. Definition, epidemiology, diagnosis and risk factors

The term autism spectrum disorders (ASDs) describes a group of early-appearing social communication deficits and repetitive sensory-motor patterns due to multiple converging causes (102). ASDs, over time, have become from barely and rare disorders of childhood onset to studied and recognized lifelong conditions with heterogeneous features. Although autistic individuals are very different from each another, the core features are based on two areas without any cultural, racial, ethnical and socio-economical differences: impaired social interaction and repetitive stereotyped motor behaviors (103). ASDs represent an economic burden, mainly for autistic patients with low functionality due to expensive provision of support: in 2014, its cost estimated $3020 for health care and $14 061 for aggregate non-health care, including $8610 for school education (104). In 2010, the global prevalence of ASDs was about 1% (105), even if a more recent review estimated an increase up to 5% in developed countries (106).

Since there are no reliable biomarkers, ASD diagnosis is based on American Psychiatric Association's Diagnostic and Statistical Manual of Mental Disorders (DSM)-5 criteria, considering specific behavioral traits (102). To identify an ASD patient, a person must show evidence of complications, in each of three social communication subdomains and/or in two of the four different stereotyped and repetitive sensory-motor behaviors (**Table 2.1**)

Persistent deficits in social communication and social interaction	**Restricted, repetitive patterns of behavior, interests, or activities**
Deficits in social–emotional reciprocity (e.g. abnormal social approach and failure of normal back-and-forth conversation; or reduced sharing of interests, emotions, or affect)	Stereotyped or repetitive motor movements, use of objects, or speech (e.g. simple motor stereotypies, lining up toys, or flipping objects)
Deficits in non-verbal communicative behaviors (e.g. poorly integrated verbal and non-verbal communication, abnormalities in eye contact and body language, or deficits in understanding and use of gestures)	Insistence on sameness, inflexible adherence to routines, or ritualized patterns of verbal and non-verbal behavior (e.g. extreme distress at small changes, difficulties with transitions, or rigid thinking patterns)
Deficits in developing, maintaining, and understanding relationships (e.g. difficulties adjusting behavior to suit various social contexts; or difficulties in sharing imaginative play or making friends)	Highly restricted, fixated interests that are abnormal in intensity or focus (e.g. strong attachment to or preoccupation with unusual objects)
	Hyperreactivity or hyporeactivity to sensory input, or unusual

	interests in sensory aspects of the environment (e.g. apparent indifference to pain or temperature, or adverse responses to specific sounds or textures)

Table 2.1. The description of ASD signs and symptoms in DSM-5.

Early diagnosis plays a crucial role to minimize the possible intellectual disabilities, reported later in underestimated and undertreated ASD adults. In addition to screening instruments, such as several standardized assessment tools (e.g. STAT, ADOS, ADI-R and DISCO), other strategies, including an increased awareness of ASDs in the family and community and an easy access to specific services, can improve the quality of life of ASD patients. The difficulty in ASD diagnosis is getting worse by accompanying comorbidities (attention-deficit hyperactivity disorder, social anxiety, generalized anxiety and phobias) (107). This concern is mainly worth for females, rather than males, who can be underdiagnosed due to the high occurrence of comorbidities (e.g. depression and severe anxiety) that hide and mask ASD symptoms (108).

Many risk factors for ASDs have been described and they are divided in two main types: environmental and genetic. The advanced parental age (≥40 years for mothers and ≥50 years for fathers) and a short interpregnancy intervals have been independently associated to an increased risk for ASD

onset in children (106, 109). The use of antibiotics and the consequent perturbations of gut microbiota during pregnancy are a potential risk factors for infantile ASD (110). Furthermore, some non-optimal conditions of mothers (excessive weight gain, hypertension, nosocomial infections or autoimmune disease) can contribute the development of ASDs (111). Although results from different studies have to be clarified, some links with air pollutants and maternal stressors during pregnancy have been found (106). Beyond maternal conditions, preterm birth (<32 weeks), low birthweight (<1500 g), small-for-gestational-age status, and large-for-gestational age status (>95th birthweight percentile) represent other important risk factors (112, 113), even if the reasons of their involvement keep still unclear. The administration of many drugs in pregnant mothers has been associated to an increased risk of ASDs. Christensen et al. (114) demonstrated that a prenatal valproic acid exposure increased the probability of ASD in offspring. In addition, de Theije et al. (115) also in rodents demonstrated that this *in utero* valproic acid exposure induced gut inflammation, altered microbiota, and ASD-like behavioral abnormalities in male offspring. Other studies did not confirm the previous belief in antidepressant-induced ASD effects (116). In last years, media and no-vax organizations strongly supported the association between ASDs and

vaccination, but, to date, no scientific evidence has clearly demonstrated their link (117).

Beyond the environmental factors, the genetic risk has assumed an even more important role in ASD pathogenic mechanisms. Tick et al. (118) showed that ASDs can be inherited in 74-93% of cases. The first evidence of this link between ASDs and genetic was the development of autistic behavior in patients affected by rare genetic syndromes, such as fragile X syndrome (119). Following studies demonstrated also that the mutations of more than 100 genes are involved in ASD risk, indicating an objective obstacle in ASD diagnosis through genetic screening (120).

2.2. Treatments of ASDs

ASDs are a group of complex diseases and as such, its treatment represents a complicated challenge. To date, psychological interventions are the most important tools to manage these disorders (103). Weitlauf et al. (121) reported that early parent-mediated interventions to coach how to interact with ASD children give immediate beneficial effects on autistic traits. Another approach is the naturalistic behavioral developmental interventions that include the most well-known Applied Behaviour Analysis (ABA). This strategy considers the presence of adult teacher or therapist who works one-

to-one with ASD child and teaches some developmental abilities, such as language, imitation and cognitive skills. Several meta-analyses demonstrated the good improvements by these interventions with a duration time of 15-20 hours or more per week (122). For school-age children and adolescents, the most common behavioral interventions are social skill groups (123). Although all these psychological interventions are necessary, unfortunately, their beneficial effects are, in any case, limited.

The pharmacological treatment of ASDs is limited to reduce symptoms and not to counteract ASDs itself. In two randomized controlled trials, risperidone (124) and aripiprazole (125) showed an improvement of irritability or agitation in ASD young patients, even if these beneficial effects were not recognized in all children. In addition, both drugs are mixed with dopamine-receptor and serotonin-receptor antagonists or partial agonists, while no other medications are used in ASDs (126). The concern in using a pharmacological treatment for ASDs is the development of adverse events that include sedation, weight gain, and an increased hearth risk.

Although basic science research has discovered about pathogenic mechanisms of ASDs, the clinical implications remain few.

2.3. Gut-brain axis in ASDs

ASDs are neuropsychological diseases with a marked peripheral component. Indeed, beyond the social and psychological pattern, ASD patients show gastrointestinal symptoms with underlying pathogenic mechanisms that are not completely clarified yet. Alterations in gut integrity and modifications of its microbiota represent features of autistic outline and the interaction between brain and gut is achieved by influx of microbiota signals (gut hormones and microbial metabolites) in CNS, via the immune system, the vagus nerve and other host microbe interactions (127). Therefore, the scaffold of this gut-brain axis is constituted by the CNS, the autonomic nervous system (both sympathetic and parasympathetic branches), the neuroendocrine and neuroimmune systems, the enteric nervous system (ENS) and, the gut microbiota (**Figure 2.1**). All these features represent main characters of a complex network, where a bidirectional communication system between gut microbes and CNS played a key role for host homeostasis (128). Indeed, genes within the gut microbiota, termed the microbiome are capable of producing a myriad of neuroactive compounds, playing a pivotal role in shaping cognitive networks underlying social cognition, emotion, and behavior (129). During the development, brain neural circuits and gut microbiota co-evolve and possible alterations of gut

microbiota composition influence the normal growth of CNS neurotransmission, particularly for serotonergic system (130). Indeed, alterations of integrity in both gut epithelium barrier and BBB, reported in ASD patients (131, 132), can cause the translocation of bacterial metabolites, inducing immunoreactions that can activate the vagal system or directly influence CNS activity, impacting on neuronal plasticity and consequently on mood and behavior (133, 134). In rats, the lack of gut microbiota colonization leads to a reduced sociability, an increased anxiety-like behavior and alterations of neurophysiology compared to control mice with no pathogen bacteria colonization (135, 136).

Several clinical studies highlighted the link between dysbiosis and ASDs. Tomova et al. (137) showed a reduction of Bacteroidetes/Firmicutes ratio in ASD patients, while Strati et al. (138) demonstrated a significant reduction in relative abundance of phylum Bacteroidetes in autistic subjects. In contrast, Son et al. (139) did not find any alteration in gut microbiota composition in a study comparing fecal microbiota in ASD children and neurotypical siblings by qPCR. These conflicting evidences and the small scale of preclinical studies demonstrated the difficulty to outline a distinctive gut microbiota composition in ASDs.

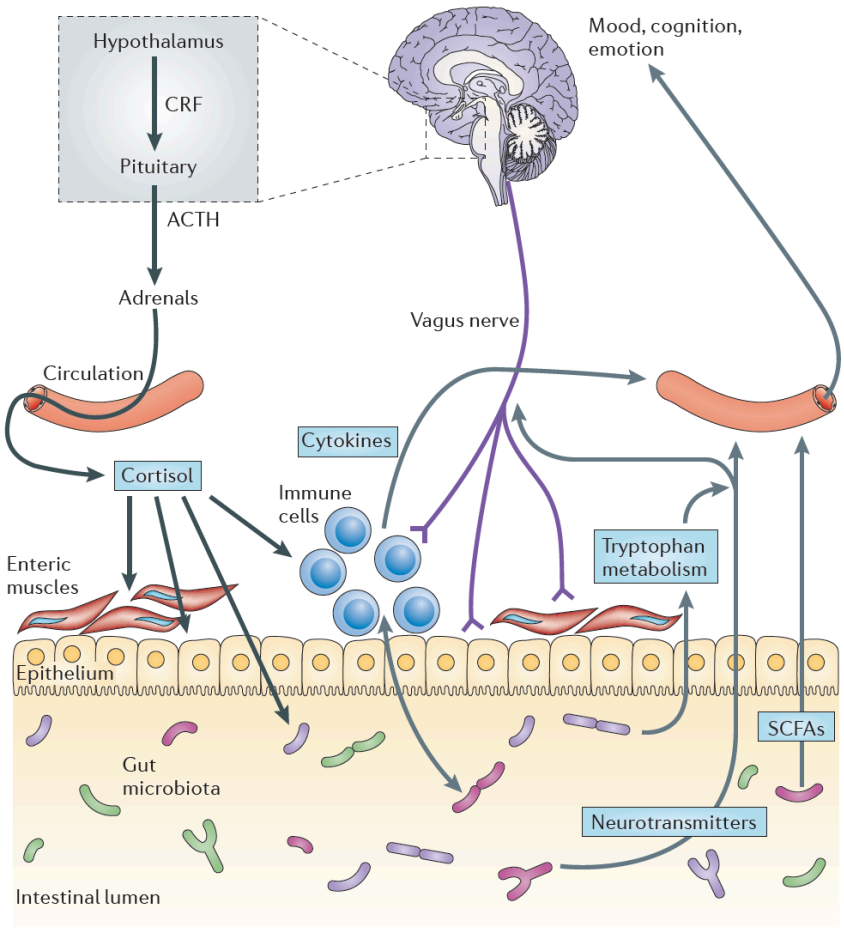

Figure 2.1. The scaffold of the gut-brain axis. The interaction between brain and gut is achieved by influx of microbiota signals, such as gut hormones and microbial metabolites, in CNS, via the immune system, the vagus nerve and other host microbe interactions.

3. Obesity-induced depression

3.1. Depression: definition, epidemiology, diagnosis and risk factors

Major depressive disorder (MDD) is a debilitating disease associated to reduced quality of life, medical morbidity, and mortality (140). Indeed, in 2013, it was considered the second leading cause of disability in all countries (141). The DSM-V identifies MDD when a person suffered from at least one discrete depressive episode lasting at least two weeks, characterized by changes in mood, interests and pleasure and by alterations of cognitive and vegetative spheres (102) (see **Figure 3.1**).

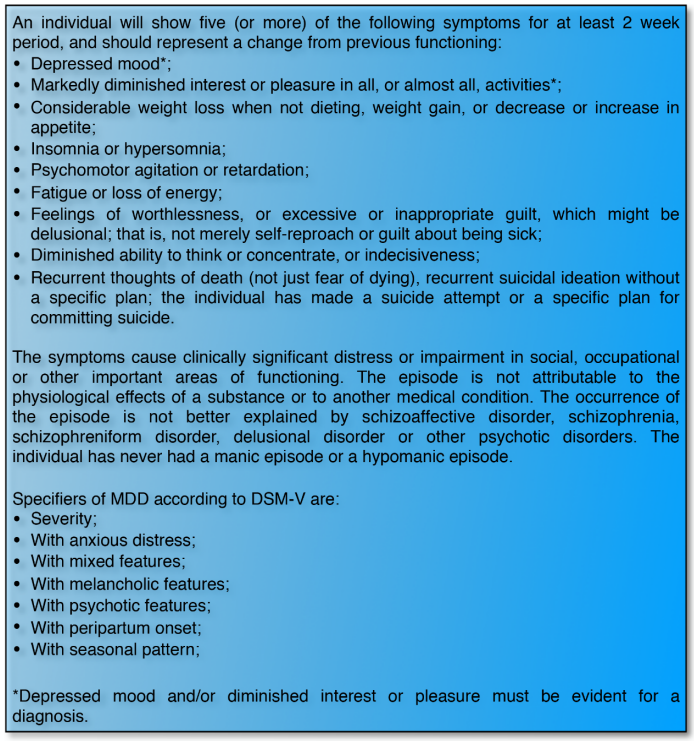

Figure 3.1. Definition of MDD according to DSM-5.

MDD represents a worldwide burden because about 6% of the adult population shows depressive episodes, mostly in women (about 2-fold) (142). In both sexes, MDD onset is approximately at 25 years of age and the range of increased risk is constituted by mid-to-late adolescence to early 40s (143). Furthermore, MDD prevalence was found to be similar between high- and low- and middle-income countries, highlighting that MDD does not represent a "modern-world" disease (**Figure 3.2**) (144).

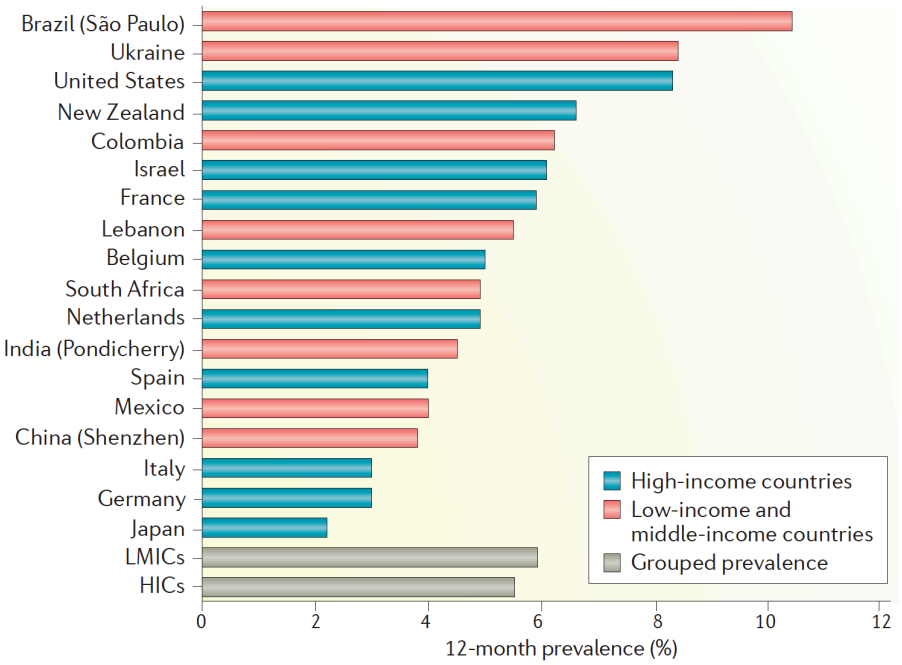

Figure 3.2. Worldwide prevalence of MDD. The overall estimates in high-income countries (5.5%) and low- and middle-income countries (5.9%) do not significantly differ.

The progress of MDD is essentially variable and it depends on its remission and chronicity. The prediction of an ill-fated course can be facilitated by higher symptom severity, other psychiatric comorbidities and the occurrence of childhood trauma (145). In population-based samples, the mean episode of MDD lasts between 13 and 30 weeks with a recovery of approximately 70–90% of patients within 1 year (146, 147), even if, in outpatient care settings, the remission rate can drastically decrease to 25% (148, 149). Furthermore, the recurrence of MDD is high, as about 80% of patients experiences at least another depressive episode during lifetime (150). Both in healthy people and other no-MDD patients, depression increases the

mortality risk by 60-80%, and its contribution of all-cause mortality is 10% (151, 152).

As mentioned above, MDD is diagnosed in patients who develop several symptoms distinguished from normal sadness or bereavement that endures at least 2 weeks (102). Beyond depressive mood, it needs only two of six symptoms such as appetite disturbances, loss of energy, reduced self-esteem, sleep disturbances, poor concentration or hopelessness. The persistent depressive disorder is a chronic disease characterized by depressive symptoms for more than 2 years. Once MDD diagnosis is made, the disorder can be classified by different specifiers (see **Scheme 3.1**).

Being MDD a multifactorial disease no established mechanisms can explain all aspects involved in its onset. The contribution of genetic factor is estimated to about 35%, highlighted more in family and twin-based studies rather than in single-nucleotide polymorphism-based estimates from genome-wide association studies (GWAS) (153). On the other side, environmental factors, such as sexual, physical or emotional abuse, contribute to the development of MDD. Indeed, epidemiological studies correlated the onset of MDD with stressful events (loss of employment, chronic or life-threatening health problems, financial insecurity, exposure to violence, separation and bereavement) usually occurred in the year preceding onset and disease itself (154). However, not only recent events

but also childhood-occurred ones, including physical and sexual abuse, psychological neglect, exposure to domestic violence or early separation from parents due to death, are clearly responsible of MDD (155).

3.2. Pathogenic mechanisms of MDD

The oldest known pathogenic mechanism of MDD is based on the lack of balance in the serotonergic, noradrenergic and dopaminergic systems (156). Indeed, for many years, MDD research focused on the metabolism of their neurotransmitters, such as noradrenaline, serotonin and dopamine, and their effect on both presynaptic and postsynaptic receptors (157).

Following studies moved their focus on connection between MDD and endocrine pathways. The hypothalamic-pituitary-adrenal (HPA) axis dysfunction represents the center of this link. Indeed, early-life stress induces the activation of corticotropin-releasing hormone (CRH)-containing neural circuits in several animal studies (158). This involvement has been confirmed by clinical studies, showing how children subjected to sexual or physical abuse showed a marked activation of HPA axis when exposed to standardized psychosocial stressors or through endocrine tests trying to stop HPA activity (159). Moreover, increased levels of cortisol, whose production is generally controlled by the hypothalamus, represented a risk factor for the onset of MDD in clinical studies (160, 161).

The immune system is another major character involved in the physiological stress-sensing pathways and interacts directly and indirectly with HPA, the autonomic nervous system and CNS in pathogenic mechanisms of MDD. Indeed, once peripheral cytokines reach and cross the BBB, they activate CNS-resident cells, such as astrocytes, microglia and neurons. In a clinical study, patients who received cytokine treatments, such as IL-2 or interferon-γ, for hepatitis or cancer therapy, showed higher rate to develop depressive episodes (162). Other meta-analyses confirmed these findings, showing high levels of serum cytokines, such as tumor necrosis factor (TNF)-α and IL-6 in MDD patients (163, 164). The increased levels of circulating cortisol and inflammatory cytokines can affect brain function, through the disruption of neuroplasticity and the reduction of neurogenesis, as demonstrated by low levels of the neurotrophin, brain-derived neurotrophic factor (BDNF) (165). Taken together, all these evidences underline how all those biological pathways, taking part into the so-called psycho-immune-neuroendocrine (PINE) network (**Figure 3.3**) are involved in MDD.

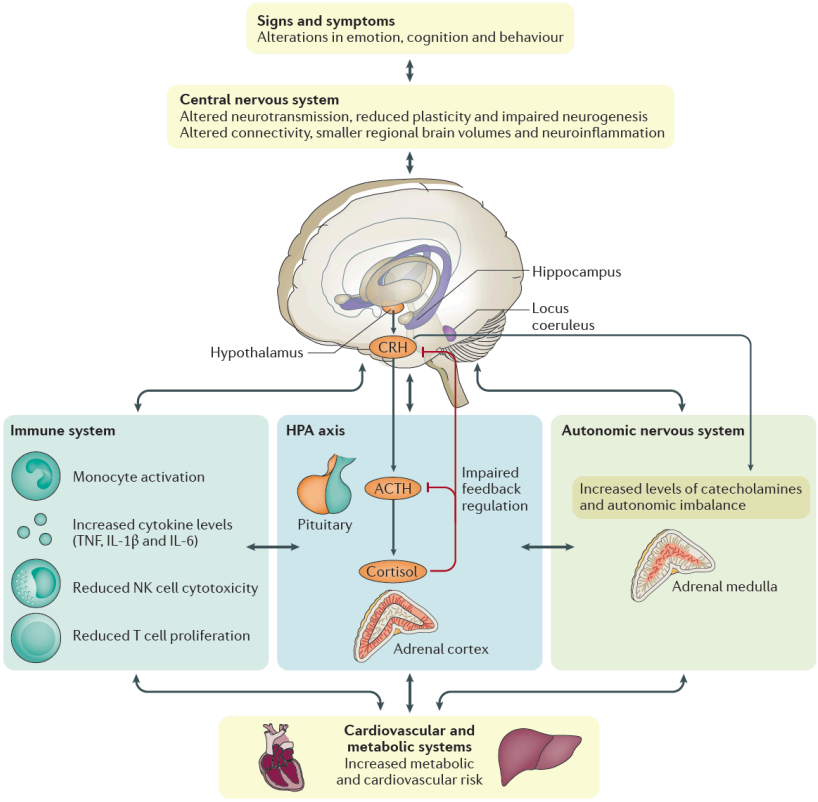

Figure 3.3. The psycho-immune-neuroendocrine (PINE) network of MDD. Beyond the impairment of CNS, the hyperstimulation of HPA axis is another pathological feature of MDD. Moreover, this pathological condition activates the immune system, increasing levels of circulating cytokines and triggering a low-grade chronic inflammation. Once MDD becomes chronic, both HPA hyperactivity and inflammation might converge towards an alteration of autonomic nervous system (ANS), contributing to MDD comorbidities, such as cardiovascular and metabolic disorders.

3.3. Depression and obesity: a bidirectional interplay

Among several risk factors, different studies highlighted the bidirectional association between obesity and depression (166, 167). Faith et al. (168) examined different studies to understand whether the association "depression-to-obesity" is stronger than "obesity-to-depression" or vice

versa. These authors reported a more significant influence of obesity to depression than the opposite (80% vs 53%).

The general mechanisms that try to explain the obesity-induced depression are two:

- Obesity and MDD share fundamental biological mechanisms (inflammatory, neuroendocrine, metabolic and gut-related patterns), and the alterations of these systems induced by obesity can lead to MDD;
- Chronic psychological stress related to lack of self-confidence induced by body-image consciousness leads to dysregulation of PINE network, triggering the onset of MDD.

According to this paradigm, the pathophysiological features of obesity, such as low-grade inflammation, ANS unbalance, leptin and ghrelin changes, and dysbiosis play a pivotal role as underlying pathogenic mechanisms of MDD. The obesity-induced systemic inflammation is characterized by the increase of serum levels of pro-inflammatory cytokines, such as IL-6 and TNF-α, that stimulate the microglial proliferation and astrocyte dysfunction with consequent neuroinflammation, mainly in areas that lack an effective BBB, including hypothalamic arcuate nucleus (ARC) (169). The ARC is strongly connected not only with other regions of the hypothalamus, but also with

other brain areas, such as mesolimbic dopamine system, hippocampus, orbitofrontal cortex, nucleus accumbens, striatum and prefrontal cortex, regulating motivation and reward pathways (170). Thus, beyond the effects on feeding signals, the inflammation in ARC can potentially impair cognitive function (**Figure 3.4**).

Moreover, neuroinflammation can trigger the PINE network to reach the critical threshold for MDD onset, even if molecular mechanisms keep still unclear.

Leptin and ghrelin are central regulators in the PINE network. Beyond their key role in food intake, these molecules are implicated in mood regulation (171-173). Leptin interacts with its receptor, particularly abundant in ARC, and, activating the proopiomelanocortin (POMC) neurons and suppressing neuropeptide Y (NPY) and agouti-related protein (AgRP) ones, reduces feeding behavior. HFD-induced obesity induces a leptin resistance, characterized by high systemic levels of leptin and reduced central leptin sensitivity. This detrimental condition can lead to a reduced neuroprotection and onset of MDD (174-176).

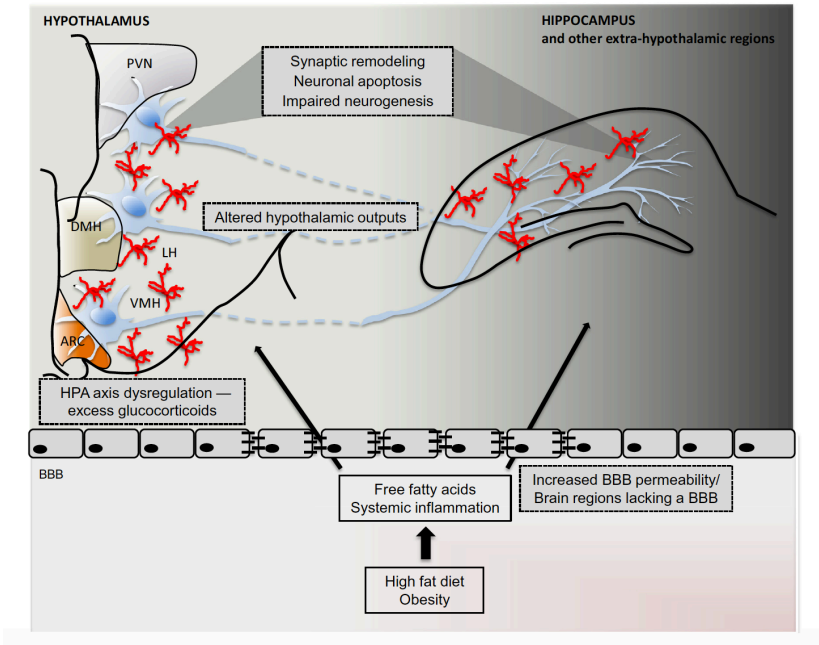

Figure 3.4. Possible mechanism of cognitive dysfunction induced by obesity. HFD/obesity induce the HPA dysfunction that can alter other brain areas, such as hippocampus, reducing neurogenesis and inducing neuronal apoptosis.

The contribution of the change in gut microbiota induced by obesity in the development of MDD has been analyzed in several studies. As mentioned above, high fat diet consumption causes the production of several inflammatory mediators that can compromise colonic epithelial barrier function, inducing the so-called "leaky gut" (177). This increased permeability allows the entrance of immunogenic molecules, such as LPS (178), in the systemic circulation, whose occurrence has been recognized in both animal (179) and human (180) affected by depression. Moreover, long-term consumption of a Western-style HFD, constituted by low levels of

fiber, may result in profound reduction of short chain fatty acids (SCFAs), endogenous molecules with marked anti-inflammatory and neurogenesis activity (181). The intestinal dysbiosis induced by obesity, may promote depression through the modulation of hippocampal BDNF. Indeed, Bercik et al. (182) demonstrated that the administration of antimicrobials was responsible of BDNF reduction in mice hippocampus, while colonization of germ-free mice with gut microbiota from other specific pathogen free mice increased the expression of neurotrophin.

3.4. Treatment of MDD

Given the complexity and high prevalence of MDD, its prevention is fundamental to limit it. These strategies include the strengthening protective factors, such as the increase of social support, and the reduction of prodromal symptoms, limiting them before that they overcome the disease threshold. Indeed, a meta-analysis demonstrated the reduction of depressive symptoms (21%) in MDD patients who received a preventive intervention (183).

The treatment of MDD depends on the severity of symptoms and include two main strategies: psychotherapy and pharmacotherapy. Mild depressive episodes could be treated only with psychotherapy, but when the grade worsens, a pharmacological treatment alone or in combination with

medication and psychotherapy should be adopted, two weeks after the beginning of symptoms (184). Several meta-analyses did not show any consistent difference among different types of psychotherapy (185-187).

The pharmacological treatment of MDD comprises the use of monoamine-based antidepressant drugs, capable to stimulate an adaptive neuronal response against MDD central perturbations (**Figure 3.5**), although the exact biomolecular mechanisms of action are not completely clarified. In addition, the wider choice of selective serotonin reuptake inhibitors (SSRIs) or serotonin–norepinephrine reuptake inhibitors (SNRIs) than that of classical antidepressant drugs is due to better adverse-effect profile rather than efficacy. However, SSRIs and SNRIs are also characterized by several adverse effects, such as headache, insomnia, gastrointestinal symptoms, dizziness, sexual dysfunction, weight gain and sleep disturbances (188). Among new therapeutic approaches for MDD, several compounds are under investigation, such as neurokinin 1 antagonists, glutamatergic system modulators, anti-inflammatory agents, opioid tone modulators and opioid κ antagonists, hippocampal neurogenesis-stimulating treatments and anti-glucocorticoid therapies (140).

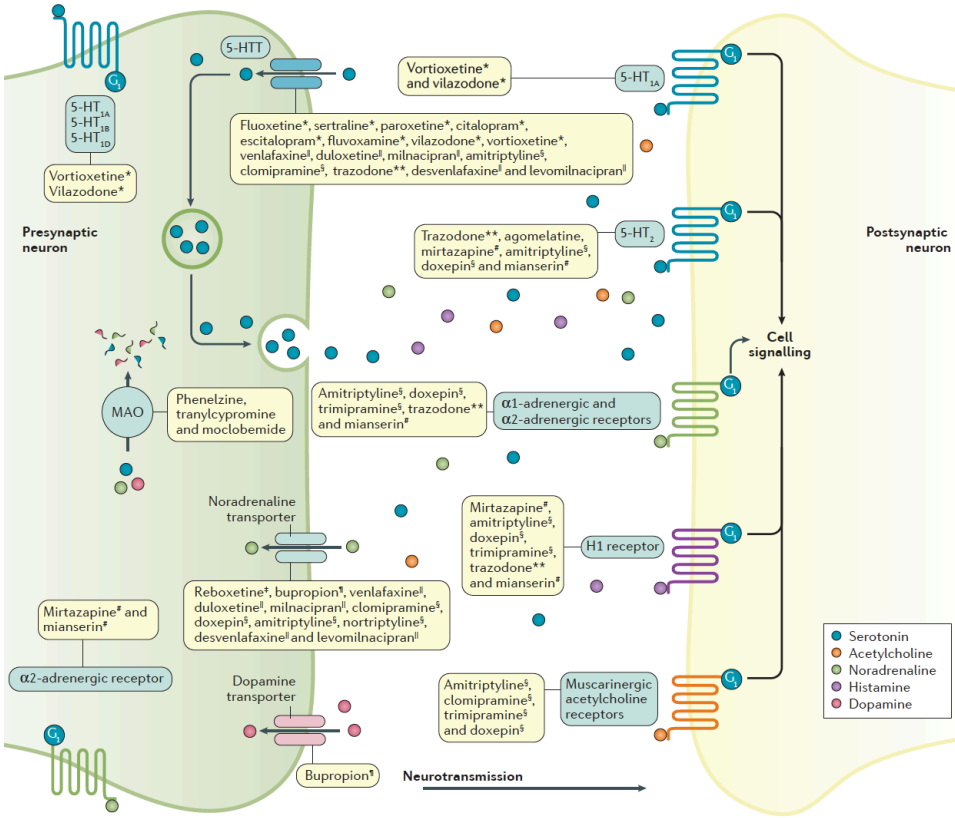

Figure 3.5. Actual pharmacological strategies for MDD treatment.

4. Material and Methods

4.1. Sex differences in gut microbiota of BTBR mice

4.1.1. Animals

C57Bl/6J (C57) and BTBR T + tf/J (BTBR) inbred strains of mice were purchased from The Jackson Laboratory (Bar Harbor, ME, USA) and a colony was established and maintained. For the study, 24 fully symptomatic BTBR mice (12 months of age, 12 for gender) and 24 C57 control mice (12 months of age, 12 for gender) were housed in the same room under standard 12-h light/12-h dark cycle with free access to water and standard laboratory chow diet. Mice were from different litters and housed by gender separately 2/3 per cage. Before killing and prior to serum and sample collection, animals, kept overnight fasted, were anesthetized by enflurane and euthanized by an intraperitoneal injection of a cocktail of ketamine/xylazine. As suggested by the animal welfare protocol, all efforts were made to minimize animal suffering and to use only the number of animals necessary to produce reliable scientific data. All procedures involving animals and their care were conducted in conformity with international and national law and policies (EU Directive 2010/63/EU for animal experiments, ARRIVE

guidelines and the Basel declaration including the 3R concept). The procedures reported here were approved by the Institutional Committee on the Ethics of Animal Experiments (CSV) of the University of Naples "Federico II" and by the Ministero della Salute under protocol no. 0022569-P-20/12/2010.

4.1.2. Marble burying test

For the performing of all behavioral tests, we considered the book of Bayley et al. (189). Male and female BTBR and C57 (n=12 each group) were individually placed in a plastic container (46 cm long x 24 cm wide x 21 cm deep) with 5 cm of clean woodchip bedding (Northeastern Products, NY). The plastic container was placed in a room used for behavioral testing. Once a mouse was gently allocated into the test container, a wire lid was placed on top and undisturbed mice were allowed to freely explore the container for 30 min, as habituation time. Twenty-four hours later, 20 glass marbles (1.5 cm in diameter) were placed on top of clean bedding, arranged in five rows of four and mice located into plastic cages for 30 minutes. After this experimental time, each mouse was removed from the testing container and replaced to their home cage. When a threshold of 75% coverage for each marble was observed, it was considered buried and recorded. After the test,

the marbles were thoroughly cleaned and new bedding was used for each mouse. The same animals tested for marble burying test were also examined for grooming behavior.

4.1.3. Self-grooming test

Mice were individually placed in an empty plastic cage (28 cm wide × 17 cm long × 12 cm high) and were freely to explore the arena for 20 minutes. The first 10 min were necessary for a habituation time. During the second phase, a trained observer, sat approximately 1.6 m from the test cage, timed the cumulative period that mice spent in self-grooming. Grooming behavior included head washing, body grooming, genital/tail grooming and paw and leg licking. After the test, the cage was thoroughly cleaned. After self-grooming test, the same animals were tested for sociability test.

4.1.4. Social interaction test

Social interaction was examined using the three-chambered apparatus as previously described (190-192). The apparatus (60 x 40 cm) has two doorways that divide it into a three chambers apparatus (20 x 40 cm each). Number of entries and time spent in each chamber were automatically

detected by a video camera coupled with a video-tracking software (Any-maze, Stoelting). The sociability test was preceded by 5-min habituation session where each mouse is restrained in the center of the middle chamber. After this phase, a novel sex, strain and age matched mouse (not used in later testing and previously habituated) is placed in one side of the chamber under an enclose cup while the other side contained an empty cup. During this sociability phase, walls between the compartments were removed and the tendency to approach a novel mouse was compared with tendency to approach a novel object is monitored and recorded. Each mouse was free to explore all three chambers for 10 minutes and both sides were alternated between the left and right chambers across subjects.

4.1.5. *In vivo* intestinal permeability assay

In vivo intestinal permeability assay was performed for a subset of mice using fluorescein isothiocyanate-labeled dextran (FITC-dextran) method, as previously described (193). Before the beginning of the test, food and water were withdrawn for 6 hours, after which mice (n=5, each group) were administrated by gavage with FITC labeled dextran 4000 (Sigma-Aldrich, Milan, Italy), as permeability tracer (60 mg/100 g body weight). After 24 hours blood of all animals was collected by intracardiac puncture and

centrifuged (3000 rpm for 15 min at RT). Then plasma FITC-dextran concentration was determined (excitation, 485 nm; emission, 535 nm; HTS-7000 Plus-plate-reader; Perkin Elmer, Wellesley, MA, USA), using a standard curve generated by serial dilution of the tracer.

4.1.6. Histological analysis

Colonic tissues of male and female mice of both strains (n=3) were removed, washed and then fixed in paraformaldehyde (4% v/v; Carlo Erba, Italy) for 12 hours. These samples were dehydrated, embedded in paraffin and cut into 5 µm thick sections before being stained with hematoxylin-eosin (H&E; Carlo Erba, Italy). Images were obtained by a Leica DFC320 video camera (Leica, Milan, Italy) connected to a Leica DM RB microscope using the Leica Application Suite software V2.4.0.

Colon sections were analyzed by the same pathologist in a blinded manner to evaluate their structure and architecture. Histopathology was quantified following: a) the severity of inflammatory cell infiltration was evaluated by percentage of leukocyte density in lamina propria area and estimated in a high-power field (HPF) representative of the section (0 for no signs of inflammation, 1 for minimal < 10%, 2 for mild 10–25% with scattered neutrophils, 3 for moderate 26–50%, 4 for marked > 51% with dense

infiltrate); b) The extent of the inflammation was estimated as expansion of leukocyte infiltration (0 for none, 1 for mucosal, 2 for mucosal and submucosal and 3 for mucosal, submucosal and transmural level).

4.1.7. Microbial DNA extraction, 16S ribosomal DNA (rDNA) library preparation and sequencing

Freshly evacuated fecal pellets were kept directly in a sterile microtube one day before the sacrifice of mice and stored at -80 °C until assayed. Bacterial genomic DNA was extracted from frozen fecal samples using the QIAamp DNA Stool Mini Kit (Qiagen) according to manufacturer's instructions. DNA concentration was measured fluorometrically using Qubit dsDNA BR assay kit (Invitrogen) and quality was assessed by spectrophotometric measurements with NanoDrop (ThermoFisher Scientific Inc). Samples were stored at -20 °C until processed for amplification. It is well documented that various compartments of the gastro-intestinal tract harbour different bacterial populations. We chose to analyze readly accessible fecal samples for gut microbiome analyses mainly because fairly representative of the whole gastro-intestinal tract, with exception of some surface-adherent bacterial species. Sequencing samples were prepared according to the protocol 16S Metagenomic Sequencing Library Preparation for Illumina

Miseq System with some modifications. The V3–V4 regions of the 16S rDNA gene were amplified starting from 200 ng of DNA template in a reaction volume of 50 µ L containg 1x Fast start High Fidelity Reaction Buffer, 5 µ M of each primer, 0.2 nM of dNTPs, 3 mM $MgCl_2$, and 2 U FastStart High Fidelity PCR System (Roche Applied Science). PCR was performed using the following cycles conditions: an initial denaturation step at 95 °C for 2 min, followed by 30 cycles of 95 °C for 30 s, 55 °C for 45 s, 72 °C for 55 s and ended with an extension

step at 72 °C for 5 minutes; products were visualized by electrophoresis on 1.2% agarose gel. After a purification step with Agencourt AMPure XP (Beckman Coulter Inc), the amplicons were indexed with 10 subsequent cycles of PCR using the Nextera XT Index Kit (Illumina). Each PCR reaction contained 10 µ L of amplicons from first PCR, 5 µl index 1 primer (N7xx), 5 µl index 2 primer (S5xx), 5 µ l 1x Fast start High Fidelity Reaction Buffer, 6 µL $MgCl_2$ (3 mM), 1 µ L dNTPs (0.2 nM), 0.4 µ L FastStart High Fidelity PCR System (2U) and 17.6 µ l PCR grade water. PCRs were carried out, visualized using gel electrophoresis and subsequently cleaned as described above.

Library sizes were assessed using a Bioanalyzer DNA 1000 chip (Agilent technologies) and quantified with Qubit. Normalized libraries were pooled,

denatured with NaOH, then diluted to 10pM and combined with 25% (v/v) denatured 10pM PhiX, according to Illumina guidelines. Sequencing run was performed on an Illumina Miseq system using v3 reagents for 2 × 281 cycles.

4.1.8. Sequencing data analysis

V3-V4 16S rDNA FASTQ paired-end reads were quality filtered and assembled using PEAR (194). Only sequences showing average PHRED score ≥ 30, read length between 400 and 500 bp and overlapping regions between mate-pair end of at least 40 nucleotides were retained in this step. Passing filter sequences were then processed with PRINSEQ (195) in order to obtain FASTA and quality files for further analyses. Metagenomic analyses on the resulting data were conducted using Quantitative Insights Into Microbial Ecology (QIIME, version 1.8.0) (196). 16S sequences were used to pick OTUs at 97% of sequences similarity from Greengenes 16S gene database (GG, may 2013 version) (197) with a closed reference-based OTU picking method. The GG database was used to taxonomically classify the identified OTUs and to compute their distribution across different taxonomic levels. To avoid sample size biases in subsequent alpha and beta diversity analyses, a sequence rarefaction procedure was applied using a

maximum depth of 32,228 sequences/sample. To assess sampling depth coverage and species heterogeneity in each sample, alpha diversity metrics were employed on rarefied OTU table using Good's coverage, Observed species and Shannon's diversity index. A two-sample permutation t-test, using 999 Monte Carlo permutations to compute p-value, was performed to compare the alpha diversities between sample groups. OTUs diversity among sample communities (beta diversity) was assessed by applying unweighted Unifrac distances. Statistical significance of beta diversities was assessed on unweighted UniFrac distances matrixes using ANOSIM method (198) with 999 permutations. Statistical differences in OTUs frequencies across sample groups at different taxonomic levels were assessed using nonparametric Kruskal-Wallis test. Next, two analyses were applied on OTU tables generated by QIIME to identify key OTUs that discriminate female and male BTBR mice from their respective controls: Metastats comparison using the online interfaces (199) and LDA Effect Size analysis (LEfSe) (200). Only those OTUs reported by both methods to be significantly different between the two groups ($p < 0.05$ for Metastats, $LDA > 2$ and $p < 0.05$ for LEfSe) have been considered as key discriminatory OTUs. Key genera that discriminate female and male BTBR mice from their respective controls were identified applying only LEfSe.

4.1.9. Quantification of gene expression using RT-PCR

Total RNA was extracted from tissues using TRIzol Reagent (Bio-Rad Laboratories), according to the manufacturer's instructions. cDNA was synthesized using a reverse transcription kit (NucleoSpin®, MACHEREY-NAGEL GmbH & Co, Düren, Germany) from 4 µg total RNA. PCRs were performed with a Bio-Rad CFX96 Connect Real-time PCR System instrument and software (Bio-Rad Laboratories). The PCR conditions were 15 min at 95 °C followed by 40 cycles of two-step PCR denaturation at 94 °C for 15 s, annealing at 55 °C for 30 s and extension at 72 °C for 30 s. Each sample contained 500 ng cDNA in 2X QuantiTect SYBRGreen PCR Master Mix and primers pairs to amplify zonuline-1 (*Tjp1*), occludin (*Ocln*), TNF-α (*Tnfa*), interleukin-6 (*Il6*), interleukin-10 (*Il10*), CD11c (*Itgax*) (Qiagen, Hilden, Germany), in a final volume of 50 µl. The relative amount of each studied mRNA was normalized to GAPDH as housekeeping gene, and data were analyzed according to the $2^{-\Delta\Delta CT}$ method.

4.1.10.Other statistical methods

Marble burying, self-grooming, plasma FITC-dextran, gene expression data were analyzed by two-way ANOVA with strain and sex as factors; social

approach behavior results were analyzed by three-way ANOVA with chamber, strain and sex as factors. Multiple comparisons were performed using Bonferroni's post-hoc test. Pearson correlation test was used to assess the eventual relationship between the amount of key genera and behavioral scores, intestinal permeability and inflammation. In this study results were considered statistically significant at p-value < 0.05. Significant differences were indicated in figures by *p<0.05, **p<0.01, ***p<0.001, ****p<0.0001. ANOSIM and permutation t-test were performed using QIIME scripts, all other analyses were performed using R 3.2.050. Bar plots were created by using GraphPad Prism 6.0.

4.2. PEA counteracts autistic-like phenotype in BTBR mice

4.2.1. Animals

Male C57Bl/6J (B6), *B6.129S4-SvJae-Pparatm1Gonz* PPARα null (KO) and BTBR T + tf/J (BTBR) (3-4 months old) mice were purchased from The Jackson Laboratory (Bar Harbor, ME, USA) and colonies maintained in our animal facility genotyped according to supplier webpage (http://jaxmice.jax.org), using the RedExtract kit (Sigma–Aldrich, Italy).

All animals were housed in groups in a room maintained at 22°C, on a 12 h:12 h light:dark cycle, with *ad libitum* access to water and standard laboratory chow diet. To minimalized litter effects, we used mice from at least 5 different litters in each experiment. All experimental procedures were carried out in compliance with the international and national law and policies (EU Directive 2010/63/EU for animal experiments, ARRIVE guidelines and the Basel declaration including the 3R concept) and approved by Italian Ministero della Salute.

4.2.2. Drugs and treatment

Ultra-micronized PEA (PEA-um®; Epitech Group, Italy) and GW6471 (N-((2S)-2-(((1Z)-1-Methyl-3-oxo-3-(4-(trifluoromethyl) phenyl)prop-1-enyl) amino)-3-(4-(2-(5-methyl-2-phenyl-1,3-oxazol-4-yl)ethoxy)phenyl)propyl) propanamide), a PPARα antagonist (GW; Tocris, Bristol, UK) were dissolved in PEG400, Tween 80 and sterile saline (Sigma-Aldrich, Milan, Italy) to obtain a final concentration of PEG400 and Tween 80 of 20 and 10% v/v, respectively and injected at a volume of 10 ml/kg body weight.

BTBR, KO and control B6 mice were daily intraperitoneal-injected (i.p.) for 10 days with vehicle, PEA (10 or 30 mg/kg), and/or GW (1mg/kg). When BTBR mice were co-treated with PEA and GW, the antagonist was injected 30 min before PEA administration. Testing began at ages 3-4 months, on day 9^{th}, one hour after the last injection. In details, behavioural tasks described below were conducted in the same mice from 5 different litters, in a battery on two separate days (9^{th}-10^{th}) according to Paylor, Spencer (201), with sufficient intervals between tests and in a sequence that begins with the least stressful quick observational tests followed by the more stressful complex tasks, except for the evaluation of locomotor activity and anxiety behaviour (elevated plus maze and open field test) that were conducted on a separate cohort of mice. All experiments and data analyses were performed

by blinded operators to genotype, when possible, and treatment. The experimental protocol is summarized in **Figure 4.2.1**.

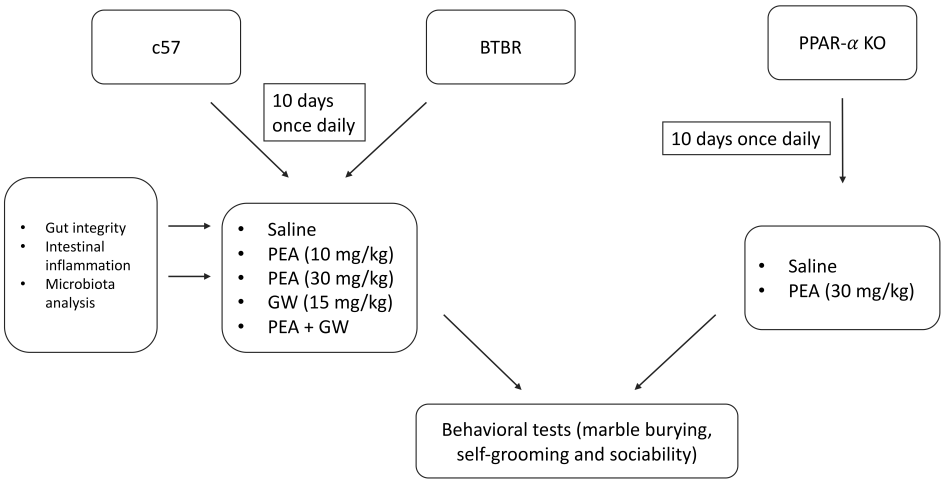

Figure 4.2.1. Experimental protocol BTBR and PEA.

4.2.3. Open field locomotion test (OFT)

The OFT represents and index of general locomotor activity and anxiety behaviour of animals (202). Mice were placed into the center of a clear square grey (40x40 cm) open-field arena and allowed to explore for 10 minutes. We measured the locomotor activity and the time spent in the centre quadrant and peripheral frame. The movements of mice were recorded by the infrared video camera and analysed by Any-maze-tracking software (Stoelting Co., Wood Dale, IL, U.S.A.).

4.2.4. Marble burying test

In marble burying test, we choose BTBR and C57 (n=10 each group) and proceeded as in previous work.

4.2.5. Self-grooming test

The same subjects tested in marble burying test were also examined for grooming behavior, as reported in previous work.

4.2.6. Three-chambered social test

The same subjects tested in marble burying and self-grooming tests were also examined for social approach behavior, as reported in previous work.

4.2.7. Elevated plus maze test (EPM)

The elevated plus maze (EPM) is test suitable for evaluation of mice anxiety, based on the test animal aversion to open spaces. The maze (Ugo Basile apparatus, Gemonio, Italy) comprised four arms (5 cm in width and 35 cm in length), with two opposing arms enclosed from the sides by black walls

(20 cm in height), defined as closed arms, whereas the other two arms remained unclosed (open arms). The intersection area for all four arms, defined as center, represented the access sector to all four arms. Mice were placed individually in the center of the apparatus, facing an open arm and allowed to explore the maze for 5 min detected by the Any-maze tracking software. We measured the number of entries in open and closed arms and time spent in these zones. An arm entry is defined as entry of all four paws into an arm. The main variable commonly associated to an 'anxiety-like' state is the percent time spent in the closed arm.

4.2.8. Serum parameters

Before sacrifice, mice were anesthetized by enflurane and blood was collected by cardiac puncture. Serum samples were obtained by centrifugation at 1500 x g at 4°C for 15 min. Serum TNF-α, IL-1β and IL-6 were measured using commercially available ELISA kits (Thermo Fisher Scientific, Rockford, IL), following the manufacturer's instructions.

4.2.9. Mitochondrial parameters

Mitochondria isolation and oxygen consumption (polarographically measured using a Clark-type electrode) were carried out. Briefly, the livers were freshly collected and washed in a medium containing 220 Mm mannitol, 70 mM sucrose, 20 mM N2-(hydroxyethyl) piperazine-N-2-ethanesulfonic acid (HEPES) (pH 7.4), 1 mM-EDTA, and 0.1 % w/v fatty acid free BSA. Tissue fragments were homogenized with the above medium (1:4, w/v) in a Potter Elvehjem homogenizer (Heidolph, Kelheim, Germany) set at 500 rpm (4 strokes/min). The homogenate was centrifuged at 1000 gav for 10 min and the resulting supernatant fraction was again centrifuged at 3000× g for 10 min. The mitochondrial pellet was washed twice and finally resuspended in a medium containing 80mMKCl, 50 mM HEPES (pH 7.0), 5 mM KH_2PO_4, and 0.1% w/v fatty acid free BSA. The protein content of the mitochondrial suspension was determined by the method of Hartree using BSA as the protein standard (203). Isolated mitochondria were then used for the determination of respiratory parameters.

Oxygen consumption was measured in the presence of substrates and ADP (state 3), in the presence of substrates alone (state 4) and their ratio (respiratory control ratio, RCR) were calculated. The substrates used for liver respiration were 10 mM succinate + 3.75 µM rotenone or 40 µM

palmitoylcarnitine + 2.5 mM malate for the determination of fatty acid oxidation rate.

The degree of coupling was determined in the liver by applying equation by Cairns et al. (204): degree of coupling = $\sqrt{\mathbf{1} - (\mathbf{Jo})_{\mathbf{sh}}/(\mathbf{Jo})_{\mathbf{unc}}}$ where (Jo)sh represents the oxygen consumption rate in the presence of oligomycin that inhibits ATP synthase, and (Jo)unc is the uncoupled rate of oxygen consumption induced by carbonyl cyanide trifluoromethoxyphenylhydrazone (FCCP), which dissipates the transmitochondrial proton gradient. (Jo)sh and (Jo)unc were measured as above using succinate (10 mmol/L) rotenone (3.75 μmol/L) in the presence of oligomycin (2 μg/mL) or FCCP (1 μmol/L), respectively. Aconitase activity was measured spectrophotometrically (at 412 nm). Determination of aconitase specific activity was carried out in amedium containing 30mM sodium citrate, 0.6mM $MnCl_2$, 0.2 mM NADP, 50 mM TRIS-HCl pH 7.4, and two units of isocitrate dehydrogenase. The formation of NADPH was followed spectrophotometrically (340 nm) at 25°C (205). The level of aconitase activity measured equals active aconitase (basal level). Aconitase inhibited by ROS in vivo was reactivated so that total activity could be measured by incubating mitochondrial extracts in a medium containing 50

mM dithiothreitol, 0.2 mM Na_2S, and 0.2 mM ferrous ammonium sulphate (206).

Carnitine-palmitoyl-transferase (CPT) activity was followed spectrophotometrically as CoA-sH production by the use of 5,5'-dithiobis (nitrobenzoic acid) (DTNB) and as substrate palmitoyl coA 10 μM. The medium consisted of 50 mM KCl, 10 mM Hepes (pH 7.4), 0.025% Triton X-100, 0.3 mM DTNB, and 10–100 pg of mitochondrial protein in a final volume of 1.0 ml. The reaction was followed at 412 nm with spectrophotometer, and enzyme activity was calculated from an E412 = 13,600/ (M X cm). The temperature was maintained at 25°C. Aconitase activity was measured spectrophotometrically (412 nm). Determination of aconitase specific activity was carried out in a medium containing 30mM sodium citrate, 0.6mM $MnCl_2$, 0.2 mM NADP, 50 mM TRIS-HCl pH 7.4, and two units of isocitrate dehydrogenase. The formation of NADPH was followed spectrophotometrically (340 nm) at 25°C. The level of aconitase activity measured equals active aconitase (basal level). Superoxide dismutase (SOD)-specific activity was carried out according to Flohe and Orting (207).

4.2.10.Oxidative stress assay

The levels of reactive oxygen species (ROS) were determined as described by Montoliu et al. (208). Briefly, fresh hippocampal homogenate was diluted in 100 mM potassium phosphate buffer (pH 7.4) and incubated with a final concentration of 5 µM dichlorofluorescein diacetate (Sigma–Aldrich) in dimethyl sulfoxide for 15 min at 37°C. The dye-loaded samples were centrifuged and the pellet suspended in 100 mM potassium phosphate buffer and incubated for 60 min at 37°C. The fluorescence measurements were performed with a HTS-7000 Plus-plate-reader spectrofluorometer (Perkin Elmer, Wellesley, Massachusetts, USA) at 488 nm for excitation and 525 nm for emission wavelengths. ROS stress was quantified from the dichlorofluorescein standard curve in dimethyl sulfoxide (0–1 mM).

4.2.11.Western blot analysis

Hippocampus was homogenized in lysis buffer (50 mM Tris–HCl, pH 7.4; 1 mM EDTA; 100 mM NaCl; 20 mM NaF; 3 mM Na_3VO_4; 1 mM PMSF with 1 % (v/v) Nonidet P-40; and protease inhibitor cocktail). Lysates were centrifuged at 20,000 g for 15 min at 4 °C. Protein concentrations were estimated using bovine serum albumin as a standard in a Bradford reagent assay. Proteins were separated on SDS-PAGE, transferred to nitrocellulose

membranes, and incubated with the following primary antibodies: PPARα (cat no P0369, Sigma Aldrich), 1: 500; Bdnf (cat no sc-546, Santa Cruz), 1: 200; pCREB (cat no 9196, Cell Signaling Technologies (CST), MA, USA), 1:1000; CREB (cat no 4820, CST) 1: 2000; β-actin (Sigma Aldrich), 1:1000. The signals were visualized with the ECL system (Pierce) by Image Quant (GE Healtcare, Milan, Italy). The protein bands were densitometrically analyzed with the Quantity One software (Bio-Rad Laboratories).

4.2.12.Quantification of gene expression using RT-PCR

RNA extraction and following Real Time-PCR analysis were performed as in previous work, even if, here, we tested primers pairs to amplify *Tjp1*, *Ocln*, *Tnfa*, *Il6*, *Il1b*, peroxisome proliferator-activator receptor α (*Ppara*), brain-derived neurotrophic factor (*Bdnf*), neurotrophic receptor tyrosine kinase 2 (*Ntrk2*) (Qiagen, Hilden, Germany), in a final volume of 50 µl.

4.2.13. 16S metagenomic sequencing and data analysis

Fecal samples were collected from a subset of six mice randomly selected from each group and quickly stored at -80°C. Fecal microbiota was studied as reported above.

4.2.14. Statistical analysis

Data are presented as mean ± SEM. All the experiments were analysed using analysis of variance (ANOVA) for multiple comparisons followed by Bonferroni's *post hoc* test, using GraphPad Prism (GraphPad software, San Diego, CA, USA). Statistical significance was set at $p<0.05$ in all the statistical analyses.

4.3. PEA limits HFD-induced depression

4.3.1. Animals and treatments

Standard chow diet had 17% fat, without sucrose while high fat diet (HFD), a diet that induces obesity (DIO, Harlan Teklad) had 45% of energy derived from fat, 7% of sucrose. Standard and HFD contained 3.3 kcal/g and 5.24 kcal/g, respectively. Ultra-micronized PEA was provided by Epitech Group Research Labs and it was suspended in carboxymethyl cellulose (1.5%) for oral administration.

Male C57BL/6J mice (Harlan, Italy) at 6 weeks of ages, were housed in stainless steel cages in a room kept at 22±1˚C with a 12:12 hours lights-dark cycle. After weaning, young mice were randomly divided into three groups (at least 10 animals for each group) as follows: control group (STD) receiving chow diet and vehicle per os by gavage; HFD group receiving vehicle; HFD group treated with PEA (HFD+PEA, 30 mg/kg/die per os). The treatments started after 12 weeks of feeding with HFD and continued for 7 weeks. The experimental protocol is outlined in Fig. **4.3.1**. All procedures involving the animals were carried out in accordance with the Institutional Guidelines and complied with the Italian D.L. no.116 of January 27, 1992 of Ministero della Salute and associated guidelines in the

European Communities Council Directive of November 24, 1986 (86/609/ECC). All animal procedures reported herein were approved by the Institutional Animal Care and Use Committee (CSV) of University of Naples Federico II under protocol no. 2011–0129170.

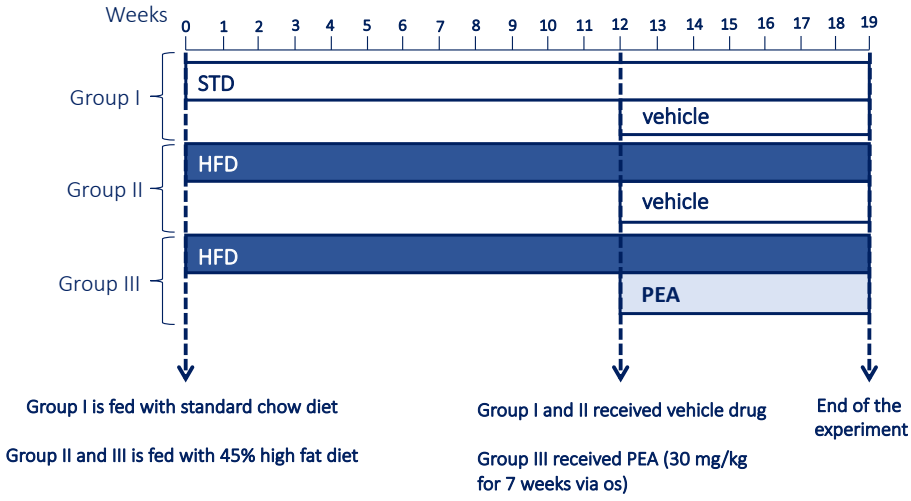

Figure 4.3.1. Experimental protocol HFD and PEA.

4.3.2. Body weight and body gain in fat

During the experimental period, body weight of mice was assessed one time for week. At the end of the experimental protocol, before sacrifice, bioelectrical impedance analysis was applied to determine fat body composition assessment using BIA 101 analyzer, modified for the mouse (Akern, Florence, Italy). Fat free mass was calculated using bioelectrical

impedance analysis and fat mass content was determined as the difference between body weight and fat-free mass.

4.3.3. Open field locomotion test

After 6 weeks of PEA treatment, STD, HFD and HFD+PEA mice were undergone to OFT, as previously reported in BTBR+PEA experiment. After OFT, the same animals were tested for forced swimming, tail suspension and novel object recognition tests.

4.3.4. Forced swimming (FST) and Tail suspension tests (TST)

The forced swimming and tail suspension tests represent the most used procedures which seek the evaluation of depressive-like behaviors in rodents, because immobility induced by exposure to an inescapable aversive situation (forced swimming or tail suspension) denotes an index of resignation (189).

The method of the FST was developed previously (209) and was subsequently modified (210-213). Briefly, mice were placed in a polymethylpentene cylinder (diameter 137 mm; height 200 mm) filled with 25 °C water to a depth of approximately 150 mm for 15 min as a pre-test

(pre-FST). After 24 h, mice were forced to swim again for 10 minutes and were recorded the entire time using a video camera. Immobility time was measured for the last 8 minutes of the swim period by observers in blinded manner. Immobility was defined as when mice stopped swimming and floated on the water.

For TST, we followed an established protocol (214, 215). Briefly, mice were acclimated to the behavior room for 1 h and then suspended by their tails to the edge of a shelf 55 cm above the floor. Adhesive tape (17 cm long) attached the tail (approximately 1 cm from the tip of the tail) to the shelf. The movements of mice were recorded by a camera for 7 minutes, even if immobility time was measured for the last 6 minutes. Mice were considered static when they hung passively and completely motionless.

4.3.5. Novel object recognition test (NORT)

NORT is a behavioral test which allow to evaluate a memory recognition deficit induced by an acute restraint stress (216). The test was done with habituation, familiarization and novel object recognition phases as described previously with some modifications (217). Mice were habituated for 10 minutes a day before the test plexiglass box (40 × 25 × 18 cm). During the familiarization phase, two identical objects were placed in the opposite

corners of the test box and the subject mice were allowed to explore for 10 min. At the end of this time, mice were kept back to their home cages. After 24 h, mice were placed in test box and kept undisturbed to explore a novel object for 5 minutes. During the recognition phase, one of the familiar objects were replaced with a new object different in shape and color. The tests were automatically detected by a video camera coupled with a video-tracking software (Any-maze, Stoelting). Object exploration was defined when the mouse was sniffing in close proximity to the object but not when the head was in another direction. After each trial, the arena floor and the objects were wiped with 70% ethanol to eliminate odour cues for the next subject.

4.3.6. Serum Parameters

STD and HFD mice, treated or not with PEA for 7 weeks, were sacrificed after overnight fasting. Blood collected by cardiac puncture was centrifuged at 2500 rpm at 4˚C for 12 minutes, and sera were stored at -80˚C for later biochemical and hormonal determinations. Alanine amino transferase (ALT), triglycerides (TG) were measured by colorimetric enzymatic method using commercial kits (SGM Italia, Italy and Randox Laboratories ltd., United Kingdom). Serum IL-1, (Thermo Scientific, Rockford, IL, USA),

TNF-α, and monocyte chemoattractant protein-1 (MCP-1) (Biovendor R&D, Brno, Czech Republic), adiponectin and leptin (B-Bridge International Mountain View, CA) and fasting insulin (cat. no. EZRMI-13K; Millipore) concentrations were measured using commercially available ELISA kits.

4.3.7. C-fos and Iba-1 staining

After overnight fasting, mice were anesthetized and transcardially perfused with 0.9% saline with heparin followed by fixative (4% paraformaldehyde, 15% picric acid, 0.1% glutaraldehyde in PBS). Brains were collected, post fixed overnight, and coronal sections were taken at every 50 µm. For c-fos staining, slides were washed and incubated with the rabbit anti-cfos antibody (Santacruz, 1:2000), and the chicken anti-GFP antibody (Life Technologies Corporation, 1:5000) in PB containing 4% normal goat serum, 0.1% glycine, and 0.2% Triton X-100 for 24 h at room temperature. For Iba-1 staining slides were washed and incubated with the mouse anti-Iba-1 antibody (Millipore, 1:1000) in PB containing 4% normal goat serum, 0.1% glycine, and 0.2% Triton X-100 for 24 h at room temperature. After several washes with PB, all sections were incubated in the secondary antibodies (for c-fos, biotinylated goat anti-rabbit, and for Iba-1, goat anti-mouse immunoglobulin

G [IgG]; 1:250 in PB; Vector Laboratories and goat antichicken Alexa-fluor 488; 1:200 in PB; Life Technologies) for 2 h at room temperature, then rinsed in PB five times, 10 min each time. Sections were then mounted with VectaShield antifade (Vector Laboratories). Fluorescent images of five to seven brain sections were captured with confocal microscope and analyzed by imaging Software (Image J), that can be downloaded from this link: https://imagej.nih.gov/ij/download.html.

4.3.8. Quantification of gene expression using RT-PCR

Total RNA was extracted using TRIzol Reagent (Bio-Rad Laboratories) and following a specific RNA extraction kit (NucleoSpin®, MACHEREY-NAGEL GmbH & Co, Düren, Germany), according to the manufacturer's instructions. cDna was synthesized using High-Capacity cDNA Reverse Transcription Kit (Applied Biosystems) from 2 µg total RNA. PCRs were performed with a Bio-Rad CFX96 Connect Real-time PCR System instrument and software (Bio-Rad Laboratories). The PCR conditions were 15 min at 95°C followed by 40 cycles of two-step PCR denaturation at 94°C for 15 s, annealing extension at 55°C for 30 s and extension at 72°C for 30 s. Each sample contained 500 ng cDNA in 2X QuantiTect SYBRGreen PCR Master Mix and primers pairs to amplify zonuline-1 (*Tjp1*), occludin (*Ocln*),

TNF-α (*Tnfa*), NF-kB (*Nfkb1*), interleukin-1β (*Il1b*), PPARα (*Ppara*), BDNF (Bdnf), Trkb (*Trkb*), (Qiagen, Hilden, Germany), in a final volume of 50 µl. The relative amount of each studied mRNA was normalized to GAPDH as housekeeping gene, and data were analyzed according to the $2^{-\Delta\Delta CT}$ method.

4.3.9. Western blotting

Hippocampus and prefrontal cortex from each mouse were homogenized and total protein lysates were subjected to SDS-PAGE. The blot was performed by transferring proteins from a slab gel to nitrocellulose membrane at 240 mA for 60 minutes at room temperature. The filter was then blocked with 1X PBS and 5% nonfat dried milk for 60 minutes at room temperature and probed with rabbit polyclonal antibody against anti-phospho-CREB and anti-CREB (dilution 1:1000; Cell Signaling Technology, Danvers, MA, USA), anti-BDNF (dilution 1:1000; Santa Cruz Biotechnology, Inc., Santa Cruz, CA), anti-PPARα (diluition 1:200, Santa Cruz Biotechnology, Inc., Santa Cruz, CA), anti-PGC1α and anti-FGF21 (1:1000, Elabscience, Bethesda, USA). Western blot for Actin (1:5000; Sigma-Aldrich, Milan, Italy) was performed to ensure equal sample loading.

4.3.10.16S metagenomic sequencing and data analysis

Fecal samples were collected from a subset of six mice randomly selected from each group and quickly stored at -80°C. Fecal microbiota was studied as reported above.

5. Results

5.1. Sex differences in gut microbiota of BTBR mice

5.1.1. Overall structure of gut microbiota of male and female BTBR mice.

We analyzed sex-related profiles of gut microbiota in BTBR mice to gain insights into relationship between autistic behavior and dysbiosis. To this purpose, fecal microbiota of fully symptomatic, 12 months old, female and male BTBR (fBTBR and mBTBR, respectively; n=6 mice each group) and female and male C57 control mice of same age (fC57 and mC57, respectively; n=6 mice each group) was analyzed by next generation sequencing (NGS) technology using the Illumina Miseq system. V3–V4 variable regions of the 16S rRNA gene were amplified and sequenced to characterize total bacterial population; 62,009.83 ± 33,665.39 high-quality sequences/sample were obtained from all 24 fecal samples, representing 3,250 operational taxonomic units (OTUs). The results shown were obtained considering a depth of 32,288 sequences/sample clustered in 2,740 OTUs; Good's coverage > of 99.3% for all sequences in the four groups indicated good sequencing depth for reliable investigation of differences in fecal

microbiota between BTBR and control mice. Among the 2,740 OTUs detected across any of the samples, 245 OTUs discriminated between fBTBR and fC57 mice, while 167 discriminated between mBTBR and mC57 mice. Discriminant OTUs were identified using two complementary analyses, LEfSe algorithm and Metastats comparison.

We evaluated ecological features of fecal bacterial communities in fBTBR and mBTBR compared to those of control groups. No significant differences in species richness (number of OTUs) and degree of homogeneity abundance of the species (Shannon index) were observed between groups (data not shown), while strong differences in phylogenetic assortment were detected comparing fBTBR and mBTBR with their respective controls (**Fig. 5.1.1**). Phylogenetic distances among samples were assessed by means of Unweighted Unifrac distance metrics, a qualitative phylogenetic measure that considers the presence/absence of a taxon. ANOSIM R statistic revealed a difference in gut bacterial assortment between BTBR of both sexes and their respective controls, with fBTBR vs fC57 displaying a higher R value compared to mBTBR vs mC57. This effect was evident in the PCoA plot, where fBTBR samples clustered to the extreme right of the plot, while mBTBR samples were positioned midway between fBTBR and control samples of both sexes (**Fig. 5.5.1A**, left plot).

Sequencing data revealed that 89.1% of total reads were taxonomically classified in Bacteroidetes and Firmicutes phyla, and the majority of discriminatory OTUs, both in females and males, were classified in these phyla. The impact of these taxa was evident when the Unweighted Unifrac analysis was repeated after negative filtering of these phyla from total sequences. After subtraction, ANOSIM analysis on remaining OTUs revealed a weaker grouping level among samples (**Fig. 5.1.1A**, right plot), indicating that Bacteroidetes and Firmicutes were the principal contributors to the BTBR and C57 gut microbiota differences both in female and male mice.

5.1.2. Gut microbiota profiling of BTBR female and male mice

Over the total of 9 identified bacterial phyla, comparison of mean abundances (by nonparametric Kruskal-Wallis test) of primary (Bacteroidetes, Firmicutes) and most of the less abundant phyla showed no significant differences between fBTBR and mBTBR compared to their respective controls (**Fig. 5.1.1B**). However, we found only a significant difference of Proteobacteria amount, with an increase in fBTBR rather than fC57 (relative abundance 13.2% ± 2.6% and 4.7% ± 1.2%, respectively), and for TM7 phylum which was found significantly less abundant in fBTBR than

fC57 (relative abundance of 0.1% ± 0.04% in fBTBR and 0.3% ± 0.05% in fC57). No significant differences were found for all phyla identified in mBTBR compared to mC57 (**Fig. 5.1.1B**).

5.1.3. Key phylotypes driving gut microbiota profiles of male and female BTBR mice

In order to identify gut microbiota key phylotypes responsible for differences between fBTBR and mBTBR compared to controls we applied LEfSe algorithm. 17/30 key genera were found within Bacteroidetes and Firmicutes phyla, mainly within Bacteroidales and Clostridiales orders, even though the comparison of the relative abundances of these phyla did not show significant differences (**Fig. 5.1.1B**). This result confirmed that Bacteroidetes and Firmicutes taxa reassortment mainly marks the differences in the gut microbiota between BTBR and C57 mice in both sexes accordingly to ANOSIM results on Unweighted Unifrac analysis (Fig. **5.1.1A**). Among key genera with relative abundance > 0.1%, *Bacteroides* and *Parabacteroides* (order Bacteroidales) were significantly more abundant in BTBR female and male compared to control mice (**Table 5.1.1**). Conversely, the genus *Dehalobacterium* (order Clostridiales) was significantly less abundant in BTBR mice of both sexes compared to

controls (**Table 5.1.1**). Notably, the identified differences in relative abundance of Bacteroides and Parabacteroides were more pronounced in fBTBR as indicated by fold change (**Table 5.1.1**). Among the other key genera, *Prevotella*, *Coprobacillus*, *Sutterella*, *Akkermansia* (*muciniphila*) and unclassified members of Desulfovibrionaceae and Enterobacteriaceae significantly increased, while *Oscillospira* and members of Rikenellaceae and TM7 (*AF12* and *U. F16*, respectively) significantly decreased in fBTBR, possibly driving a female-specific microbial signature in BTBR mice. Key genera specifically altered in mBTBR were *Lactobacillus*, *Ruminococcus*, *Desulfovibrio* and unclassified member of Helicobacteriaceae (**Table 5.1.1**). Genus *Oscillospira* accounted for 13.7% in fC57 and was found significantly reduced to 5.4% in fBTBR.

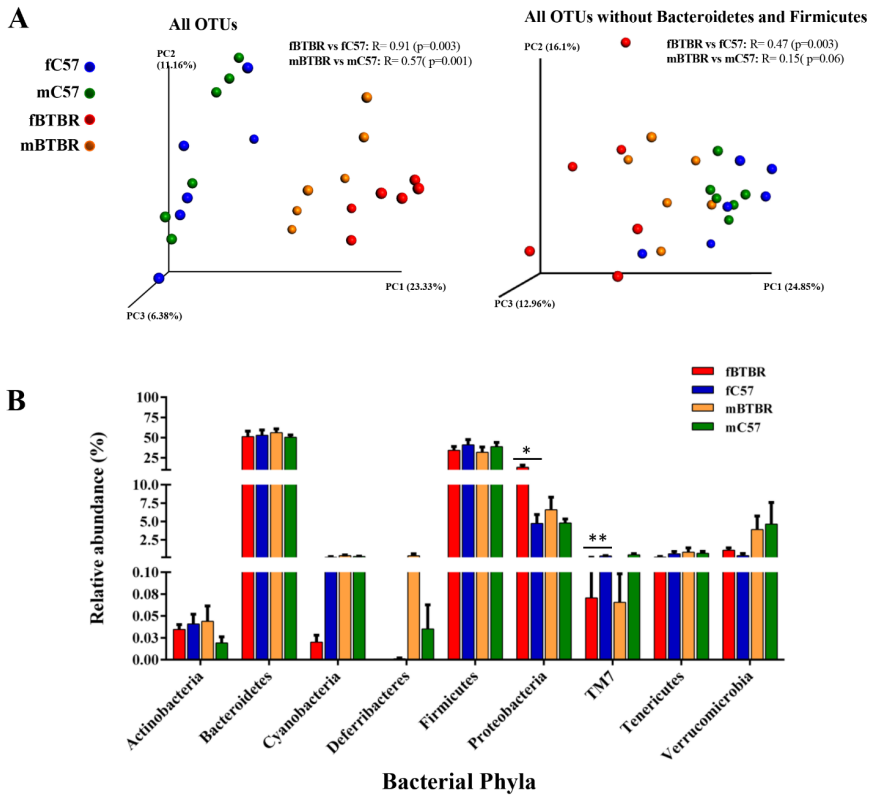

Figure 5.1.1. Female and male BTBR mice exhibit an altered gut microbial composition. (A) Unweighted UniFrac-based 3D PCoA plot constructed on all OTUs (32,288 reads per sample, left) or all OTUs without Bacteroidetes and Firmicutes reads (850 reads per sample, right) of fecal community of BTBR and C57 mice of both sexes. Analysis of similarity (ANOSIM) with 999 permutations was used to detect the statistical significant differences in microbial community composition between fBTBR and mBTBR compared to their controls (fC57 and mC57); on the top of plots are reported both R statistics and p values. **(B)** Relative abundance of all identified OTUs classified at phylum level. Mean values ± SEM are plotted (n=6/group). Significant differences are indicated by *p<0.05 and **p<0.01 for comparison of fBTBR vs. fC57 and mBTBR vs. mC57. Abbreviations: fBTBR (BTBR female mice); mBTBR (BTBR male mice); fC57 (C57 female mice); mC57 (C57 male mice).

	fBTBR	fC57	p-value; Fold Change	mBTBR	mC57	p-value; Fold Change
Prevotella	4.18 ± 1.70	1.50 ± 1.20	0.037; 2.8	1.95 ± 0.50	0.72 ± 0.39	p > 0.05
Bacteroides	9.85 ± 3.53	0.93 ± 0.45	0.006; 10.5	6.94 ± 2.47	0.80 ± 0.16	0.004; 8.7
Parabacteroides	6.40 ± 1.43	0.79 ± 0.30	0.004; 8.1	4.02 ± 0.84	1.08 ± 0.36	0.025; 3.7
AF12 (Rikenellaceae)	0.31 ± 0.07	0.76 ± 0.07	0.006; 0.4	0.57 ± 0.18	0.71 ± 0.11	p > 0.05
Lactobacillus	0.27 ± 0.08	0.11 ± 0.04	p > 0.05	3.48 ± 2.10	0.15 ± 0.04	0.016; 22.7
Dehalobacterium	0.06 ± 0.02	0.20 ± 0.04	0.025; 0.3	0.11 ± 0.04	0.27 ± 0.04	0.025; 0.4
Oscillospira	5.39 ± 0.68	13.71 ± 1.76	0.010; 0.4	7.16 ± 1.75	8.88 ± 0.74	p > 0.05
Ruminococcus	0.71 ± 0.17	1.11 ± 0.16	p > 0.05	0.68 ± 0.18	1.19 ± 0.16	0.037; 0.6
Coprobacillus	0.13 ± 0.07	0	0.003; 244	0.09 ± 0.03	0.01 ± 0.01	0.014; 9
Sutterella	4.51 ± 1.05	1.07 ± 0.48	0.016; 4.2	3.01 ± 0.87	1.71 ± 0.66	p > 0.05
U. Desulfovibrionaceae	2.78 ± 1.24	0.16 ± 0.12	0.010; 17.3	0.55 ± 0.22	0.63 ± 0.34	p > 0.05
Desulfovibrio	0.39 ± 0.11	1.15 ± 0.44	p > 0.05	0.11 ± 0.08	1.14 ± 0.34	0.006; 0.1
U. Helicobacteraceae	0.67 ± 0.57	0.05 ± 0.01	p > 0.05	0.13 ± 0.03	0.03 ± 0.01	0.025; 4.2
U. Enterobacteriaceae	3.38 ± 1.84	0.03 ± 0.01	0.004; 109	1.66 ± 1.11	0.13 ± 0.07	p > 0.05
U. F16 (TM7)	0.07 ± 0.04	0.29 ± 0.05	0.004; 0.2	0.07 ± 0.03	0.44 ± 0.17	p > 0.05
Akkermansia	1.08 ± 0.32	0.35 ± 0.27	0.016; 3.1	3.90 ± 1.85	4.62 ± 2.96	p > 0.05

Table 5.1.1. Relative abundance of key genera discriminating female and male BTBR from their sex-matched control mice. Key genera were identified applying the metagenomic biomarker discovery approach of LEfSe and only genera with an LDA significant threshold > 2 and relative abundance > 0.1% in at least one group of mice, are shown. Fold change was expressed as ratio between the value of mean relative abundance of each genus in fBTBR and mBTBR groups and the value found in the sex-matched controls. Data are shown as average and SEM (n = 6/group). Abbreviations: fBTBR (BTBR female mice); mBTBR (BTBR male mice); fC57 (C57 female mice); mC57 (C57 male mice).

5.1.4. Alteration in behavioral phenotype, intestinal integrity, and immunity in female and male BTBR mice: correlation with gut microbiota modifications

After a deep description of BTBR gut microbiota composition, the next step was to investigate the possible correlation between the levels of specific bacterial taxa and peculiar pathological traits dysregulated in ASD patients such as behavioral abnormalities, gut permeability and immune

abnormalities (131, 218). For all behavioral tests, both female and male BTBR mice showed deficits compared to controls, however a significant sex-related alteration was observed with fBTBR displaying higher self-grooming scores (**Fig. 5.1.2A–C**). Alteration of gut permeability, as evidenced by increased FITC-dextran translocation across the intestinal epithelium into blood, was observed both in female and male BTBR mice (**Fig. 5.1.3A**). Consistently, a significant reduction of transcription of occludin and zonuline-1 was detected in colon of mBTBR mice and a similar trend was observed in fBTBR (**Fig. 5.1.3B**). In addition, expression of a subset of cytokines (TNF-α, IL-6 and IL-10) and CD11c integrin were determined in colon tissue of male and female BTBR and C57 mice (**Fig. 5.1.3C**). Increased expression of TNF-α was observed in BTBR mice of both sexes. Significant increase of IL-6 and CD11c was observed in mBTBR compared to both sex-matched controls and fBTBR. Furthermore, histological evaluation of colon tissues showed tissue damage and evident inflammatory cells infiltration in both mBTBR and fBTBR (**Fig. 5.1.4**). Pearson correlation was applied to correlate the abundance of key genera, that discriminated fBTBR and mBTBR from sex-matched controls, with behavioral tests, colon mRNA expression of occludin, zonuline-1 and immune-markers (**Fig. 5.1.5**). In particular, increase of *Parabacteroides* and

Sutterella, together with decrease of *Dehalobacterium*, *Oscillospira* and unclassified member of TM7 were strongly associated to altered behavior and TNF-α expression in fBTBR. Unclassified members of Helicobacteriaceae associated to autistic phenotype and low IL-10 expression in mBTBR. Finally, in mBTBR mice lower levels of *Dehalobacterium*, *Ruminococcus* and *Desulfovibrio* were associated to increased gut permeability (**Fig. 5.1.5**).

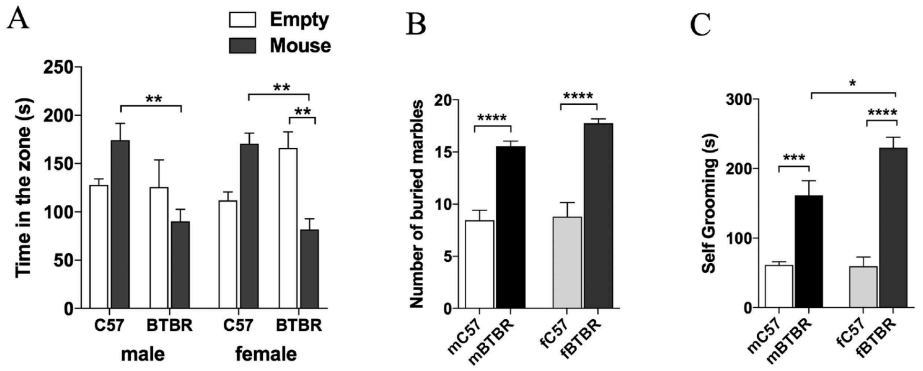

Figure 5.1.2. Analysis of social interaction, stereotyped and repetitive behavior in female and male BTBR mice. (A) Three-chamber social interaction test showing time spent in each chamber by BTBR and C57 mice of both sexes (n=12/group; p = 0.7424 for chamber, p=0.0077 for strain, p=0.7761 for sex, p<0.0001 for chamber x strain and p = 0.1671 for chamber x strain x sex, by three-way ANOVA). **(B)** Number of buried marble by BTBR and C57 mice of both sexes after 30 min testing session (n=12/group; p<0.0001 for strain, p=0.1322 for sex and p=0.2689 for strain x sex, by two-way ANOVA). **(C)** Seconds spent in repetitive grooming measured for BTBR and C57 mice of both sexes during 10 min test session (n=12/group; p<0.0001 for strain, p=0.0372 for sex, and p=0.0269 for strain x sex, by two-way ANOVA). Significant differences are indicated by *p<0.05, **p<0.01, ***p<0.001 and ****p<0.0001 using Bonferroni post-hoc tests following three-way ANOVA with chamber, strain and sex as factors **(A)** or two-way ANOVA with strain and sex as factors **(B and C)**. Abbreviations: fBTBR (BTBR female mice); mBTBR (BTBR male mice); fC57 (C57 female mice); mC57 (C57 male mice). Data are shown as mean values ± SEM.

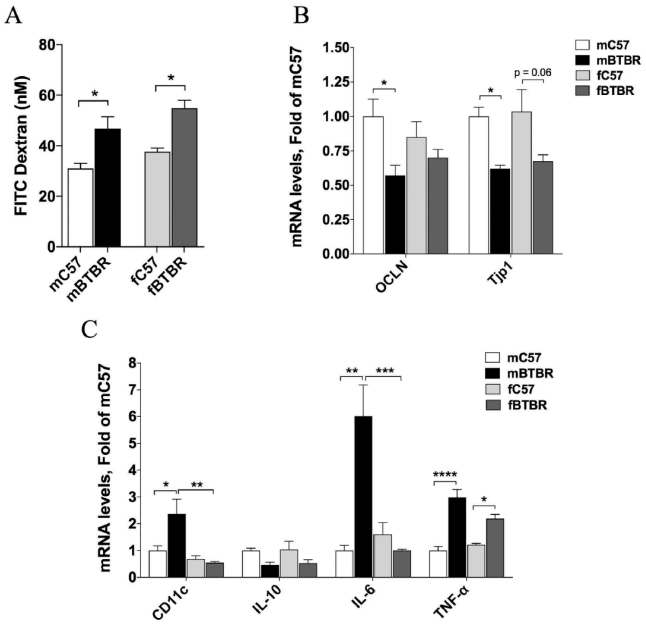

Figure 5.1.3. Analysis of intestinal integrity and inflammation levels in female and male BTBR mice. (A) Intestinal epithelial permeability to fluorescein isothiocyanate (FITC)-dextran 4 kDa of BTBR and C57 mice of both sexes. Data are represented as plasma concentration of FITC dextran (nM) (n=5/group; p=0.0002 for strain, p=0.0469 for sex and p=0.8187 for strain x sex, by two-way ANOVA). **(B)** Colon occludin (*Ocln*) and zonuline-1 (*Tjp1*), gene expression normalized to GAPDH gene in BTBR and C57 mice of both sexes. Data were normalized to mC57 control (n=6/group; *Ocln*: p=0.0067 for strain, p=0.9105 for sex and p=0.1623 for strain x sex; *Tjp1*: p=0.0004 for strain, p=0.6202 for sex and p=0.9105 for strain x sex, by two-way ANOVA). **(C)** Colon mRNA levels of inflammatory markers (CD11c, IL-10, IL-6 and TNF-α) normalized to GAPDH in BTBR and C57 mice of both sexes. Data for each gene were normalized to mC57 controls (n=6/group; CD11c: p=0.0529 for strain, p=0.0018 for sex and p=0.019 for strain x sex; IL-10: p=0.0041 for strain, p=0.7827 for sex and p=0.9739 for strain x sex; IL-6: p=0.0106 for strain, p=0.0107 for sex and p=0.002 for strain x sex; TNF-α: p<0.0001 for strain, p=0.2196 for sex and p=0.0354 for strain x sex, by two-way ANOVA). In bar charts, all data are expressed as mean values ± SEM; significant differences are indicated by *p<0.05, **p<0.01, ***p<0.001 and ****p<0.0001; near-significant differences are also reported (Bonferroni post-hoc tests following two-way ANOVA with strain and sex as factors). Abbreviations: fBTBR (BTBR female mice); mBTBR (BTBR male mice); fC57 (C57 female mice); mC57 (C57 male mice).

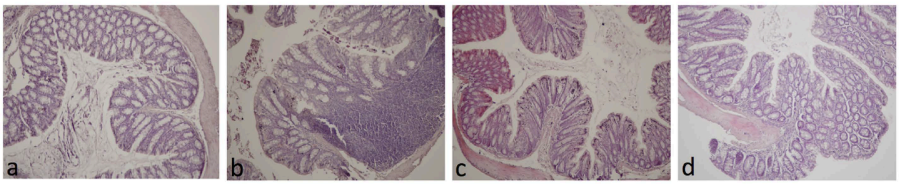

Figure 5.1.4. Histological evaluation of colon inflammatory cell infiltration in female and male BTBR mice. Representative hematoxylin and eosin–stained sections from colon tissues of mice. **(a)** Colon tissue from mC57 mice showing absence of inflammatory cells. **(b)** Colon tissue of mBTBR group showing leukocyte infiltration in the mucosa and submucosa. **(c)** Colon tissue of fC57 group, showing absence of inflammatory cells. **(d)** Colon tissue from fBTBR group showing moderate leukocyte infiltration in the mucosa. Original magnification 10x. Histological evaluation of inflammatory cells infiltration was scored along the entire colon length, inspecting the colon mucosa, submucosa and transmural areas considering the following parameters: leukocyte density (mC57 = 0.33 ± 0.58, mBTBR = 2 ± 1, fC57 = 0, fBTBR = 2.67 ± 0.58) and expansion of leukocyte infiltration (mC57 = 0.33 ± 0.58, mBTBR = 1.33 ± 0.58, fC57 = 0, fBTBR = 1.67 ± 0.58). The histologic scoring system is reported in Material and Methods section. Data reported as mean ± SD, n=3/group.

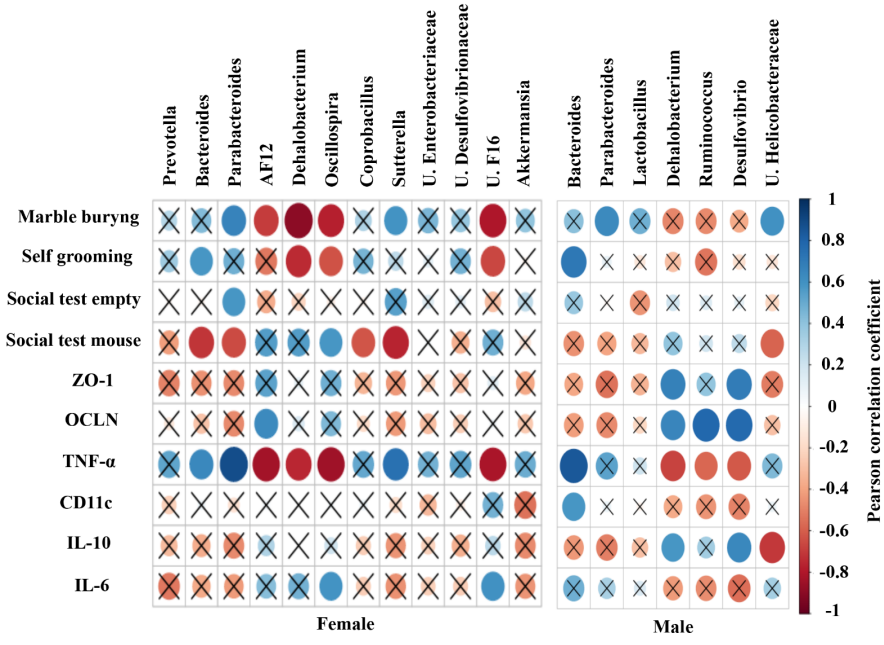

Figure 5.1.5. Correlogram showing the Pearson's correlation between key genera and behavioral scores, gut integrity and immune-markers in BTBR and C57 mice of both sexes. Blue circles designate a positive correlation while red ones designate a negative correlation. With X are barred no significant results according to the significance level of 0.05.

5.2. PEA counteracts autistic-like phenotype in BTBR mice

5.2.1. PEA reduced repetitive behaviour and increased sociability in BTBR mice

The number of buried marbles and the time spent in home cage self-grooming represent indexes of the repetitive/perseverative phenotype, typical of autistic-like behaviour. We observed that BTBR mice buried a greater number of marbles (**Fig. 5.2.1A**) and displayed higher self-grooming scores (**Fig. 5.2.1B**) compared to control mice. PEA at low dose (10 mg/kg) induced a slight improvement in the repetitive behaviour, whereas at the highest dose (30 mg/kg) this drug significantly decreased stereotyped behaviours in both marble buried (**Fig. 5.2.1A**) and self-grooming scores (**Fig. 5.2.1B**).

To assess PPAR-α involvement in PEA effect, BTBR mice were treated with the PPAR-α antagonist GW6471 before PEA administration. The highest dose of PEA failed in exerting its effect on both repetitive behaviours when it was associated to PPAR-α antagonist (**Fig. 5.2.1C-D**). GW alone had no effect on BTBR mice in both behavioural paradigms. Consistently, PEA treatment did not modify the autistic-like traits showed by PPAR-α null mice

in both behavioural tests (**Fig. 5.2.1E-F**), indicating the essential involvement of PPAR-α activation.

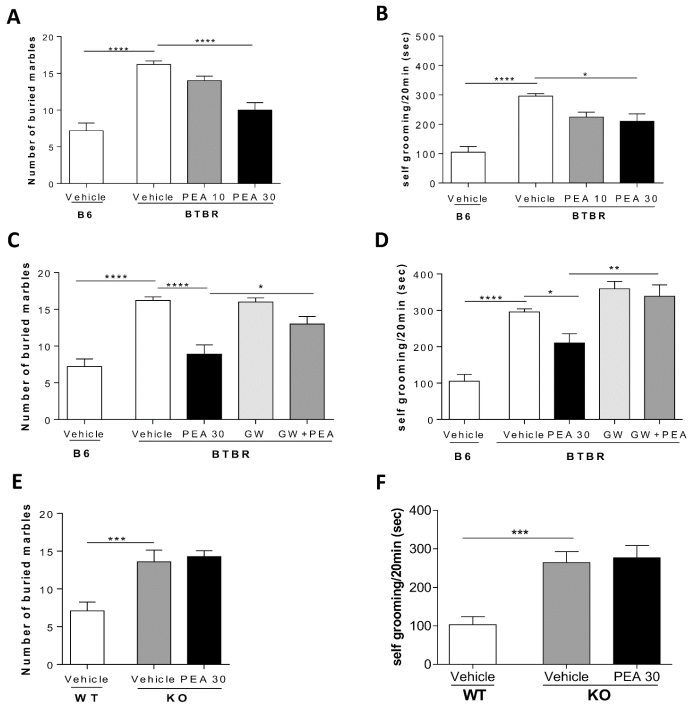

Figure 5.2.1. Effect of PEA on repetitive stereotyped autist-like behaviour of BTBR mice and involvement of PPAR-α. (A-B) Number of buried marbles and self-grooming time of control B6 and BTBR mice following i.p. daily administration of Vehicle, PEA (10–30 mg/kg) for 10 days (n=10 each group). **(C-D)** Number of buried marbles and self-grooming time of control B6 and BTBR mice following daily GW 6471 (GW, 1 mg/kg i.p.) treatment alone or 1 hr before PEA (30 mg/kg) for 10 days (n=10 each group). **(E-F)** Number of buried marbles and self-grooming time of WT (n=9) and PPAR-α null mice (KO) daily i.p. treated with Vehicle (n=10) or PEA 30 mg/kg (n=10) for 10 days. All data are presented as means ± S.E.M. *p<0.05; **p<0.01; ***p<0.001; ****p<0.0001.

The following step was to investigate the possible effect of PEA on social interaction of BTBR mice, using the three-chambered social test. BTBR mice failed to display significant sociability both on time in the zone (**Fig.**

5.2.2A) and on time in social sniffing (**Fig. 5.2.2B**) during the second phase of the automated three-chambered social approach task compared to control mice. PEA treatment improved sociability of BTBR mice: at the dose of 10 mg/kg, mice spent equal time in the zone and in sniffing the novel mouse and the novel object, while, at 30 mg/kg, they significantly spent more time in the mouse chamber and in sniffing the mouse compared to the object (**Fig. 5.2.2A-B**).

Then, PPAR-α involvement was assess in social behaviour of BTBR mice. Results showed that PEA failed to improve sociability both in time in the zone and in sniffing time of BTBR mice, when pre-treated with GW (**Fig. 5.2.2C**). These findings were confirmed by reduced sniffing for mouse in pre-treated mice with GW than PEA group (**Fig. 5.2.2D**). The treatment with GW alone had no effect on BTBR mice. PEA treated PPAR-α null mice showed equal time spent in the mouse zone and in sniffing time with the mouse and the object (**Fig. 5.2.2E-F**). Vehicle treated PPAR-α null mice showed a not significant preference for the object side (**Fig. 5.2.2E-F**).

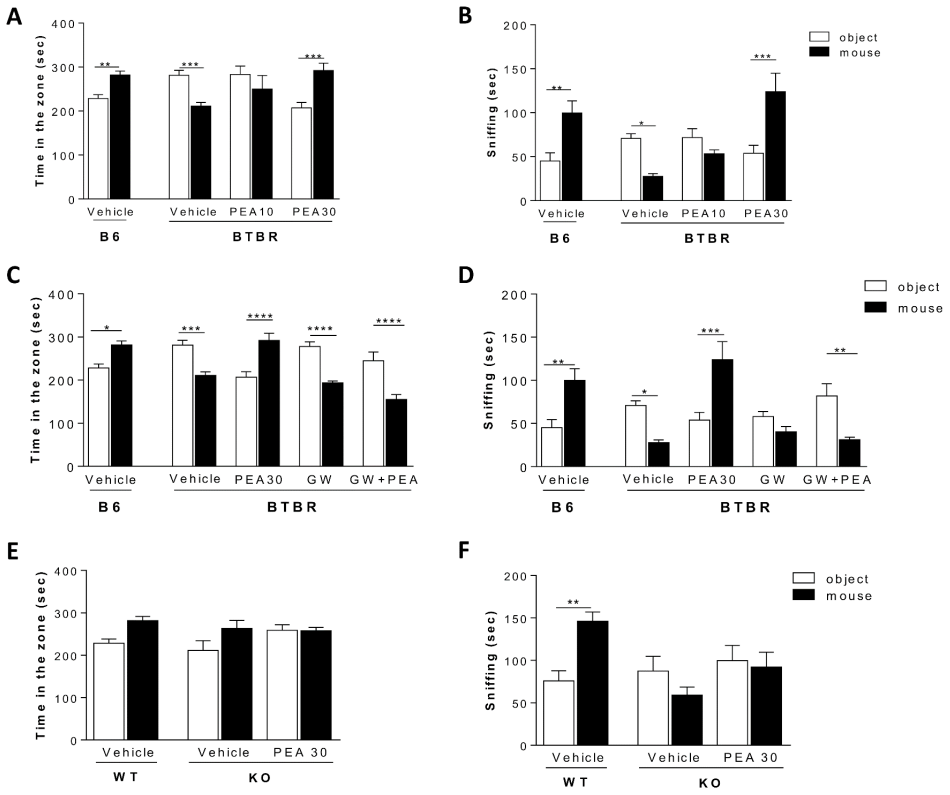

Figure 5.2.2. Effect of PEA on social behaviour of BTBR mice and involvement of PPAR-α. (A) Time in the zone **(B)** and sniffing time during the second social preference phase of 3-chambered social test of control B6 and BTBR mice following i.p. daily administration of Vehicle, PEA (10–30 mg/kg) for 10 days (n=10 each group). **(C)** Time in the zone **(D)** and sniffing time during the sociability phase of 3-chambered social test of control B6 and BTBR mice following daily GW 6471 (GW, 1 mg/kg i.p.) treatment alone or 1 hr before PEA (30 mg/kg) for 10 days (n=10 each group). **(E)** Time in the zone **(F)** and sniffing time during the sociability phase of 3-chambered social test of WT (n=9) and PPAR-α null mice (KO) daily i.p. treated with Vehicle (n=10) or PEA 30 mg/kg (n=10) for 10 days. All data are presented as means ± S.E.M. *p<0.05; **p<0.01; ***p<0.001; ****p<0.0001.

During the last phase of the test, we analysed the time spent in area and the time spent in sniffing familiar or new mouse (**Figure 5.2.3**). All BTBR and B6 groups spent more time in the chamber with the novel mouse than the

familiar mouse, as well as in sniffing time, indicating no behavioural impairment in this phase of the test in vehicle- or treated BTBR mice. Instead, vehicle- or PEA-treated PPAR-α null mice showed a significant preference for the familiar mouse.

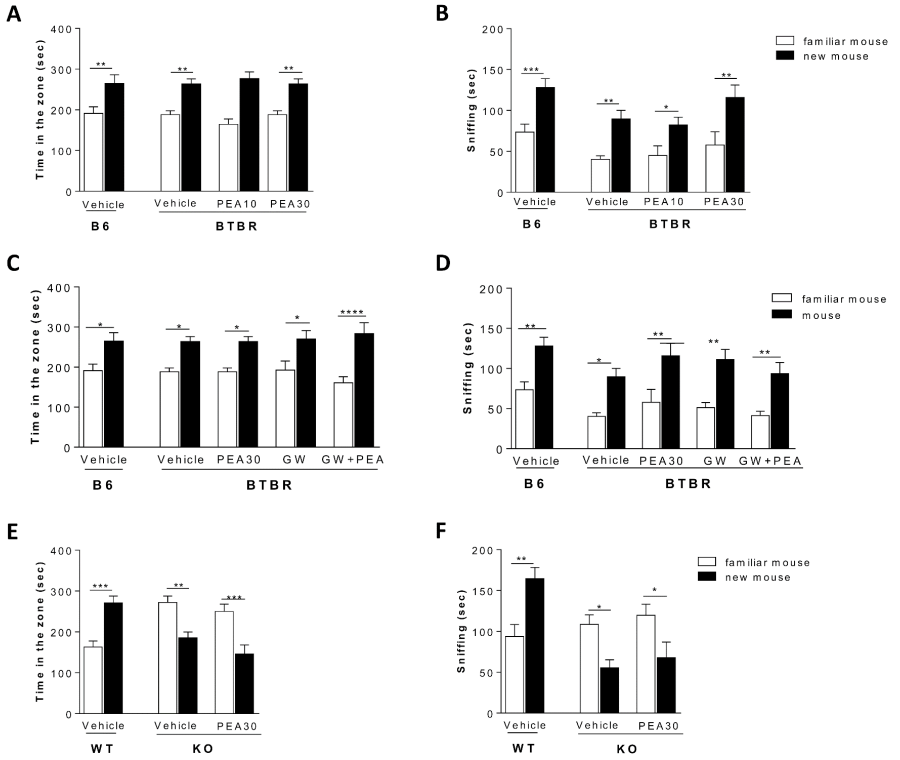

Figure 5.2.3. Effect of all treatments on social novelty behaviour in mice. Social novelty was measured as time spent with the new mouse versus the familiar mouse during the last phase of the 3-chambered social test. **(A, C)** All groups significantly prefer to spent time in the new mouse side compared to the familiar mouse side as well as sniffing time **(B, D)**. **(E)** KO mice spent more time in the zone with familiar mouse and in **(F)** sniffing the familiar mouse than the new mouse. Here, PEA at the dose of 30 mg/kg did not change mouse behaviour. Results are showed as mean ± S.E.M., n= 10 for each group; * $p<0.05$; ** $p<0.01$; *** $p<0.001$; **** $p<0.0001$.

A single PEA administration (30 mg/kg i.p.) in BTBR mice was also tested, revealing no effect after 1 hour on all behavioural tests (**Figure 5.2.4A-F**) demonstrating no early fast effect of PEA.

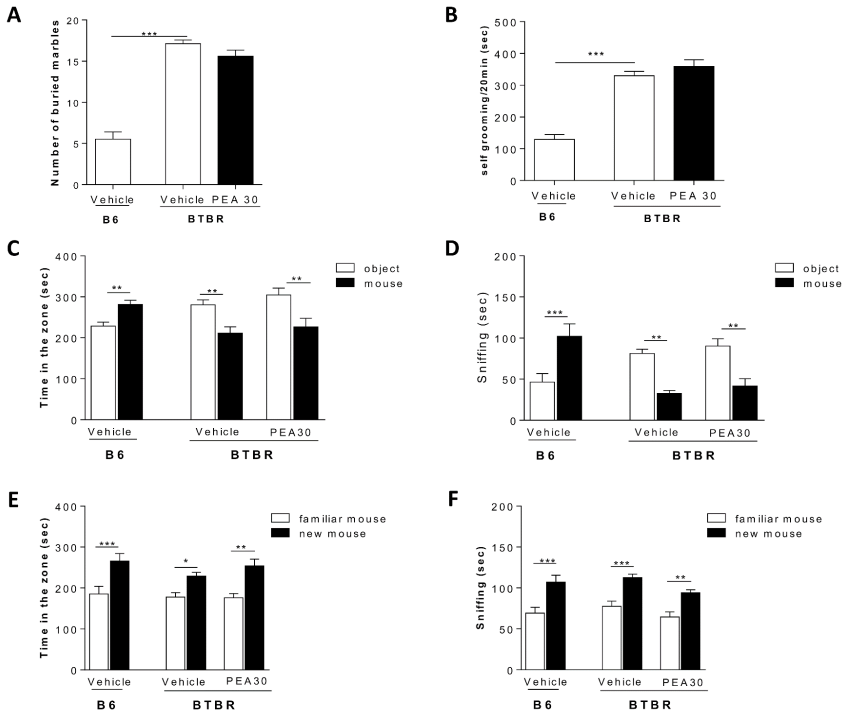

Figure 5.2.4. Effect of a single i.p. administration of PEA 30mg/kg in BTBR mice. (A) No significant difference in number of buried marbles and **(B)** self-grooming time was found between PEA 30 mg/kg and vehicle treated BTBR mice. **(C)** Time spent in the zone and **(D)** sniffing time between the chamber containing the mouse and the chamber containing the object showed no behavioural difference between PEA and vehicle treated BTBR mice; both groups significantly prefer to spend time in the object side compared to the mouse side. **(E)** Time spent in the zone and **(F)** sniffing time between the chamber containing the familiar mouse and the new mouse showed no behavioural difference between PEA and vehicle-treated BTBR mice. Here, both treated and untreated BTBR mice significantly prefer to spend time in the new mouse side compared to the familiar mouse side. Results are showed as mean ± S.E.M.; n=10 for each group. * $p<0.05$; ** $p<0.01$; *** $p<0.001$.

Moreover, all behavioural skills were not affected by PEA in control mice, indicating that this drug had no behavioural effects *per se* (**Figure 5.2.5A-C**).

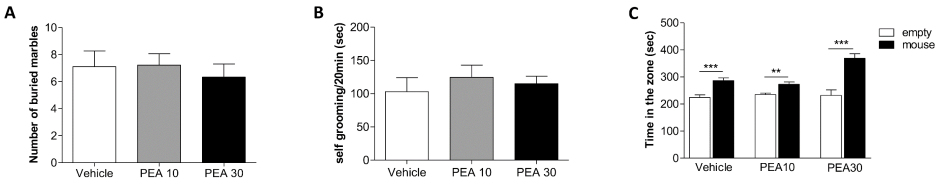

Figure 5.2.5. Effect of daily i.p. administration of PEA 10 mg/kg and 30 mg/kg for 10 days in B6 control mice. (A) No significant difference in number of buried marbles and **(B)** self-grooming time was found in control B6 mice treated with PEA or vehicle. **(C)** Social novelty was measured as time spent in the new mouse side versus the familiar mouse side during the last phase of 3-chambered social test. Here, both PEA-treated and vehicle-treated B6 mice significantly prefer to spend time in the new mouse side compared to the familiar mouse side. Results are showed as mean ± S.E.M.; n=9 for each group. **p<0.01; ***p<0.001; ****p<0.0001.

In order to exclude the induction of anxiety and/or locomotor deficits by treatments, we tested all mice in open field and EPM test, revealing no difference due to treatments, but only an overall difference between strains (**Figure 5.2.6A-H**).

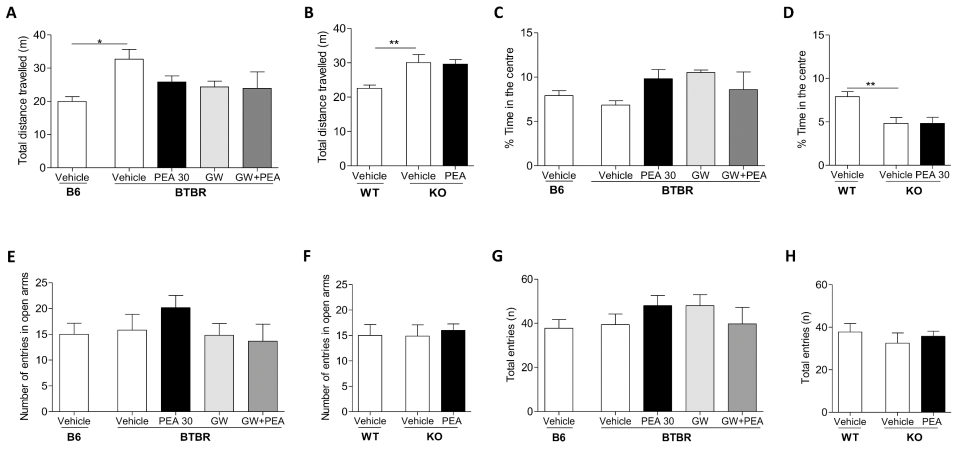

Figure 5.2.6. Effect of all treatments on locomotor activity and anxiety behaviour. BTBR and PPAR-α KO mice treated with PEA (30 m/kg), GW6471 (1 mg/kg) alone or in combination with PEA, compared to vehicle treated control B6 mice, were subject to **(A-D)** open field and **(E-H)** elevated plus maze test. **(A, B)** Both BTBR and vehicle PPAR-α KO mice exhibit an increased locomotor activity compared to B6 mice, during 10 minutes of freely movement in the open field test. **(C)** BTBR mice spent the same percentage of time in the centre of the arena compared to B6 mice. **(D)** PPAR-α KO mice significantly spent less percentage of time in the centre of the arena compared to control mice. No significant differences were found in the number of entries in open arms of **(E, F)** BTBR mice and PPAR-α KO mice compared to B6 mice and in the number of total arms entries **(G, H)** of BTBR and PPAR-α KO mice compared to B6 mice during the EPM test. No significant effect of all drug treatments was detected on both tests. Results are shown as mean ± S.E.M. *p<0.05; **p<0.01.

5.2.2. PEA improves BDNF/TrkB system, increasing hippocampal PPAR-α expression

As well known by literature, ASD is characterized by an impairment of BDNF/TrkB system signalling and its downstream CREB activation (219). Here, BTBR mice showed lower level of hippocampal BDNF and a partial reduction of TrkB in both mRNA and protein expression than B6 control

mice (**Fig. 5.2.7A-D**). PEA treatment (30 mg/kg) restored both BDNF (**Fig. 5.2.7A-B**) and TrkB expression (**Fig. 5.2.7C-D**) in BTBR mice. Furthermore, although CREB mRNA level did not significant change by PEA treatment (30 mg/kg) (**Fig. 5.2.7E**) in BTBR mice, the phosphorylation of protein CREB was significantly increased by PEA administration (**Fig. 5.2.7F**).

To strengthen PPAR-α role in autism, we subsequently evaluated PPAR-α expression in the hippocampus. BTBR mice displayed a significant reduction in PPAR-α mRNA and protein expression, that were significantly reconstituted by PEA treatment (30 mg/kg) at both mRNA and protein level (**Fig. 5.2.7G-H**).

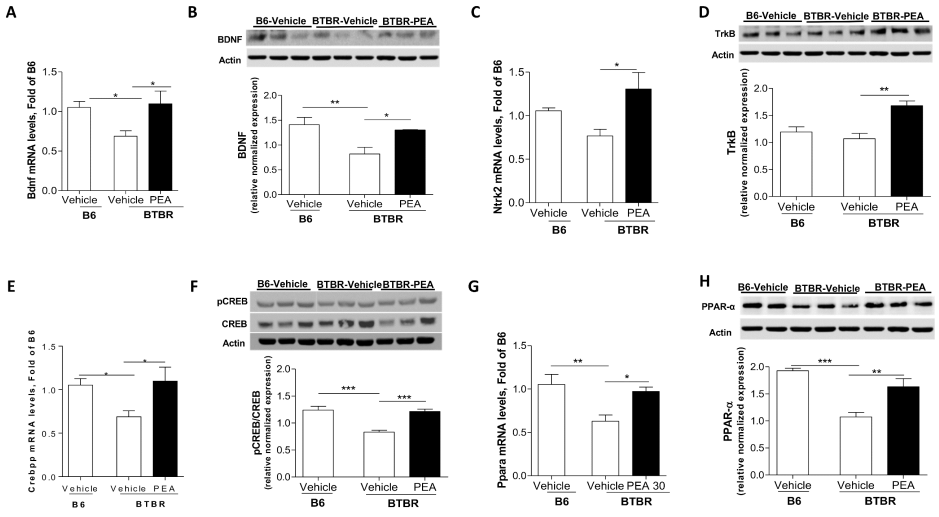

Figure 5.2.7. PEA effect on hippocampal gene transcription and protein expression. RT-PCR detection of **(A)** BDNF, **(C)** TrkB, **(E)** CREB, and **(G)** PPARα and western blot analysis of **(B)** BDNF, **(D)** TrkB, **(F)** p-CREB and CREB, and **(H)** PPARα in the hippocampus were performed from B6 and BTBR mice treated with vehicle or PEA 30 mg/kg (n=7–11 per group) for 10 days. Representative immunoblots from 2–3 animals each group following the above treatments are shown. Signals from each animal were quantified and peptide expression was shown as a ratio of housekeeping gene β-Actin (Actin) and with total CREB. Results are expressed as mean ± S.E.M. *p<0.05; **p<0.01; ***p<0.001; ****p<0.001.

5.2.3. PEA treatment improves hippocampal mitochondrial function and reduces oxidative stress

Mitochondrial state 3 respiration using succinate as substrate was decreased in BTBR mice compared with B6. Repeated treatments of PEA restored mitochondrial respiration (**Fig. 5.2.8A left side**), whereas no variation was observed in mitochondrial state 4 respiration (**Fig. 5.2.8A right side**). No variation was found in oligomycin state 4 respiration (**Fig. 5.2.8B left side**), while a significant decrease was found in maximal FCCP-stimulated respiration in PEA treated mice compared BTBR mice (**Fig. 5.2.8B right side**). As a consequence, hippocampal mitochondrial energetic efficiency (q), assessed as degree of coupling, was significantly lower in PEA treated mice compared to BTBR mice (**Fig. 5.2.8C**).

ROS production was significantly increased in hippocampus from BTBR mice and blunted by PEA treatment (**Fig. 5.2.8D**); consistently, BTBR mice

showed a significant lower SOD activity, which was restored by PEA (**Fig. 5.2.8E**).

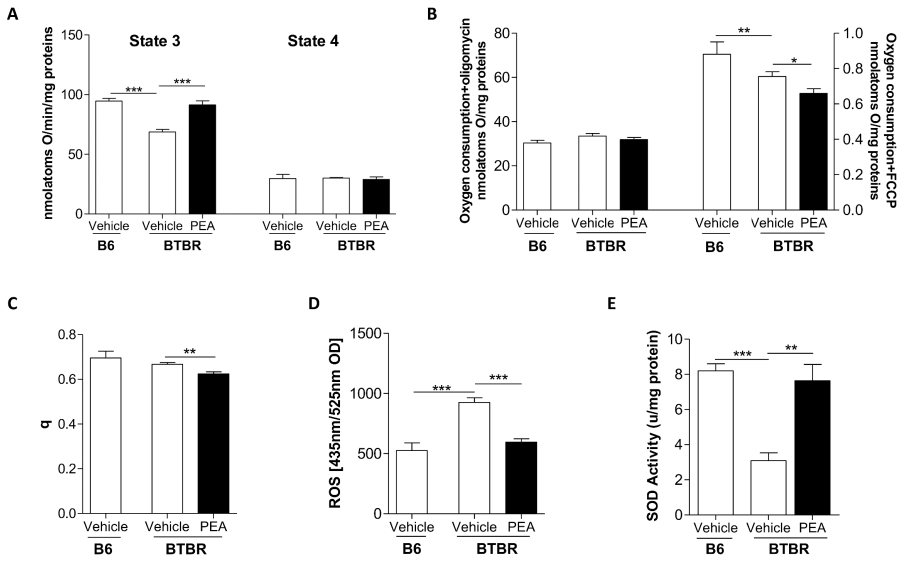

Figure 5.2.8. Effect of PEA on mitochondrial and oxidative stress. (A) Mitochondrial respiration in the presence of succinate as substrate, **(B)** oxygen consumption in the presence of oligomycin **(left side)**, or FCCP **(right side)** and **(C)** degree of coupling values calculated from oxygen consumption in the presence of oligomycin and FCCP in the hippocampus from B6 and BTBR mice following daily i.p. administration of vehicle or PEA 30 mg/kg for 10 days (n=12 per group). **(D)** ROS production in the hippocampus from mice of all groups (n=12 per group). **(E)** SOD activity in the hippocampus (n=5) All data are presented as mean ± S.E.M. *p<0.05; **p<0.01; ***p<0.001.

5.2.4. PEA reduces central, systemic and intestinal inflammation

Neuroinflammation represents one of the crucial basis of ASD pathogenesis and progression. Indeed, pro-inflammatory cytokines are correlated with

impaired sociability and aberrant behaviour linked to ASD in both humans and mice (220, 221). BTBR mice showed increased level of TNF-α, IL-1β, and IL-6 in the hippocampus compared to B6 mice and PEA was able to reduce them (**Fig. 5.2.9A-C**). Similarly, we demonstrated the same cytokine profile at serum and colonic level (**Fig. 5.2.9D-I**). These results revealed both peripheral and central effects of PEA in autistic mice, opening a new scenario on the mechanism of action of PEA.

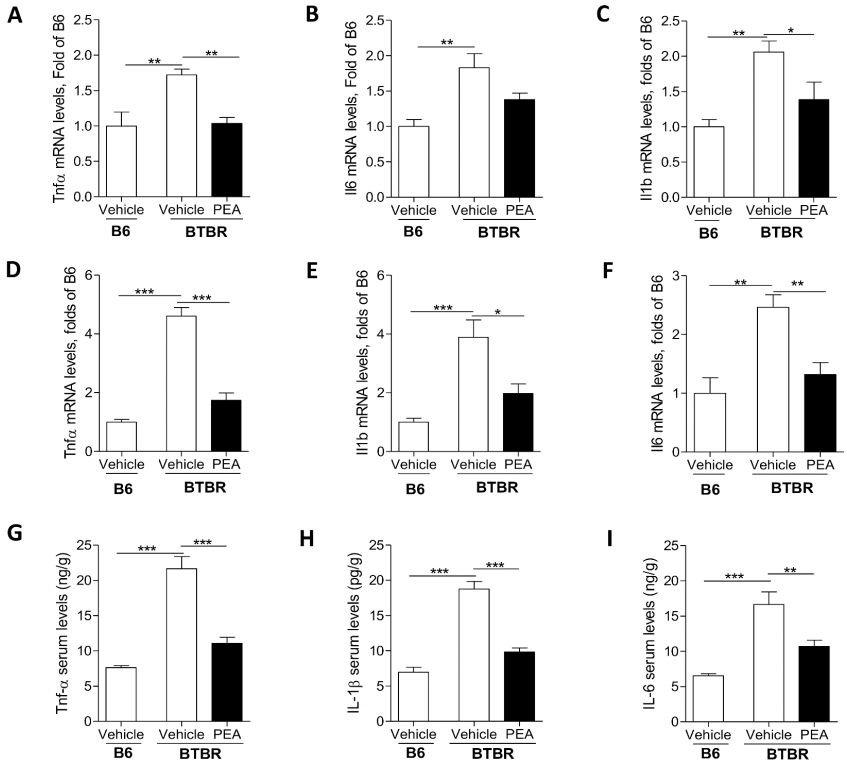

Figure 5.2.9. PEA modulation of central and peripheral inflammatory cytokines. Changes in TNF-α, IL-1β, and IL-6 mRNA levels in **(A-C)** hippocampus, **(D-F)** colon, and **(G-I)** serum of B6 or BTBR mice following daily i.p. administration of vehicle or PEA 30

mg/kg for 10 days (n=6 per group). Results are shown as mean ± S.E.M. *p<0.05; **p<0.01; ***p<0.001.

5.2.5. PEA effects on gut permeability and microbiota

BTBR mice are characterized by a compromised epithelial barrier integrity: a significant increase in gut permeability was shown in vivo in BTBR mice evaluating the plasmatic levels of FITC-labelled dextran 24 h after its oral administration (**Fig. 5.2.10A**). Molecular analysis showed PEA-induced improvement of epithelial barrier integrity of BTBR mice, increasing of *Tjp1* and *Ocln* mRNA transcripts in colonic tissues found significantly reduced in BTBR mice compared to B6 control mice (**Fig. 5.2.10 B-C**).

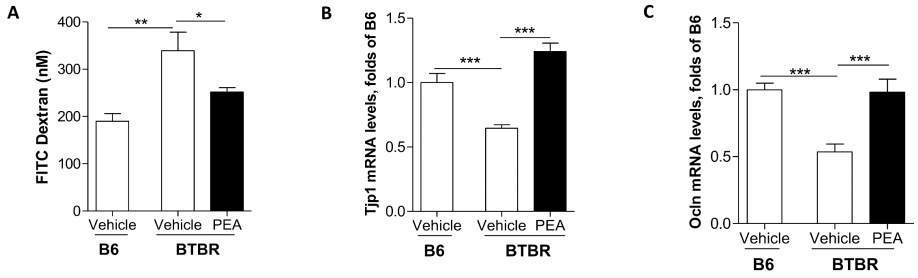

Figure 5.2.10. PEA effect on intestinal permeability. (A) *In vivo* permeability was detected by plasmatic levels of FITC-labelled dextran from B6 or BTBR mice following daily i.p. administration of vehicle or PEA 30 mg/kg for 10 days (n=6 per group). Changes in mRNA expression of zonuline-1 **(B)** and occludin **(C)** in colon tissue from B6 or BTBR mice following daily i.p. administration of vehicle or PEA 30 mg/kg for 10 days (n=6 per group).

Faecal microbiota composition was analysed by next-generation sequencing method to evaluate the effect of PEA administration on gut microbial communities of BTBR mice with respect to similar ages of cases of untreated BTBR and B6 control mice. Alpha diversity analyses did not show significant alteration in bacterial species richness and diversity within groups. On the contrary, measuring phylogenetic distances by beta diversity analyses, we found significant differences in microbial species assortment (unweighted beta diversity) among groups (see **Table 5.2.1**). Interestingly, R statistic ANOSIM, computed on phylogenetic distances among samples, revealed that upon PEA treatment the overall microbial community of BTBR mice was restructured and resulted significantly different from that of untreated BTBR mice (**Table 5.2.1**).

Alpha diversity			
	C57	**BTBR**	**BTBR PEA**
Observed species	430.9 ± 51.1	425.3 ± 46.7	505.25 ± 38.5
Shannon	6.2 ± 0.3	6.1 ± 0.4	6.4 ± 0.05
Good's coverage	0.987 ± 0.001	0.986 ± 0.001	0.984 ± 0.001

Beta diversity			
	C57 vs BTBR	**BTBR vs BTBR PEA**	**C57 vs BTBR PEA**
Unweighted UniFrac distances	R= 0.937 ($p < 0.01$)	R= 0.0522 ($p < 0.01$)	R= 0.917 ($p < 0.01$)
Weighted UniFrac distances	R= 0.293 ($p < 0.05$)	R= 0.0513 ($p = 0.01$)	R= 0.398 ($p < 0.01$)

Table 5.2.1. Significant differences in microbial species assortment among groups. Alpha diversity indexes reported as mean ± SD (Upper panel). R statistics and *p*-values of analysis of similarity (ANOSIM) with 999 permutations computed on unweighted and weighted UniFrac distances between groups (Lower panel).

PEA treatment strongly impacted on levels of definite identified phyla. Among the 9 phyla detected, Bacteroidetes and Firmicutes were the most abundant and primarily affected by PEA treatment (**Fig. 5.2.11A**); Firmicutes/Bacteroidetes ratio was considerably higher in BTBR mice treated with PEA due to significant increase in Firmicutes and decrease in Bacteroidetes (**Fig. 5.2.11A**). At genus level, the increase of Firmicutes/Bacteroidetes ratio upon PEA administration was mainly a

consequence of diminution of *Bacteroides*, *U. g. of Rikenellaceae*, *U.g. of S24-7* (phylum Bacteroidetes) and increase of *U.g. of Clostridiales* (phylum Firmicutes) (**Fig. 5.2.11B**). Thus, PEA treatment establishes a new microbiota profile, marking differences with microbiota composition found in untreated BTBR mice and recovering similarities for some aspects with microbial assortment of B6 control mice.

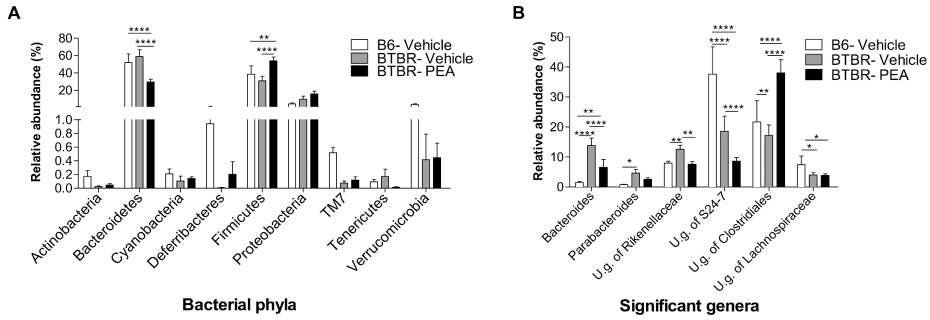

Figure 5.2.11. PEA effect on faecal microbiota composition. (A) Phylum level composition of fecal microbiota from B6 and BTBR mice following daily i.p. administration of vehicle or PEA 30 mg/kg for 10 days (n=6 per group). **(B)** Bacterial genera belonging to Bacteroidetes and Firmicutes phyla found to be significantly different among groups (n=6 per group). Results are showed as mean ± S.E.M. *p<0.05; **p<0.01; ***p<0.001 ****p<0.0001.

5.3. PEA limits HFD-induced depression

5.3.1. PEA lessens depressive-like behaviour and memory deficit

In forced swimming test (**Fig. 5.3.1A**) and tail suspension test (**Fig. 5.3.1B**), HFD caused a significant increase in immobility time, related to depressive-like behaviour of mice. After 7 weeks of treatment, PEA induced an increase in HFD mice responsiveness and effort to escape than untreated HFD group. Furthermore, during the novel object recognition test, we have evaluated the time (**Fig. 5.3.1C**) and the number of entries (**Fig. 5.3.1D**) of mice in the areas, in which the new and the old object were placed. While HFD induced an impairment in the recognition of old object, PEA was able to restore the curiosity of mice. The open field test highlighted that PEA partially stimulated the movement of HFD mice, reduced by HFD intake (**Fig. 5.3.1E-H**).

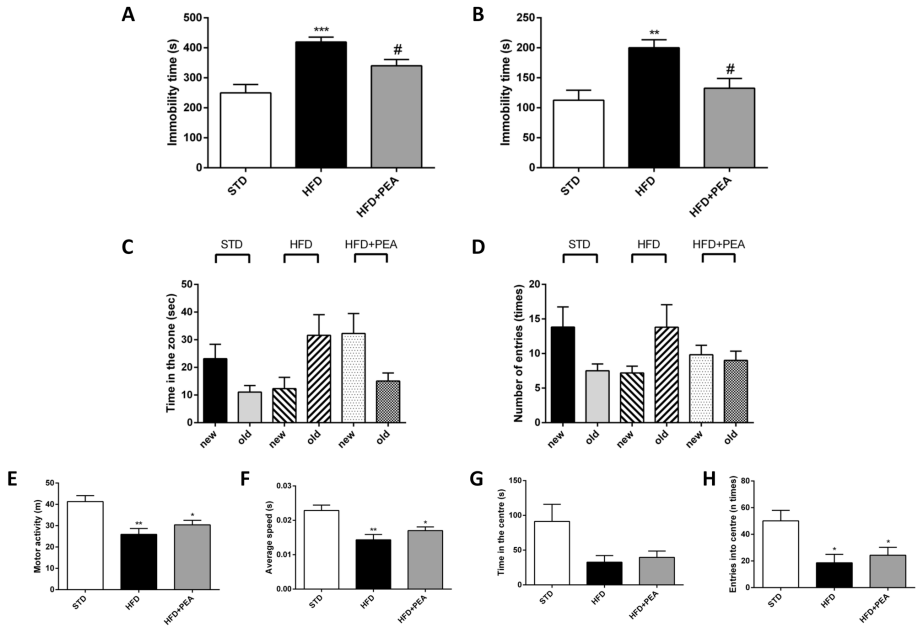

Figure 5.3.1. PEA effects on depressive-like behavior, memory recognition and locomotor activity. STD, HFD and PEA-treated HFD mice (n=10 each group) were subjected to forced swimming test **(A)**, tail suspension test **(B)**, novel object recognition test **(C-D)** and open field test **(E-H)**. **(A-B)** HFD group mice showed an increased immobility time in both tests for depressive-like behaviour that was significantly improved by PEA treatment. During NORT, PEA stimulated the curiosity on new object similar to that of STD group, both in the **(C)** time and the **(D)** number of entries. **(E-H)** The locomotor activity of HFD and HFD+PEA was reduced compared to STD group, even if the treatment with PEA induced a trend of improvement. Results are shown as mean ± S.E.M. *p<0.05, **p<0.01, ***p<0.001 vs STD and #p<0.05 vs HFD.

5.3.2. PEA improves serum metabolic and inflammatory parameters

After 19 weeks of HFD feeding, serum triglycerides and ALT (**Fig. 5.3.2A-B**) were altered compared to STD group and PEA significantly reduced these parameters. Similarly, the hormonal profile drastically compromised by high

fat feeding was improved by PEA, as shown by leptin and adiponectin serum levels (**Fig. 5.3.2C-D**). PEA carried out its anti-inflammatory activity reducing serum levels of inflammatory mediators (TNF-α, IL-1β and MCP-1) (**Fig. 5.3.2E-G**), elevated by HFD.

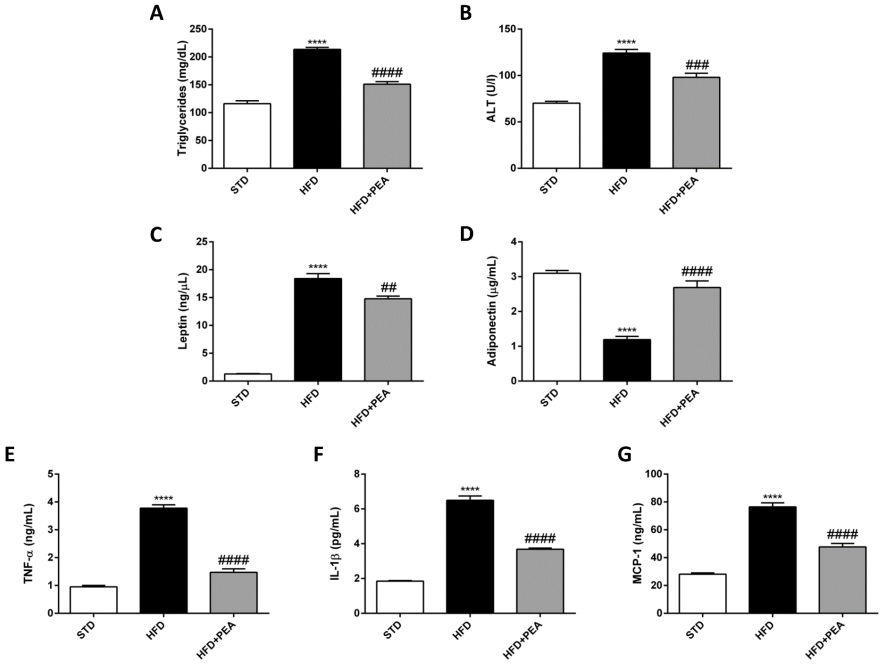

Figure 5.3.2. PEA restored serum metabolic parameters and decreased pro-inflammatory mediators. HFD feeding compromised serum metabolic profile, altering **(A)** triglycerides, **(B)** ALT, **(C)** leptin and **(D)** adiponectin levels. PEA was able to improve these parameters. In addition, this molecule decreased serum levels of pro-inflammatory mediators, such as **(E)** TNF-α, **(F)** IL-1β and **(G)** MCP-1, significantly increased in HFD mice. Results are shown as mean ± S.E.M from n = 6 animals/group. ****p<0.0001 vs STD; ##p<0.01, ###p<0.001 ####p<0.0001 vs HFD.

5.3.3. Activation of POMC neurons by PEA in ARC

To evaluate the activation of anorexigenic POMC neurons in ARC of hypothalamus, we performed the staining of c-fos in POMC in both all three experimental groups (**Fig. 5.3.3A**). As shown by **Fig. 5.3.3B**, the number of activated POMC neurons in HFD mice was significantly reduced compared to STD group and increased after PEA treatment. Furthermore, we also demonstrated PEA capability in increasing the transcription of BDNF in hypothalamus, altered by HFD (**Fig. 5.3.3C**).

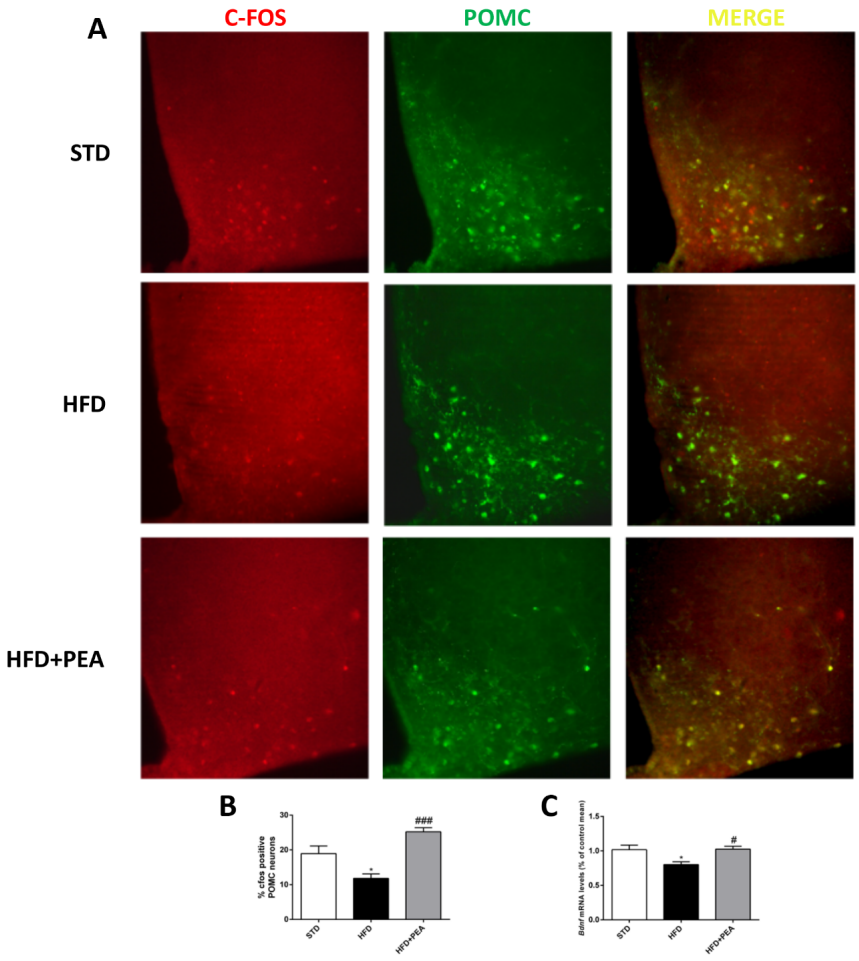

Figure 5.3.3. PEA stimulated POMC neurons in ARC and neurogenesis in hypothalamus. As shown by immunostaining of **(A)** c-fos in POMC neurons in ARC, PEA was able to increase **(B)** the number of activated POMC neurons, significantly diminished by HFD. Moreover, PEA also increased the transcription of **(C)** BDNF in hypothalamus. Results are showed as mean ± S.E.M from n=6 animals/group for immunostaining and n=10 animals/group for real time PCR. *p<0.05 vs STD; #p<0.05, ###p<0.001 vs HFD.

5.3.4. PEA reduces neuro-inflammation in hypothalamus

IBA-1, a protein generally expressed by microglia, resulted up-regulated during inflammation. Indeed, HFD caused an increase of IBA-1 cells in

ARC of hypothalamus and PEA was able to reduce this parameter, indicating PEA protective effect on microgliosis (**Fig. 5.3.4A-B**). Furthermore, this acylethanolamide also reduced NF-κB and IL-1β transcription in hypothalamus, altered by HFD (**Fig. 5.3.4C-D**).

These experiments were performed in the laboratory of Prof. Sabrina Diano at Yale University, Department of Obstetrics, Gynecology & Reproductive Sciences, located in New Haven (Connecticut, USA), from January 2017 to January 2018.

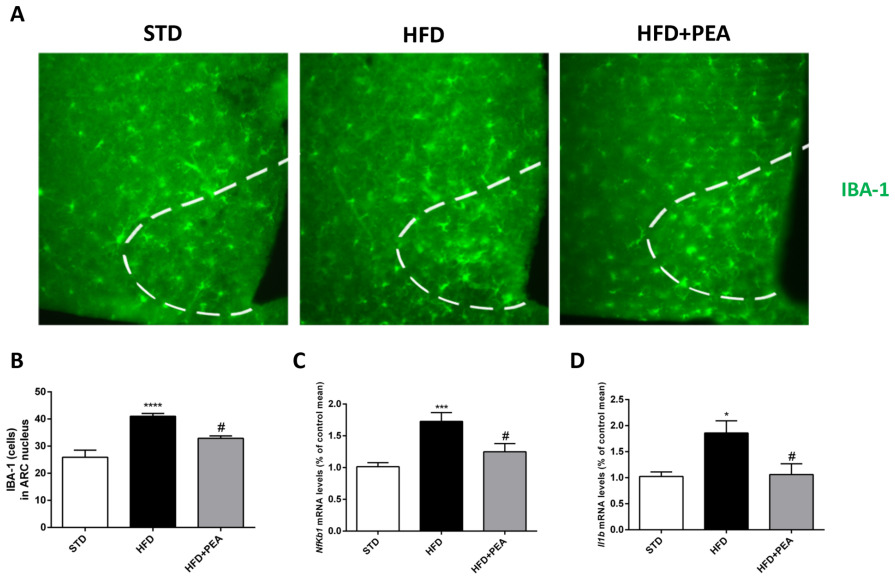

Figure 5.3.4. PEA reduces microgliosis and inflammation in hypothalamus. As shown by immunostaining of **(A)** IBA-1 in ARC of hypothalamus, PEA was able to decrease the number of activated microglia, markedly altered by HFD. Moreover, PEA reduced the transcription of pro-inflammatory mediators, such as (B) NF-kB and (C) IL-1β in hypothalamus. Results are shown as mean ± S.E.M from n=6 animals/group for immunostaining and n=10 animals/group for real time PCR. *p<0.05, ***p<0.001 and ****p<0.0001 vs STD; #p<0.05 vs HFD.

5.3.5. PEA improves BDNF/CREB system and reduces HFD-induced inflammation in hippocampus

The hippocampal dysfunction of BDNF/CREB system as pathogenic mechanism of MDD is well known (222). In our experimental condition, 19 week-HFD caused a significant reduction of the phosphorylation of CREB and protein expression of BDNF, improved by PEA treatment (**Fig. 5.3.5 A-B**). These data were confirmed by the improvement of PEA in mRNA levels of BDNF and TrkB (**Fig. 5.3.5C-D**). Furthermore, PEA carried out its anti-inflammatory activity reducing the mRNA levels of IL-1β and TNF-α, significantly increased by HFD (**Fig. 5.3.5 E-F**).

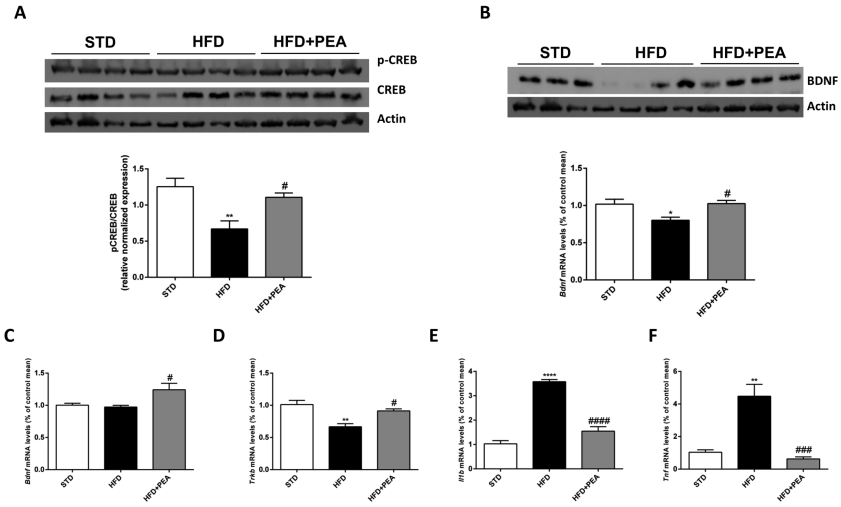

Figure 5.3.5. PEA restored BDNF/CREB pathway and reduced inflammation in hippocampus of HFD mice. In hippocampus of HFD mice there was a reduction of **(A)**

phosphorylated CREB and **(B)** BDNF expression. PEA was able to increase these parameters, as also demonstrated by mRNA levels of **(C)** BDNF and **(D)** TrkB. In addition, PEA reduced also inflammatory mediators, such as **(E)** IL-1β and **(F)** TNF-α, altered by HFD. Results are shown as mean ± S.E.M from n=10 animals/group. *p<0.05, **p<0.01 and ****p<0.0001 vs STD; #p<0.05, ###p<0.001 and ####p<0.0001 vs HFD.

5.3.6. PEA ameliorating effect on HFD-induced depression: possible involvement of PPAR-α

To explore the hypothesis that PEA activity was mediated by PPAR-α, we evaluated the hippocampal expression of PPAR-α, at mRNA and protein level, its coactivator PGC1α and the downstream factor FGF21 (**Fig.5.3.6**). PEA treatment was able to increase the expression of PPAR-α, PGC1α, and FGF21 in the hippocampus, indicating the involvement of PPAR-α and its downstream pathway in PEA mechanism of action.

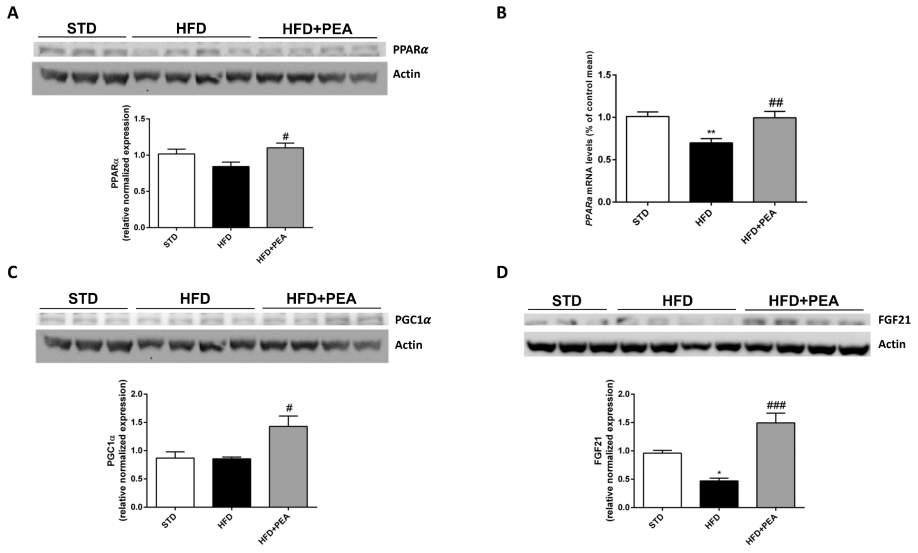

Figure 5.3.6. PPARα involvement in beneficial effects of PEA in HFD hippocampus. **(A)** protein expression and **(B)** mRNA level of PPARα, and the protein expression of **(C)** PGC1α and **(D)** FGF21 were analysed. Results are shown as mean ± S.E.M from n=10 animals/group. *p<0.05, **p<0.01 vs STD; #p<0.05, ##p<0.01, ###p<0.001 vs HFD.

5.3.7. PEA restores BBB integrity of HFD-mice hippocampus

The tight junctions, such as occludin and zonuline-1, play a key role in maintaining the integrity of endothelial membrane of BBB. The membrane disruption, due to the reduction of these proteins at hippocampal level, is related to neurodegenerative disorders, such as Alzheimer's Disease (AD) (223). Here, HFD caused a significant reduction of mRNA levels of occludin (**Fig. 5.3.7A**) and zonuline-1 (**Fig.5.3.7B**), indicating an increase of BBB permeability. PEA was able to restore its integrity, inducing the transcription of these two tight junctions (**Fig. 5.3.7**).

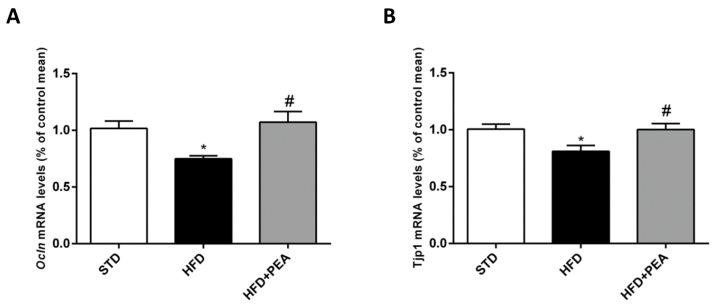

Figure 5.3.7. PEA induces the transcription of TJs in hippocampus of HFD mice. mRNA levels of **(A)** occludin and **(B)** zonuline-1 are shown. Results are shown mean ± S.E.M from n=10 animals/group. *p<0.05 vs STD; #p<0.05 vs HFD.

5.3.8. PEA effects on BDNF/CREB system in prefrontal cortex of HFD mice

To evaluate the possible impact of hippocampus neuroinflammation on prefrontal cortex, we investigated whether HFD induced also the impairment in prefrontal cortex of BDNF/CREB pathway. As shown in **Fig. 5.3.8**, 19 week-HFD caused a partial reduction of phosphorylated CREB and a significant decrease of BDNF, that were restored by PEA treatment. In addition, this molecule was able to reduce inflammatory mediators, such as IL-1β (**Fig. 5.3.8C**) and TNF-α (**Fig. 5.3.8D**), significantly and partially altered by HFD, respectively.

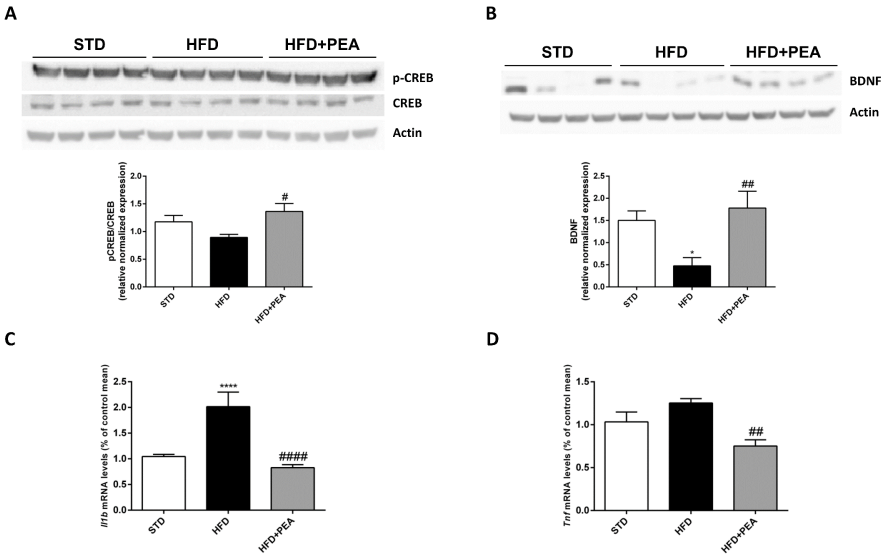

Figure 5.3.8. PEA restored BDNF/CREB system and reduced inflammation in prefrontal cortex of HFD mice. In prefrontal cortex of HFD mice there was a reduction of **(A)** phosphorylated CREB and **(B)** BDNF expression. PEA was able to increase these parameters. Moreover, PEA reduced also inflammatory mediators, such as **(C)** IL-1β and **(D)** TNF-α, altered by HFD. Results are shown as mean ± S.E.M from n=10 animals/group. *p<0.05 and ****p<0.0001 vs STD; #p<0.05, ##p<0.01 and ####p<0.0001 vs HFD.

5.3.9. PEA effects on gut microbiota composition

A total of 606,533 quality-filtered 16S rRNA gene sequences from 12 mouse fecal samples were available for meta-analysis (n=4/group). Of these, 241,734 were at least 97% similar to a sequence in the GG database and represented 2,104 bacterial operational taxonomic units (OTUs), prior to random subsampling. It was necessary to randomly subsample to a level of 7,032 sequences per sample to describe the microbiota composition that have been shown to be sufficient to analyse differences between sample

groups (Goods Coverage>96%). After this sample rarefaction procedure, the resulting sequences represented 1,745 OTUs taxonomically classified in 11 phyla and 87 genera.

The alpha and beta diversity among the three groups were measured in order to evaluate the bacterial diversity in terms of species richness and community diversity. Alpha diversity results revealed that the intestinal bacterial population of HFD and HFD+PEA groups exhibited a significant decrease of microbial diversity (Shannon index; $P<0.05$; **Fig. 5.3.9B**), compared with STD group. Beta diversity, representing the distances among samples and groups in terms of bacterial community composition, was then measured. Using the ANOSIM R statistic, an index based on rank dissimilarity, dissimilarity between groups based on unweighted and weighted Unifract distances was measured (**Fig. 5.3.9C-D**, respectively).

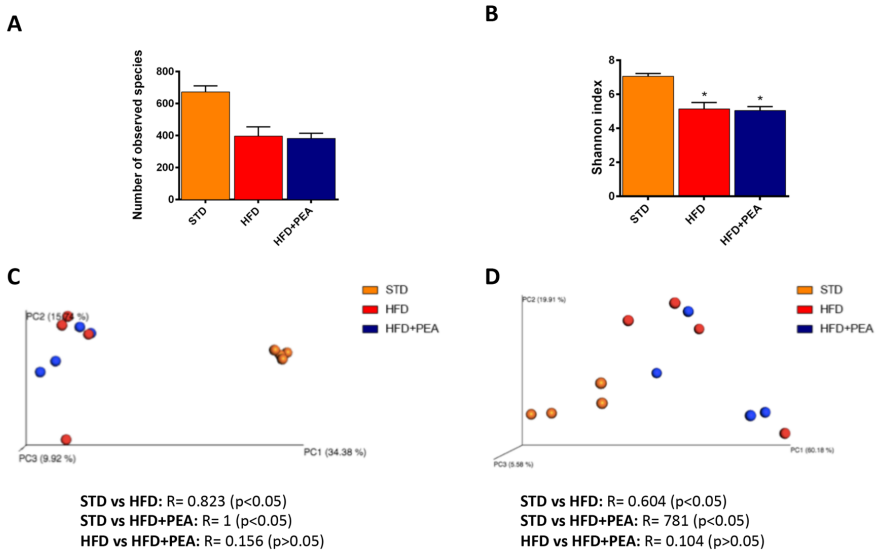

Figure 5.3.9. Comparison of fecal microbial diversity among STD, HFD and HFD+PEA groups. Diversity within bacterial communities is demonstrated by the number of observed species **(A)** and the Shannon Index **(B)**. Results are presented as the mean ± standard deviation. *p<0.05 vs STD, by nonparametric t-test. Diversity among bacterial communities is displayed in the principal coordinate analysis plot, based on unweighted **(C)** and weighted **(D)** Unifrac distances, with the amount of variance along each axis in brackets. Analysis of similarity (ANOSIM) with 999 permutations was used to detect the statistical signicant differences in microbial community composition among groups; on the bottom of plots are reported both R statistics and p values.

ANOSIM analysis revealed significant differences in bacterial assortment of HFD and HFD+PEA samples compared to STD ones both in terms of type and relative abundance of shared species, while no significant differences in bacterial assortment were identified between HFD and HFD+PEA groups. These results indicated the detrimental effect on gut microbiota richness and variety induced by HFD.

Sequencing analysis revealed that Bacteroidetes, Firmicutes and Proteobacteria were the dominant phyla of faecal microbiota in all groups (**Fig. 5.3.10A**). Among the 11 bacterial phyla identified, comparison of relative abundances by Kruskal Wallis test revealed significant differences among groups in the levels of Actinobacteria, Bacteroidetes and Cyanobacteria (**Fig. 5.3.10B**). The treatment with PEA induced a trend of decrease in Proteobacteria, increased by HFD feeding.

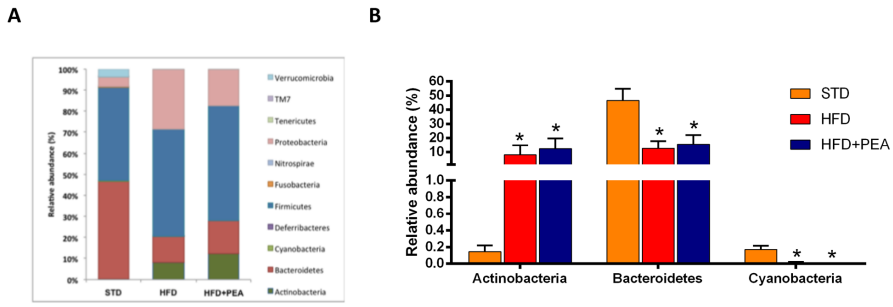

Fig. 5.3.10. Faecal microbiota composition at phylum level. Mean relative abundance of all identified OTUs classified at phylum level **(A)**. Mean values ± SEM of bacterial phyla found to be significantly different among groups **(B)**. Significant differences are indicated by *p<0.05 vs STD.

At the genus level, five genera belonging to Bacteroidetes phylum were altered in HFD mice compared to STD. Among these, unclassified genera of *Prevotellaceae* and *S24-7* families were altered both in HFD and HFD+PEA, whereas *Af12* and *Prevotella* were changed only in the HFD group and unclassified genus of *Bacteroidales* only in HFD+PEA group

(**Fig. 5.3.11A**). Among Proteobacteria phyla, although *Sutterella*, an unclassified genus of *Desulfovibrionaceae*, and of *Helicobacteraceae* were different both in HFD and HFD+PEA group, PEA was able to induce a partial reduction of *Desulfovibrio* (**Fig. 5.3.11B**). Moreover, a total of 13 Firmicutes genera were changed by treatments, with a substantially decrease of relative abundance of an unclassified genus of *Clostridiales* and an increase of genera *Lactococcus*, *Ruminococcus* and *Allobaculum*. Genera *Lactobacillus*, *Clostridium* and an unclassified genus of *Mogibacteriaceae* were influenced specifically by HFD and restored by PEA administration. While unclassified genera of *Clostridiaceae* and *Lacnospiraceae* were different only in HFD+PEA group (**Fig. 5.3.11C**).

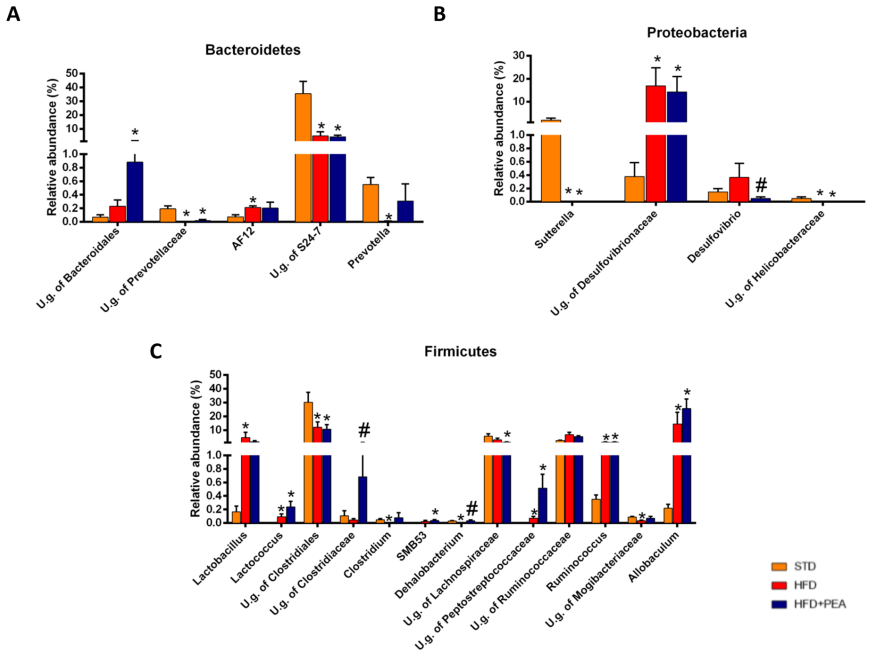

Figure 5.3.11. Faecal microbiota composition at genus level. Genera are grouped according to belonged phyla, **(A)** Bacteroidetes, **(B)** Proteobacteria and **(C)** Firmicutes. Results are shown as mean ± S.E.M from n=4 animals/group. *$p<0.05$ and vs STD; #$p<0.05$ vs HFD.

6. Discussion and conclusions

6.1 Gut-brain axis in ASDs: focus on PEA beneficial effects

ASDs are multifactorial disorders, characterized by multiple converging mechanisms based on genetic, epigenetic and environmental risk factors, even if the specific molecular and cellular features keep still unclear (224). In ASDs, it is usual the incidence of medical comorbidities, such as seizures, intellectual disability, gastrointestinal disorders, metabolic impairment and sleep deficiency (225, 226). In particular, several studies have focused on the ever-increasing relationship between gut disorders and ASDs, showing the presence of diarrhea/constipation, abdominal pain, gastric reflux and the so-called leaky gut in ASDs patients (227-229). Accordingly, previous studies demonstrated the beneficial effects of short-term treatment with antibiotics and probiotics in ASDs patients (230, 231), supporting the possible role of gut microbiota modulation in ASDs. Mouse models of ASDs have often represented a support to study and understand, not only the mechanisms underlying ASD pathogenesis and behavior, but also the communication between gut microbes and CNS. During the first part of the PhD programme, a gender study was performed on gut microbiota

composition, behavioral features, such as social interaction, stereotyped and repetitive movement, intestinal integrity and architecture of adult male and female BTBR mice, one of the most used animal model of ASDs.

From the analysis of gut microbiota, we observed that Bacteroidetes and Firmicutes were the principal contributors to the BTBR and C57 gut microbiota differences both in female and male mice. In particular, among the key genera belonging to Bacteroidetes phyla, *Bacteroides* and *Parabacteroides* were significantly more abundant in both male and female BTBR mice than control group. These two genera of microrganisms are producers of lipopolysaccharide, an endotoxin detected in serum of autistic patients (232). In another clinical study, high levels of *Bacteroides* were found in fecal samples of ASDs children (233).

Interestingly, among other phyla, we demonstrated also a gender difference. Indeed, we found an increase of Proteobacteria and a reduction of TM7 phylum in fBTBR compared with fC57, not recognized between mBTBR and mC57. Although comparison between animal model and human studies should be critically analyzed for great heterogenic differences, several families among Proteobacteria, gut commensal species with potential pathogenic features, were detected in gut of ASDs children (234). In Proteobacteria phylum, genus *Sutterella*, found elevated in fBTBR, was also detected in fecal samples of children with ASDs or gut disorders (235, 236).

The unbalance of gut microbiota in BTBR mice was accompanied, in both males and females, by an increased gut permeability and inflammation, related to the occurrence of marked colonic damage, underlining again the strong link between ASDs and gut disturbances (131).

Beyond the description of gut microbiota profile, we also investigated whether there was a possible correlation between specific microorganisms and behavioral or peripheral pathological features. In particular, the increase of *Parabacteroides* and *Sutterella* amount, associated with the reduction of *Dehalobacterium*, *Oscillospira*, and unclassified member of TM7, were strongly related to autistic behavior and high colonic expression of TNF-α in fBTBR. This finding goes along with Onore et al. (237), whose work highlighted the relationship between colonic inflammation and repetitive grooming behavior of BTBR mice. After the characterization of the mouse model of ASDs, our focus moved to the evaluation of possible central and peripheral activities evoked by PEA in improving autistic-like traits, focusing on the effects on gut-brain axis.

PPARα targeting, using PEA as PPARα agonist, represents a novel therapeutic approach for ASDs treatment: indeed, some recent but still preliminary studies highlighted the beneficial effects of PEA in autistic animals and patients (96, 238, 239).

To this purpose, during the second part of the PhD programme, the beneficial and dose-dependent effects of PEA on autistic-like behavior was investigated using a mouse model of ASDs. In particular, we assessed the contribution of converging mechanisms underlying PEA effect and the obligatory role of PPARα in its mechanism of action.

In BTBR mice, the treatment with PEA at higher dosage improved repetitive behavior and sociability. These effects were not related to possible drug-induced confounding hyper- or hypoactivity, as confirmed by OFT and EPM test. In addition, a single PEA administration had no positive effect, demonstrating the consolidation of PEA-induced mechanisms for a delayed effect. We directly correlated the improved social behavior to PPARα activation mediated by PEA, because of the loss of its activity in both PPARα null mice and BTBR mice pretreated with PPARα antagonist, GW. These findings were strengthened by the increased PPARα mRNA and protein expression in the hippocampus of PEA-treated BTBR mice. In two preclinical studies, PPARα activation prevented cognitive dysfunction (240) and induced hippocampal neurogenesis after cerebral ischemia (241). In particular, this receptor regulates the expression and functions of several plasticity-related molecules through the direct transcriptional control of CREB (64, 65). Interestingly, ASDs are characterized by an alteration of

BDNF/TrkB signaling pathway and a significant reduction of BDNF-induced synaptic transmission (219, 242, 243). Here, we found lower BDNF level and no significant changes of TrkB expression between BTBR and control mice, while PEA was able to induce both mRNA and protein expression compared to autistic mice. The involvement of BDNF signalling pathway in the molecular mechanisms contributing to PEA effect, was confirmed by the increase in the phosphorylation of CREB, involved in BDNF signalling pathway (244).

As above mentioned, the pathogenic mechanism of ASDs is multifactorial. Indeed, beyond the involvement of synapse development and plasticity, it includes other different alterations, such as mitochondrial dysfunction, dysregulated immune response and chronic neuroinflammation (245).

During their energy-generating activity, mitochondria are main responsible for the production of free radical species. In brain, where the demand of mitochondrial energy is high, these waste products can trigger pathological conditions. Therefore, mitochondrial dysfunction may be a key feature common to a wide spectrum of neurological and neurodevelopmental diseases, including ASDs (246). Furthermore, Anitha et al. (247) had already observed an altered expression of electron transport chain genes in brains of autistic patients. Accordingly, hippocampal mitochondria in BTBR mice exhibited a reduced respiratory capacity, as indicated by the decrease in

succinate State 3 oxygen consumption, which would partially block electron flow within the respiratory chain and consequently increase oxidative stress. Moreover, the decreased SOD activity could contribute to excessive ROS formation in BTBR mice. Notably, PEA treatment restored mitochondrial function and decreased oxidative stress partially due to the increase in SOD activity. A concomitant decline in mitochondrial energy efficiency, as evidenced by the decreased degree of coupling in PEA treatment, may also contribute to counteract excessive ROS formation in PEA-treated BTBR mice. These evidences confirm that PEA rescues hippocampal functionality, balancing ROS production and antioxidant defences. Therefore, PEA could limit all those events related to excessive ROS, such as the destruction of cellular components including lipids, protein, and DNA, and the trigger of inflammation.

In ASDs, neuroinflammation is driven by microglial cells that acquire a M1 phenotype and induce the production of several pro-inflammatory cytokines, including TNF-α, IL-1β and IL-6 (248). Indeed, in both BTBR and VPA-induced autistic mice, Cipriani et al. (249) discovered high levels of pro-inflammatory cytokines in brain and serum samples. Furthermore, as shown in the first part, the inflammatory state is also mediated by the

gastrointestinal system, due to increased gut permeability, synthesis of cytokines and alteration of gut microbiota.

Here, PEA was able to reduce cytokine production at colonic, central and systemic levels, and improved intestinal permeability. Therefore, it is conceivable to hypothesise that systemic administration of PEA could directly impact neuroinflammation, being able to cross BBB, but also indirectly reduce peripheral inflammatory input to the brain, through its anti-inflammatory properties in periphery. Therefore, our hypothesis is that PEA would reduce the trafficking of inappropriate gut-derived detrimental factors into the portal circulation and the crossing through a permissive BBB, leading to a reduction in systemic and ultimately central inflammation.

Finally, PEA peripheral effect could be also mediated by the modulation of gut microbiota. Indeed, we observed several modifications of faecal microbial communities and, in particular, a variation in amount of Firmicutes and Bacteroidetes in BTBR mice upon PEA treatment. A marked augment of Firmicutes, mainly due to the increase of Unclassified genus of *Clostridiales*, to the expense of Bacteroidetes, is the most evident change induced by PEA administration. Clostridia include the majority of species able to produce butyrate as metabolic product of anaerobic fermentation. Indeed, it has been demonstrated the key role of butyrate in the maintenance of gut physiology, regulating gut barrier permeability, suppressing

inflammation and modulating immune functions (250). Although further studies are needed, here, we demonstrated that PEA modulated gut bacterial species composition, whose remodelling may be associated to gut homeostasis.

In conclusion, PEA showed beneficial effects on complex disorders such as ASDs, due to its pleiotropic mechanism of action, evidenced by neuroprotection, anti-inflammatory effects, and the modulation of gut-brain axis, through restoring gut integrity and remodelling gut microbiota composition.

6.2. PEA and obesity-induced depression

MDD and obesity represent often two inter-related burdens. These two disorders are strictly interconnected, composing a bi-directional axis, although the description of underlying mechanisms is not completely clarified (251). Several clinical studies demonstrated that obesity is prospectively associated to the onset of MDD, highlighting a significant obesity-to-depression association (168). In the last part of this PhD programme, we investigated the effects induced by high fat feeding in the onset of depressive episodes, elucidating biomolecular mechanisms that combine the two sides of the same coin. Furthermore, we assessed PEA improvement of this pathological condition induced by HFD overnutrition.

Recently, Wu et al. (252) demonstrated that young mice on HFD for 6 weeks, showed depressive-like behaviour associated to an impairment of hippocampal neurogenesis, due to a reduction of phosphorylated CREB and BDNF expression. Here, after 19 weeks of HFD, mice exhibited a depressive mood, evidencing by an increased immobility time in FST and TST and an impairment of CREB/BDNF pathway in hippocampus. The treatment with PEA induced a significant improvement in depressive state with a restoration of hippocampal BDNF signalling. These findings reinforced

previous preliminary data where a single administration of PEA in mice at different dosage reduced immobility time in FST and TST more than the anti-depressant drug fluoxetine (92).

As previously demonstrated, high fat diet feeding is characterized by increased levels of circulating LPS, pro-inflammatory cytokines and chemokines (253). Consistently, here we showed an alteration of serum inflammatory and metabolic profile, restored by PEA treatment. All detrimental factors elevated in the bloodstream, could reach the hypothalamus and cross BBB, mainly in areas where barrier integrity is more rarefied, such as ARC, a zone involved not only in the regulation of food intake, but also in the modulation of cognitive function through the connection with other brain areas (mesolimbic dopamine system, hippocampus, orbitofrontal cortex, nucleus accumbens, striatum and prefrontal cortex) (254). The occurrence of these detrimental molecules in ARC induces an impairment of anorexigen POMC neurons, whose dysfunction precedes inflammation and represents a leading factor for the progression of obesity (255). Moreover, in obese mice, HFD can induce neuroinflammation, characterized by microglial infiltration, activation and proliferation; activation of the pro-inflammatory transcription factor NF-kB; and increased expression of pro-inflammatory cytokines (256-259).

Here, we demonstrated that HFD caused a decreased activation of POMC neurons in ARC accompanied by microglial activation addressed by IBA-1 increased expression. In addition, in hypothalamus from HFD mice we found an alteration of inflammatory mediators and a reduced transcription of the neurotrophin BDNF. Interestingly, PEA treatment restored POMC neuron activation and limited the neuroinflammation.

The disruption of internal hypothalamic circuitry can lead to the dysfunction of other brain regions, such as hippocampus, through defective outputs. The loss of hippocampal integrity and function induced by HFD represents another pivotal factor that induces the progression of MDD (260). Lu et al. (261) demonstrated that 20 week-HFD feeding caused a hippocampal inflammation mediated by IKKB/NF-kB activity and production of several pro-inflammatory players, such as TNF-α, COX-2 and iNOS. This deleterious condition also leads to the loss of BBB integrity, triggering further neuroinflammation and activating a vicious self-feeding loop (262). In our experimental condition, HFD mice showed an impairment of BDNF signaling, an occurrence of inflammation and loss of hippocampal tight junctions, such as zonuline-1 and occludin. The treatment with PEA improved this pathological condition, restoring the functionality and integrity of hippocampus.

Hippocampus and prefrontal cortex interplay mainly for prolonged process by which new memories are converted into permanent storehouse of knowledge (263). The difficulty in recognizing the old object by HFD mice during NORT, prompted us to examine the possible impairment of BDNF/CREB pathway in prefrontal cortex. 19-week HFD was able to reduce the expression of these parameters, confirming a previous study where the exposure to HFD led to detrimental effect on prefrontal cortex function (264). Consistently with the improvement in recognition activity, PEA was able to restore the levels of BDNF and its signaling pathway in prefrontal cortex of HFD mice.

In last years, several studies have demonstrated the presence of PPARα in hippocampus, more than other brain areas. This receptor plays a pivotal role in the modulation of synaptic function, through the up-regulation of the transcription factor CREB. Indeed, in PPARα KO, but not PPARβ KO mice, CREB was down-regulated and a decreased spatial learning and memory was shown (64). Moreover, the same group demonstrated also that statin-mediated nuclear activation of PPARα modulated the expression of neurotrophins in different brain cells (265). Yang et al. (266) showed the antidepressive effect of PPARα agonist, WY-14643, in improving BDNF signaling pathway both in hippocampus and prefrontal cortex, and preventing neuroinflammation and oxidative-nitrosative stress in the mouse

model of lipopolysaccharide-induced depression. PEA, as a PPARα agonist, stimulate the expression of PPARα, its coactivator PGC1α and the downstream FGF21, parameters altered by HFD, indicating a possible role of PPARα in ameliorating the obesity-induced depression.

Potential neurobehavioral disruptions following exposure to HFD may be mediated by gut microbiota alterations, i.e. through the gut-microbiome-brain axis. HFD-fed mice treated with PEA showed mild changes in the composition of the gut microbiota compared to HFD fed mice: in particular *Desulfovibrio* was reduced by PEA treatment, while U.g. of Clostridiaceae and *Dehalobacterium* were increased. Studies have demonstrated a significant increase in Desulfovibrionaceae, potential endotoxin producers, in the gut microbiomes of both HFD-induced obese mice and obese human subjects compared with lean individuals (267-269). Here, HFD-fed mice treated with PEA showed a decrease in endotoxin-producing *Desulfovibrio* bacteria, whose increase has been positively correlated with obesity and inflammation. The significant reduction in the relative abundance of this endotoxin-producing opportunistic pathogens *Desulfovibrio* by PEA is indeed also consistent with a possible concomitant reduction in endotoxemia, whose increase correlates with depression mood.

On the other hand, we have found a marked increase of an U.g. of Clostridiaceae, belonging to Clostridiales, by PEA treatment. This

modification is consistent with what we have already shown in BTBR mice, suggesting a peculiar effect of PEA in increasing *Clostridiales* genus relative abundance, and consistently Clostridiales-producing metabolites. In particular, an increase in SCFAs could be hypothesized, also considering the beneficial effect they exert in gut homeostasis. Moreover, among SCFAs, butyrate has been shown to counteract LPS-induced depressive state in mice, an effect related to decreased IBA-1 hippocampal expression (270). Finally, we have shown a reduction of *Dehalobacterium* genus in HFD-fed mice. Actually, Javurek et al in 2017 (271), have correlated this alteration with behavioural modifications. Indeed, we have also reported that the reduction in this genus was found in BTBR mice, where the autistic phenotype was also accompanied by leaky gut and inflammation. These preliminary data on PEA-induced gut microbiota remodelling need further investigation, however suggest a novel possible peripheral mechanism underlying not only gut homeostasis but also all related-ailments profoundly modulated by gut-brain axis.

Highlights

- Autistic mice turned gut homeostasis upside down, showing a pronounced dysbiosis, the loss of its barrier integrity and inflammation.
- PEA limited stereotyped behavior and improve social interaction of autistic mice, through the reduction of inflammation and the modulation gut microbiota.
- High fat diet feeding induced a depressive-like behavior in mice triggered by an extent neuroinflammation and gut dysbiosis.
- PEA improved depressive behavior and memory deficit induced by HFD, improved BBB integrity, reducing hypothalamic, hippocampal and cortical inflammation and modulating microbiota composition.
- All the effects of PEA were contingent to PPAR-α activation.

General conclusions: PEA and CNS disorders

In the light of obtained data, we can hypothesise that systemic administration of PEA could directly impact neuroinflammation, being able to cross the BBB, but also indirectly reduce peripheral inflammatory input to the brain, through its anti-inflammatory properties at colonic and systemic level. Therefore, our hypothesis is that PEA would reduce the trafficking of inappropriate gut-derived detrimental factors into the portal circulation and the crossing through a permissive BBB, leading to a reduction in systemic and ultimately central inflammation.

In conclusion, PEA may be considered a multifunctional compound for an integrative and innovative approach against complex diseases, such as metabolic illness and CNS disorders, due to its pleiotropic mechanism of action, supporting neuroprotection, anti-inflammatory effects, and the modulation of gut-brain axis, through restoring gut integrity and remodeling gut microbiota composition.

7. References

1. **Geschwind, D.H.**, *Autism: many genes, common pathways?* Cell, 2008. **135**(3): p. 391-5.
2. **Lo Verme, J., J. Fu, G. Astarita, G. La Rana, R. Russo, A. Calignano, and D. Piomelli**, *The nuclear receptor peroxisome proliferator-activated receptor-alpha mediates the anti-inflammatory actions of palmitoylethanolamide.* Mol Pharmacol, 2005. **67**(1): p. 15-9.
3. **LoVerme, J., R. Russo, G. La Rana, J. Fu, J. Farthing, G. Mattace-Raso, R. Meli, A. Hohmann, A. Calignano, and D. Piomelli**, *Rapid broad-spectrum analgesia through activation of peroxisome proliferator-activated receptor-alpha.* J Pharmacol Exp Ther, 2006. **319**(3): p. 1051-61.
4. **D'Agostino, G., G. La Rana, R. Russo, O. Sasso, A. Iacono, E. Esposito, G. Mattace Raso, S. Cuzzocrea, J. Loverme, D. Piomelli, R. Meli, and A. Calignano**, *Central administration of palmitoylethanolamide reduces hyperalgesia in mice via inhibition of NF-kappaB nuclear signalling in dorsal root ganglia.* Eur J Pharmacol, 2009. **613**(1-3): p. 54-9.
5. **Hansen, H.S.**, *Palmitoylethanolamide and other anandamide congeners. Proposed role in the diseased brain.* Exp Neurol, 2010. **224**(1): p. 48-55.
6. **Sasso, O., G. La Rana, S. Vitiello, R. Russo, G. D'Agostino, A. Iacono, E. Russo, R. Citraro, S. Cuzzocrea, P.V. Piazza, G. De Sarro, R. Meli, and A. Calignano**, *Palmitoylethanolamide modulates pentobarbital-evoked hypnotic effect in mice: involvement of allopregnanolone biosynthesis.* Eur Neuropsychopharmacol, 2010. **20**(3): p. 195-206.
7. **Mattace Raso, G., A. Santoro, R. Russo, R. Simeoli, O. Paciello, C. Di Carlo, S. Diano, A. Calignano, and R. Meli**, *Palmitoylethanolamide prevents metabolic alterations and restores leptin sensitivity in ovariectomized rats.* Endocrinology, 2014. **155**(4): p. 1291-301.
8. **Cadas, H., S. Gaillet, M. Beltramo, L. Venance, and D. Piomelli**, *Biosynthesis of an endogenous cannabinoid precursor in neurons and its control by calcium and cAMP.* J Neurosci, 1996. **16**(12): p. 3934-42.
9. **Piomelli, D.**, *The molecular logic of endocannabinoid signalling.* Nat Rev Neurosci, 2003. **4**(11): p. 873-84.

10. **Aloe, L., A. Leon, and R. Levi-Montalcini**, *A proposed autacoid mechanism controlling mastocyte behaviour.* Agents Actions, 1993. **39 Spec No**: p. C145-7.
11. **Balvers, M.G., K.C. Verhoeckx, J. Meijerink, H.M. Wortelboer, and R.F. Witkamp**, *Measurement of palmitoylethanolamide and other N-acylethanolamines during physiological and pathological conditions.* CNS Neurol Disord Drug Targets, 2013. **12**(1): p. 23-33.
12. **Hansen, H.S., B. Moesgaard, G. Petersen, and H.H. Hansen**, *Putative neuroprotective actions of N-acyl-ethanolamines.* Pharmacol Ther, 2002. **95**(2): p. 119-26.
13. **Mattace Raso, G., R. Russo, A. Calignano, and R. Meli**, *Palmitoylethanolamide in CNS health and disease.* Pharmacol Res, 2014. **86**: p. 32-41.
14. **Schmid, H.H. and E.V. Berdyshev**, *Cannabinoid receptor-inactive N-acylethanolamines and other fatty acid amides: metabolism and function.* Prostaglandins Leukot Essent Fatty Acids, 2002. **66**(2-3): p. 363-76.
15. **Sugiura, T., Y. Kobayashi, S. Oka, and K. Waku**, *Biosynthesis and degradation of anandamide and 2-arachidonoylglycerol and their possible physiological significance.* Prostaglandins Leukot Essent Fatty Acids, 2002. **66**(2-3): p. 173-92.
16. **Di Marzo, V., A. Fontana, H. Cadas, S. Schinelli, G. Cimino, J.C. Schwartz, and D. Piomelli**, *Formation and inactivation of endogenous cannabinoid anandamide in central neurons.* Nature, 1994. **372**(6507): p. 686-91.
17. **Okamoto, Y., J. Morishita, K. Tsuboi, T. Tonai, and N. Ueda**, *Molecular characterization of a phospholipase D generating anandamide and its congeners.* J Biol Chem, 2004. **279**(7): p. 5298-305.
18. **Deutsch, D.G., N. Ueda, and S. Yamamoto**, *The fatty acid amide hydrolase (FAAH).* Prostaglandins Leukot Essent Fatty Acids, 2002. **66**(2-3): p. 201-10.
19. **McKinney, M.K. and B.F. Cravatt**, *Structure and function of fatty acid amide hydrolase.* Annu Rev Biochem, 2005. **74**: p. 411-32.
20. **Ueda, N., K. Tsuboi, and T. Uyama**, *Metabolism of endocannabinoids and related N-acylethanolamines: canonical and alternative pathways.* FEBS J, 2013. **280**(9): p. 1874-94.
21. **Bojesen, I.N. and H.S. Hansen**, *Membrane transport of anandamide through resealed human red blood cell membranes.* J Lipid Res, 2005. **46**(8): p. 1652-9.

22. **Iannotti, F.A., V. Di Marzo, and S. Petrosino**, *Endocannabinoids and endocannabinoid-related mediators: Targets, metabolism and role in neurological disorders.* Prog Lipid Res, 2016. **62**: p. 107-28.
23. **De Petrocellis, L., T. Bisogno, A. Ligresti, M. Bifulco, D. Melck, and V. Di Marzo**, *Effect on cancer cell proliferation of palmitoylethanolamide, a fatty acid amide interacting with both the cannabinoid and vanilloid signalling systems.* Fundam Clin Pharmacol, 2002. **16**(4): p. 297-302.
24. **Zoete, V., A. Grosdidier, and O. Michielin**, *Peroxisome proliferator-activated receptor structures: ligand specificity, molecular switch and interactions with regulators.* Biochim Biophys Acta, 2007. **1771**(8): p. 915-25.
25. **Echeverria, F., M. Ortiz, R. Valenzuela, and L.A. Videla**, *Long-chain polyunsaturated fatty acids regulation of PPARs, signaling: Relationship to tissue development and aging.* Prostaglandins Leukot Essent Fatty Acids, 2016. **114**: p. 28-34.
26. **Kersten, S., B. Desvergne, and W. Wahli**, *Roles of PPARs in health and disease.* Nature, 2000. **405**(6785): p. 421-4.
27. **Tan, C.K., Y. Zhuang, and W. Wahli**, *Synthetic and natural Peroxisome Proliferator-Activated Receptor (PPAR) agonists as candidates for the therapy of the metabolic syndrome.* Expert Opin Ther Targets, 2017. **21**(3): p. 333-348.
28. **Kliewer, S.A., K. Umesono, D.J. Noonan, R.A. Heyman, and R.M. Evans**, *Convergence of 9-cis retinoic acid and peroxisome proliferator signalling pathways through heterodimer formation of their receptors.* Nature, 1992. **358**(6389): p. 771-4.
29. **Gearing, K.L., M. Gottlicher, M. Teboul, E. Widmark, and J.A. Gustafsson**, *Interaction of the peroxisome-proliferator-activated receptor and retinoid X receptor.* Proc Natl Acad Sci U S A, 1993. **90**(4): p. 1440-4.
30. **Keller, H., C. Dreyer, J. Medin, A. Mahfoudi, K. Ozato, and W. Wahli**, *Fatty acids and retinoids control lipid metabolism through activation of peroxisome proliferator-activated receptor-retinoid X receptor heterodimers.* Proc Natl Acad Sci U S A, 1993. **90**(6): p. 2160-4.
31. **Juge-Aubry, C., A. Pernin, T. Favez, A.G. Burger, W. Wahli, C.A. Meier, and B. Desvergne**, *DNA binding properties of peroxisome proliferator-activated receptor subtypes on various natural peroxisome proliferator response elements. Importance of the 5'-flanking region.* J Biol Chem, 1997. **272**(40): p. 25252-9.

32. **Feige, J.N., L. Gelman, L. Michalik, B. Desvergne, and W. Wahli**, *From molecular action to physiological outputs: peroxisome proliferator-activated receptors are nuclear receptors at the crossroads of key cellular functions.* Prog Lipid Res, 2006. **45**(2): p. 120-59.
33. **Cowell, R.M., P. Talati, K.R. Blake, J.H. Meador-Woodruff, and J.W. Russell**, *Identification of novel targets for PGC-1alpha and histone deacetylase inhibitors in neuroblastoma cells.* Biochem Biophys Res Commun, 2009. **379**(2): p. 578-82.
34. **Bagattin, A., L. Hugendubler, and E. Mueller**, *Transcriptional coactivator PGC-1alpha promotes peroxisomal remodeling and biogenesis.* Proc Natl Acad Sci U S A, 2010. **107**(47): p. 20376-81.
35. **Chen, S.D., T.K. Lin, J.W. Lin, D.I. Yang, S.Y. Lee, F.Z. Shaw, C.W. Liou, and Y.C. Chuang**, *Activation of calcium/calmodulin-dependent protein kinase IV and peroxisome proliferator-activated receptor gamma coactivator-1alpha signaling pathway protects against neuronal injury and promotes mitochondrial biogenesis in the hippocampal CA1 subfield after transient global ischemia.* J Neurosci Res, 2010. **88**(14): p. 3144-54.
36. **Wenz, T.**, *Regulation of mitochondrial biogenesis and PGC-1alpha under cellular stress.* Mitochondrion, 2013. **13**(2): p. 134-42.
37. **Braissant, O., F. Foufelle, C. Scotto, M. Dauca, and W. Wahli**, *Differential expression of peroxisome proliferator-activated receptors (PPARs): tissue distribution of PPAR-alpha, -beta, and -gamma in the adult rat.* Endocrinology, 1996. **137**(1): p. 354-66.
38. **Kainu, T., A.C. Wikstrom, J.A. Gustafsson, and M. Pelto-Huikko**, *Localization of the peroxisome proliferator-activated receptor in the brain.* Neuroreport, 1994. **5**(18): p. 2481-5.
39. **Benani, A., P. Kremarik-Bouillaud, A. Bianchi, P. Netter, A. Minn, and M. Dauca**, *Evidence for the presence of both peroxisome proliferator-activated receptors alpha and beta in the rat spinal cord.* J Chem Neuroanat, 2003. **25**(1): p. 29-38.
40. **Moreno, S., S. Farioli-Vecchioli, and M.P. Ceru**, *Immunolocalization of peroxisome proliferator-activated receptors and retinoid X receptors in the adult rat CNS.* Neuroscience, 2004. **123**(1): p. 131-45.
41. **Desvergne, B., L. Michalik, and W. Wahli**, *Transcriptional regulation of metabolism.* Physiol Rev, 2006. **86**(2): p. 465-514.
42. **Montagner, A., G. Rando, G. Degueurce, N. Leuenberger, L. Michalik, and W. Wahli**, *New insights into the role of PPARs.* Prostaglandins Leukot Essent Fatty Acids, 2011. **85**(5): p. 235-43.

43. **Zolezzi, J.M., C. Silva-Alvarez, D. Ordenes, J.A. Godoy, F.J. Carvajal, M.J. Santos, and N.C. Inestrosa**, *Peroxisome proliferator-activated receptor (PPAR) gamma and PPARalpha agonists modulate mitochondrial fusion-fission dynamics: relevance to reactive oxygen species (ROS)-related neurodegenerative disorders?* PLoS One, 2013. **8**(5): p. e64019.
44. **Wang, G., X. Liu, Q. Guo, and S. Namura**, *Chronic treatment with fibrates elevates superoxide dismutase in adult mouse brain microvessels.* Brain Res, 2010. **1359**: p. 247-55.
45. **Santos, M.J., R.A. Quintanilla, A. Toro, R. Grandy, M.C. Dinamarca, J.A. Godoy, and N.C. Inestrosa**, *Peroxisomal proliferation protects from beta-amyloid neurodegeneration.* J Biol Chem, 2005. **280**(49): p. 41057-68.
46. **Cimini, A., L. Cristiano, E. Benedetti, B. D'Angelo, and M.P. Ceru**, *PPARs Expression in Adult Mouse Neural Stem Cells: Modulation of PPARs during Astroglial Differentiaton of NSC.* PPAR Res, 2007. **2007**: p. 48242.
47. **Cimini, A. and M.P. Ceru**, *Emerging roles of peroxisome proliferator-activated receptors (PPARs) in the regulation of neural stem cells proliferation and differentiation.* Stem Cell Rev, 2008. **4**(4): p. 293-303.
48. **Roberts, R.A., S. Chevalier, S.C. Hasmall, N.H. James, S.C. Cosulich, and N. Macdonald**, *PPAR alpha and the regulation of cell division and apoptosis.* Toxicology, 2002. **181-182**: p. 167-70.
49. **Strakova, N., J. Ehrmann, J. Bartos, J. Malikova, J. Dolezel, and Z. Kolar**, *Peroxisome proliferator-activated receptors (PPAR) agonists affect cell viability, apoptosis and expression of cell cycle related proteins in cell lines of glial brain tumors.* Neoplasma, 2005. **52**(2): p. 126-36.
50. **Melis, M., G. Carta, M. Pistis, and S. Banni**, *Physiological role of peroxisome proliferator-activated receptors type alpha on dopamine systems.* CNS Neurol Disord Drug Targets, 2013. **12**(1): p. 70-7.
51. **Melis, M., S. Scheggi, G. Carta, C. Madeddu, S. Lecca, A. Luchicchi, F. Cadeddu, R. Frau, L. Fattore, P. Fadda, M.G. Ennas, M.P. Castelli, W. Fratta, B. Schilstrom, S. Banni, M.G. De Montis, and M. Pistis**, *PPARalpha regulates cholinergic-driven activity of midbrain dopamine neurons via a novel mechanism involving alpha7 nicotinic acetylcholine receptors.* J Neurosci, 2013. **33**(14): p. 6203-11.
52. **Melis, M., S. Carta, L. Fattore, S. Tolu, S. Yasar, S.R. Goldberg, W. Fratta, U. Maskos, and M. Pistis**, *Peroxisome proliferator-*

activated receptors-alpha modulate dopamine cell activity through nicotinic receptors. Biol Psychiatry, 2010. **68**(3): p. 256-64.

53. **Hajjar, T., G.Y. Meng, M.A. Rajion, S. Vidyadaran, F. Othman, A.S. Farjam, T.A. Li, and M. Ebrahimi**, *Omega 3 polyunsaturated fatty acid improves spatial learning and hippocampal peroxisome proliferator activated receptors (PPARalpha and PPARgamma) gene expression in rats.* BMC Neurosci, 2012. **13**: p. 109.
54. **Campolongo, P., B. Roozendaal, V. Trezza, V. Cuomo, G. Astarita, J. Fu, J.L. McGaugh, and D. Piomelli**, *Fat-induced satiety factor oleoylethanolamide enhances memory consolidation.* Proc Natl Acad Sci U S A, 2009. **106**(19): p. 8027-31.
55. **Mazzola, C., J. Medalie, M. Scherma, L.V. Panlilio, M. Solinas, G. Tanda, F. Drago, J.L. Cadet, S.R. Goldberg, and S. Yasar**, *Fatty acid amide hydrolase (FAAH) inhibition enhances memory acquisition through activation of PPAR-alpha nuclear receptors.* Learn Mem, 2009. **16**(5): p. 332-7.
56. **Benani, A., T. Heurtaux, P. Netter, and A. Minn**, *Activation of peroxisome proliferator-activated receptor alpha in rat spinal cord after peripheral noxious stimulation.* Neurosci Lett, 2004. **369**(1): p. 59-63.
57. **de Novellis, V., L. Luongo, F. Guida, L. Cristino, E. Palazzo, R. Russo, I. Marabese, G. D'Agostino, A. Calignano, F. Rossi, V. Di Marzo, and S. Maione**, *Effects of intra-ventrolateral periaqueductal grey palmitoylethanolamide on thermoceptive threshold and rostral ventromedial medulla cell activity.* Eur J Pharmacol, 2012. **676**(1-3): p. 41-50.
58. **Di Cesare Mannelli, L., G. D'Agostino, A. Pacini, R. Russo, M. Zanardelli, C. Ghelardini, and A. Calignano**, *Palmitoylethanolamide is a disease-modifying agent in peripheral neuropathy: pain relief and neuroprotection share a PPAR-alpha-mediated mechanism.* Mediators Inflamm, 2013. **2013**: p. 328797.
59. **Khasabova, I.A., Y. Xiong, L.G. Coicou, D. Piomelli, and V. Seybold**, *Peroxisome proliferator-activated receptor alpha mediates acute effects of palmitoylethanolamide on sensory neurons.* J Neurosci, 2012. **32**(37): p. 12735-43.
60. **Chakravarthy, M.V., Y. Zhu, M. Lopez, L. Yin, D.F. Wozniak, T. Coleman, Z. Hu, M. Wolfgang, A. Vidal-Puig, M.D. Lane, and C.F. Semenkovich**, *Brain fatty acid synthase activates PPARalpha to maintain energy homeostasis.* J Clin Invest, 2007. **117**(9): p. 2539-52.

61. **Fu, J., S. Gaetani, F. Oveisi, J. Lo Verme, A. Serrano, F. Rodriguez De Fonseca, A. Rosengarth, H. Luecke, B. Di Giacomo, G. Tarzia, and D. Piomelli**, *Oleylethanolamide regulates feeding and body weight through activation of the nuclear receptor PPAR-alpha.* Nature, 2003. **425**(6953): p. 90-3.
62. **Schwartz, G.J., J. Fu, G. Astarita, X. Li, S. Gaetani, P. Campolongo, V. Cuomo, and D. Piomelli**, *The lipid messenger OEA links dietary fat intake to satiety.* Cell Metab, 2008. **8**(4): p. 281-288.
63. **Konig, B., C. Rauer, S. Rosenbaum, C. Brandsch, K. Eder, and G.I. Stangl**, *Fasting Upregulates PPARalpha Target Genes in Brain and Influences Pituitary Hormone Expression in a PPARalpha Dependent Manner.* PPAR Res, 2009. **2009**: p. 801609.
64. **Roy, A., M. Jana, G.T. Corbett, S. Ramaswamy, J.H. Kordower, F.J. Gonzalez, and K. Pahan**, *Regulation of cyclic AMP response element binding and hippocampal plasticity-related genes by peroxisome proliferator-activated receptor alpha.* Cell Rep, 2013. **4**(4): p. 724-37.
65. **Rivera, P., S. Arrabal, A. Vargas, E. Blanco, A. Serrano, F.J. Pavon, F. Rodriguez de Fonseca, and J. Suarez**, *Localization of peroxisome proliferator-activated receptor alpha (PPARalpha) and N-acyl phosphatidylethanolamine phospholipase D (NAPE-PLD) in cells expressing the Ca(2+)-binding proteins calbindin, calretinin, and parvalbumin in the adult rat hippocampus.* Front Neuroanat, 2014. **8**: p. 12.
66. **Skaper, S.D., L. Facci, and P. Giusti**, *Glia and mast cells as targets for palmitoylethanolamide, an anti-inflammatory and neuroprotective lipid mediator.* Mol Neurobiol, 2013. **48**(2): p. 340-52.
67. **Di Marzo, V., T. Bisogno, L. De Petrocellis, D. Melck, and B.R. Martin**, *Cannabimimetic fatty acid derivatives: the anandamide family and other endocannabinoids.* Curr Med Chem, 1999. **6**(8): p. 721-44.
68. **De Petrocellis, L., J.B. Davis, and V. Di Marzo**, *Palmitoylethanolamide enhances anandamide stimulation of human vanilloid VR1 receptors.* FEBS Lett, 2001. **506**(3): p. 253-6.
69. **Mechoulam, R., E. Fride, L. Hanus, T. Sheskin, T. Bisogno, V. Di Marzo, M. Bayewitch, and Z. Vogel**, *Anandamide may mediate sleep induction.* Nature, 1997. **389**(6646): p. 25-6.
70. **Smart, D., K.O. Jonsson, S. Vandevoorde, D.M. Lambert, and C.J. Fowler**, *'Entourage' effects of N-acyl ethanolamines at human*

vanilloid receptors. Comparison of effects upon anandamide-induced vanilloid receptor activation and upon anandamide metabolism. Br J Pharmacol, 2002. **136**(3): p. 452-8.

71. **Jonsson, K.O., S. Vandevoorde, D.M. Lambert, G. Tiger, and C.J. Fowler**, *Effects of homologues and analogues of palmitoylethanolamide upon the inactivation of the endocannabinoid anandamide.* Br J Pharmacol, 2001. **133**(8): p. 1263-75.
72. **De Petrocellis, L., C.J. Chu, A.S. Moriello, J.C. Kellner, J.M. Walker, and V. Di Marzo**, *Actions of two naturally occurring saturated N-acyldopamines on transient receptor potential vanilloid 1 (TRPV1) channels.* Br J Pharmacol, 2004. **143**(2): p. 251-6.
73. **Ho, W.S., D.A. Barrett, and M.D. Randall**, *'Entourage' effects of N-palmitoylethanolamide and N-oleoylethanolamide on vasorelaxation to anandamide occur through TRPV1 receptors.* Br J Pharmacol, 2008. **155**(6): p. 837-46.
74. **Godlewski, G., L. Offertaler, J.A. Wagner, and G. Kunos**, *Receptors for acylethanolamides-GPR55 and GPR119.* Prostaglandins Other Lipid Mediat, 2009. **89**(3-4): p. 105-11.
75. **Ryberg, E., N. Larsson, S. Sjogren, S. Hjorth, N.O. Hermansson, J. Leonova, T. Elebring, K. Nilsson, T. Drmota, and P.J. Greasley**, *The orphan receptor GPR55 is a novel cannabinoid receptor.* Br J Pharmacol, 2007. **152**(7): p. 1092-101.
76. **Overton, H.A., A.J. Babbs, S.M. Doel, M.C. Fyfe, L.S. Gardner, G. Griffin, H.C. Jackson, M.J. Procter, C.M. Rasamison, M. Tang-Christensen, P.S. Widdowson, G.M. Williams, and C. Reynet**, *Deorphanization of a G protein-coupled receptor for oleoylethanolamide and its use in the discovery of small-molecule hypophagic agents.* Cell Metab, 2006. **3**(3): p. 167-75.
77. **Sharir, H. and M.E. Abood**, *Pharmacological characterization of GPR55, a putative cannabinoid receptor.* Pharmacol Ther, 2010. **126**(3): p. 301-13.
78. **Sasso, O., R. Russo, S. Vitiello, G.M. Raso, G. D'Agostino, A. Iacono, G.L. Rana, M. Vallee, S. Cuzzocrea, P.V. Piazza, R. Meli, and A. Calignano**, *Implication of allopregnanolone in the antinociceptive effect of N-palmitoylethanolamide in acute or persistent pain.* Pain, 2012. **153**(1): p. 33-41.
79. **Di Paola, R., D. Impellizzeri, A. Torre, E. Mazzon, A. Cappellani, C. Faggio, E. Esposito, F. Trischitta, and S. Cuzzocrea**, *Effects of palmitoylethanolamide on intestinal injury and inflammation caused*

by ischemia-reperfusion in mice. J Leukoc Biol, 2012. **91**(6): p. 911-20.
80. **Fidaleo, M., F. Fanelli, M.P. Ceru, and S. Moreno**, *Neuroprotective properties of peroxisome proliferator-activated receptor alpha (PPARalpha) and its lipid ligands.* Curr Med Chem, 2014. **21**(24): p. 2803-21.
81. **Lombardi, G., G. Miglio, F. Varsaldi, A. Minassi, and G. Appendino**, *Oxyhomologation of the amide bond potentiates neuroprotective effects of the endolipid N-palmitoylethanolamine.* J Pharmacol Exp Ther, 2007. **320**(2): p. 599-606.
82. **Sun, Y., S.P. Alexander, M.J. Garle, C.L. Gibson, K. Hewitt, S.P. Murphy, D.A. Kendall, and A.J. Bennett**, *Cannabinoid activation of PPAR alpha; a novel neuroprotective mechanism.* Br J Pharmacol, 2007. **152**(5): p. 734-43.
83. **Bisogno, T. and V. Di Marzo**, *Cannabinoid receptors and endocannabinoids: role in neuroinflammatory and neurodegenerative disorders.* CNS Neurol Disord Drug Targets, 2010. **9**(5): p. 564-73.
84. **Schomacher, M., H.D. Muller, C. Sommer, S. Schwab, and W.R. Schabitz**, *Endocannabinoids mediate neuroprotection after transient focal cerebral ischemia.* Brain Res, 2008. **1240**: p. 213-20.
85. **Duncan, R.S., K.D. Chapman, and P. Koulen**, *The neuroprotective properties of palmitoylethanolamine against oxidative stress in a neuronal cell line.* Mol Neurodegener, 2009. **4**: p. 50.
86. **Koch, M., S. Kreutz, C. Bottger, A. Benz, E. Maronde, C. Ghadban, H.W. Korf, and F. Dehghani**, *Palmitoylethanolamide protects dentate gyrus granule cells via peroxisome proliferator-activated receptor-alpha.* Neurotox Res, 2011. **19**(2): p. 330-40.
87. **Raso, G.M., E. Esposito, S. Vitiello, A. Iacono, A. Santoro, G. D'Agostino, O. Sasso, R. Russo, P.V. Piazza, A. Calignano, and R. Meli**, *Palmitoylethanolamide stimulation induces allopregnanolone synthesis in C6 Cells and primary astrocytes: involvement of peroxisome-proliferator activated receptor-alpha.* J Neuroendocrinol, 2011. **23**(7): p. 591-600.
88. **Esposito, E., D. Impellizzeri, E. Mazzon, I. Paterniti, and S. Cuzzocrea**, *Neuroprotective activities of palmitoylethanolamide in an animal model of Parkinson's disease.* PLoS One, 2012. **7**(8): p. e41880.
89. **Avagliano, C., R. Russo, C. De Caro, C. Cristiano, G. La Rana, G. Piegari, O. Paciello, R. Citraro, E. Russo, G. De Sarro, R.**

Meli, G. Mattace Raso, and A. Calignano, *Palmitoylethanolamide protects mice against 6-OHDA-induced neurotoxicity and endoplasmic reticulum stress: In vivo and in vitro evidence.* Pharmacol Res, 2016. **113**(Pt A): p. 276-289.

90. **Scuderi, C., G. Esposito, A. Blasio, M. Valenza, P. Arietti, L. Steardo, Jr., R. Carnuccio, D. De Filippis, S. Petrosino, T. Iuvone, V. Di Marzo, and L. Steardo**, *Palmitoylethanolamide counteracts reactive astrogliosis induced by beta-amyloid peptide.* J Cell Mol Med, 2011. **15**(12): p. 2664-74.
91. **D'Agostino, G., R. Russo, C. Avagliano, C. Cristiano, R. Meli, and A. Calignano**, *Palmitoylethanolamide protects against the amyloid-beta25-35-induced learning and memory impairment in mice, an experimental model of Alzheimer disease.* Neuropsychopharmacology, 2012. **37**(7): p. 1784-92.
92. **Yu, H.L., X.Q. Deng, Y.J. Li, Y.C. Li, Z.S. Quan, and X.Y. Sun**, *N-palmitoylethanolamide, an endocannabinoid, exhibits antidepressant effects in the forced swim test and the tail suspension test in mice.* Pharmacol Rep, 2011. **63**(3): p. 834-9.
93. **Crupi, R., I. Paterniti, A. Ahmad, M. Campolo, E. Esposito, and S. Cuzzocrea**, *Effects of palmitoylethanolamide and luteolin in an animal model of anxiety/depression.* CNS Neurol Disord Drug Targets, 2013. **12**(7): p. 989-1001.
94. **Ghazizadeh-Hashemi, M., A. Ghajar, M.R. Shalbafan, F. Ghazizadeh-Hashemi, M. Afarideh, F. Malekpour, A. Ghaleiha, M.E. Ardebili, and S. Akhondzadeh**, *Palmitoylethanolamide as adjunctive therapy in major depressive disorder: A double-blind, randomized and placebo-controlled trial.* J Affect Disord, 2018. **232**: p. 127-133.
95. **Kerr, D.M., L. Downey, M. Conboy, D.P. Finn, and M. Roche**, *Alterations in the endocannabinoid system in the rat valproic acid model of autism.* Behav Brain Res, 2013. **249**: p. 124-32.
96. **Bertolino, B., R. Crupi, D. Impellizzeri, G. Bruschetta, M. Cordaro, R. Siracusa, E. Esposito, and S. Cuzzocrea**, *Beneficial Effects of Co-Ultramicronized Palmitoylethanolamide/Luteolin in a Mouse Model of Autism and in a Case Report of Autism.* CNS Neurosci Ther, 2017. **23**(1): p. 87-98.
97. **Olusanmi, D., D. Jayawickrama, D. Bu, G. McGeorge, H. Sailes, J. Kelleher, J.F. Gamble, U.V. Shah, and M. Tobyn**, *A control strategy for bioavailability enhancement by size reduction: effect of micronization conditions on the bulk, surface and blending*

characteristics of an active pharmaceutical ingredient. Powder Technology, 2014. **258**: p. 222-233.
98. **Joshi, J.T.**, *A review on micronization techniques.* J Pharmaceutical Sci Technol, 2011. **3**: p. 651-681.
99. **Bisrat, M. and C. Nyström**, *Physicochemical aspects of drug release. VIII. The relation between particle size and surface specific dissolution rate in agitated suspensions.* International journal of pharmaceutics, 1988. **47**(1-3): p. 223-231.
100. **Oh, D.-M., R.L. Curl, C.-S. Yong, and G.L. Amidon**, *Effect of micronization on the extent of drug absorption from suspensions in humans.* Archives of Pharmacal Research, 1995. **18**(6): p. 427-433.
101. **Petrosino, S., M. Cordaro, R. Verde, A. Schiano Moriello, G. Marcolongo, C. Schievano, R. Siracusa, F. Piscitelli, A.F. Peritore, R. Crupi, D. Impellizzeri, E. Esposito, S. Cuzzocrea, and V. Di Marzo**, *Oral Ultramicronized Palmitoylethanolamide: Plasma and Tissue Levels and Spinal Anti-hyperalgesic Effect.* Front Pharmacol, 2018. **9**: p. 249.
102. **Association, A.P.**, *Diagnostic and statistical manual of mental disorders (DSM-5®)*. 2013: American Psychiatric Pub.
103. **Lord, C., M. Elsabbagh, G. Baird, and J. Veenstra-Vanderweele**, *Autism spectrum disorder.* Lancet, 2018. **392**(10146): p. 508-520.
104. **Lavelle, T.A., M.C. Weinstein, J.P. Newhouse, K. Munir, K.A. Kuhlthau, and L.A. Prosser**, *Economic burden of childhood autism spectrum disorders.* Pediatrics, 2014. **133**(3): p. e520-9.
105. **Elsabbagh, M., G. Divan, Y.J. Koh, Y.S. Kim, S. Kauchali, C. Marcin, C. Montiel-Nava, V. Patel, C.S. Paula, C. Wang, M.T. Yasamy, and E. Fombonne**, *Global prevalence of autism and other pervasive developmental disorders.* Autism Res, 2012. **5**(3): p. 160-79.
106. **Lyall, K., L. Croen, J. Daniels, M.D. Fallin, C. Ladd-Acosta, B.K. Lee, B.Y. Park, N.W. Snyder, D. Schendel, H. Volk, G.C. Windham, and C. Newschaffer**, *The Changing Epidemiology of Autism Spectrum Disorders.* Annu Rev Public Health, 2017. **38**: p. 81-102.
107. **Tromans, S., V. Chester, R. Kiani, R. Alexander, and T. Brugha**, *The Prevalence of Autism Spectrum Disorders in Adult Psychiatric Inpatients: A Systematic Review.* Clin Pract Epidemiol Ment Health, 2018. **14**: p. 177-187.
108. **Halladay, A.K., S. Bishop, J.N. Constantino, A.M. Daniels, K. Koenig, K. Palmer, D. Messinger, K. Pelphrey, S.J. Sanders, A.T. Singer, J.L. Taylor, and P. Szatmari**, *Sex and gender differences*

in autism spectrum disorder: summarizing evidence gaps and identifying emerging areas of priority. Mol Autism, 2015. **6**: p. 36.

109. **Zerbo, O., C. Yoshida, E.P. Gunderson, K. Dorward, and L.A. Croen**, *Interpregnancy Interval and Risk of Autism Spectrum Disorders.* Pediatrics, 2015. **136**(4): p. 651-7.
110. **Isaksson, J., E. Pettersson, E. Kostrzewa, R. Diaz Heijtz, and S. Bolte**, *Brief Report: Association Between Autism Spectrum Disorder, Gastrointestinal Problems and Perinatal Risk Factors Within Sibling Pairs.* J Autism Dev Disord, 2017. **47**(8): p. 2621-2627.
111. **Lyall, K., P. Ashwood, J. Van de Water, and I. Hertz-Picciotto**, *Maternal immune-mediated conditions, autism spectrum disorders, and developmental delay.* J Autism Dev Disord, 2014. **44**(7): p. 1546-55.
112. **Moore, G.S., A.W. Kneitel, C.K. Walker, W.M. Gilbert, and G. Xing**, *Autism risk in small- and large-for-gestational-age infants.* Am J Obstet Gynecol, 2012. **206**(4): p. 314 e1-9.
113. **Lampi, K.M., L. Lehtonen, P.L. Tran, A. Suominen, V. Lehti, P.N. Banerjee, M. Gissler, A.S. Brown, and A. Sourander**, *Risk of autism spectrum disorders in low birth weight and small for gestational age infants.* J Pediatr, 2012. **161**(5): p. 830-6.
114. **Christensen, J., T.K. Gronborg, M.J. Sorensen, D. Schendel, E.T. Parner, L.H. Pedersen, and M. Vestergaard**, *Prenatal valproate exposure and risk of autism spectrum disorders and childhood autism.* JAMA, 2013. **309**(16): p. 1696-703.
115. **de Theije, C.G., H. Wopereis, M. Ramadan, T. van Eijndthoven, J. Lambert, J. Knol, J. Garssen, A.D. Kraneveld, and R. Oozeer**, *Altered gut microbiota and activity in a murine model of autism spectrum disorders.* Brain Behav Immun, 2014. **37**: p. 197-206.
116. **Brown, H.K., J.G. Ray, A.S. Wilton, Y. Lunsky, T. Gomes, and S.N. Vigod**, *Association Between Serotonergic Antidepressant Use During Pregnancy and Autism Spectrum Disorder in Children.* JAMA, 2017. **317**(15): p. 1544-1552.
117. **Zerbo, O., Y. Qian, C. Yoshida, B.H. Fireman, N.P. Klein, and L.A. Croen**, *Association Between Influenza Infection and Vaccination During Pregnancy and Risk of Autism Spectrum Disorder.* JAMA Pediatr, 2017. **171**(1): p. e163609.
118. **Tick, B., P. Bolton, F. Happe, M. Rutter, and F. Rijsdijk**, *Heritability of autism spectrum disorders: a meta-analysis of twin studies.* J Child Psychol Psychiatry, 2016. **57**(5): p. 585-95.

119. **Niu, M., Y. Han, A.B.C. Dy, J. Du, H. Jin, J. Qin, J. Zhang, Q. Li, and R.J. Hagerman**, *Autism Symptoms in Fragile X Syndrome.* J Child Neurol, 2017. **32**(10): p. 903-909.
120. **Geschwind, D.H. and M.W. State**, *Gene hunting in autism spectrum disorder: on the path to precision medicine.* Lancet Neurol, 2015. **14**(11): p. 1109-20.
121. **Weitlauf, A.S., M.L. McPheeters, B. Peters, N. Sathe, R. Travis, R. Aiello, E. Williamson, J. Veenstra-VanderWeele, S. Krishnaswami, R. Jerome, and Z. Warren**, in *Therapies for Children With Autism Spectrum Disorder: Behavioral Interventions Update*. 2014: Rockville (MD).
122. **Reichow, B., K. Hume, E.E. Barton, and B.A. Boyd**, *Early intensive behavioral intervention (EIBI) for young children with autism spectrum disorders (ASD).* Cochrane Database Syst Rev, 2018. **5**: p. CD009260.
123. **Gates, J.A., E. Kang, and M.D. Lerner**, *Efficacy of group social skills interventions for youth with autism spectrum disorder: A systematic review and meta-analysis.* Clin Psychol Rev, 2017. **52**: p. 164-181.
124. **Kent, J.M., S. Kushner, X. Ning, K. Karcher, S. Ness, M. Aman, J. Singh, and D. Hough**, *Risperidone dosing in children and adolescents with autistic disorder: a double-blind, placebo-controlled study.* J Autism Dev Disord, 2013. **43**(8): p. 1773-83.
125. **Owen, R., L. Sikich, R.N. Marcus, P. Corey-Lisle, G. Manos, R.D. McQuade, W.H. Carson, and R.L. Findling**, *Aripiprazole in the treatment of irritability in children and adolescents with autistic disorder.* Pediatrics, 2009. **124**(6): p. 1533-40.
126. **Politte, L.C. and C.J. McDougle**, *Atypical antipsychotics in the treatment of children and adolescents with pervasive developmental disorders.* Psychopharmacology (Berl), 2014. **231**(6): p. 1023-36.
127. **Kelly, J.R., C. Minuto, J.F. Cryan, G. Clarke, and T.G. Dinan**, *Cross Talk: The Microbiota and Neurodevelopmental Disorders.* Front Neurosci, 2017. **11**: p. 490.
128. **Cryan, J.F. and T.G. Dinan**, *Mind-altering microorganisms: the impact of the gut microbiota on brain and behaviour.* Nat Rev Neurosci, 2012. **13**(10): p. 701-12.
129. **Dinan, T.G., R.M. Stilling, C. Stanton, and J.F. Cryan**, *Collective unconscious: how gut microbes shape human behavior.* J Psychiatr Res, 2015. **63**: p. 1-9.
130. **Clarke, G., S. Grenham, P. Scully, P. Fitzgerald, R.D. Moloney, F. Shanahan, T.G. Dinan, and J.F. Cryan**, *The microbiome-gut-*

brain axis during early life regulates the hippocampal serotonergic system in a sex-dependent manner. Mol Psychiatry, 2013. **18**(6): p. 666-73.

131. **de Magistris, L., V. Familiari, A. Pascotto, A. Sapone, A. Frolli, P. Iardino, M. Carteni, M. De Rosa, R. Francavilla, G. Riegler, R. Militerni, and C. Bravaccio**, *Alterations of the intestinal barrier in patients with autism spectrum disorders and in their first-degree relatives.* J Pediatr Gastroenterol Nutr, 2010. **51**(4): p. 418-24.
132. **Fiorentino, M., A. Sapone, S. Senger, S.S. Camhi, S.M. Kadzielski, T.M. Buie, D.L. Kelly, N. Cascella, and A. Fasano**, *Blood-brain barrier and intestinal epithelial barrier alterations in autism spectrum disorders.* Mol Autism, 2016. **7**: p. 49.
133. **Yarandi, S.S., D.A. Peterson, G.J. Treisman, T.H. Moran, and P.J. Pasricha**, *Modulatory Effects of Gut Microbiota on the Central Nervous System: How Gut Could Play a Role in Neuropsychiatric Health and Diseases.* J Neurogastroenterol Motil, 2016. **22**(2): p. 201-12.
134. **Ashwood, P., P. Krakowiak, I. Hertz-Picciotto, R. Hansen, I. Pessah, and J. Van de Water**, *Elevated plasma cytokines in autism spectrum disorders provide evidence of immune dysfunction and are associated with impaired behavioral outcome.* Brain Behav Immun, 2011. **25**(1): p. 40-5.
135. **Desbonnet, L., G. Clarke, F. Shanahan, T.G. Dinan, and J.F. Cryan**, *Microbiota is essential for social development in the mouse.* Mol Psychiatry, 2014. **19**(2): p. 146-8.
136. **Stilling, R.M., F.J. Ryan, A.E. Hoban, F. Shanahan, G. Clarke, M.J. Claesson, T.G. Dinan, and J.F. Cryan**, *Microbes & neurodevelopment--Absence of microbiota during early life increases activity-related transcriptional pathways in the amygdala.* Brain Behav Immun, 2015. **50**: p. 209-220.
137. **Tomova, A., V. Husarova, S. Lakatosova, J. Bakos, B. Vlkova, K. Babinska, and D. Ostatnikova**, *Gastrointestinal microbiota in children with autism in Slovakia.* Physiol Behav, 2015. **138**: p. 179-87.
138. **Strati, F., D. Cavalieri, D. Albanese, C. De Felice, C. Donati, J. Hayek, O. Jousson, S. Leoncini, D. Renzi, A. Calabro, and C. De Filippo**, *New evidences on the altered gut microbiota in autism spectrum disorders.* Microbiome, 2017. **5**(1): p. 24.
139. **Son, J.S., L.J. Zheng, L.M. Rowehl, X. Tian, Y. Zhang, W. Zhu, L. Litcher-Kelly, K.D. Gadow, G. Gathungu, C.E. Robertson, D. Ir, D.N. Frank, and E. Li**, *Comparison of Fecal Microbiota in*

Children with Autism Spectrum Disorders and Neurotypical Siblings in the Simons Simplex Collection. PLoS One, 2015. **10**(10): p. e0137725.

140. **Otte, C., S.M. Gold, B.W. Penninx, C.M. Pariante, A. Etkin, M. Fava, D.C. Mohr, and A.F. Schatzberg**, *Major depressive disorder.* Nat Rev Dis Primers, 2016. **2**: p. 16065.
141. **Global Burden of Disease Study, C.**, *Global, regional, and national incidence, prevalence, and years lived with disability for 301 acute and chronic diseases and injuries in 188 countries, 1990-2013: a systematic analysis for the Global Burden of Disease Study 2013.* Lancet, 2015. **386**(9995): p. 743-800.
142. **Seedat, S., K.M. Scott, M.C. Angermeyer, P. Berglund, E.J. Bromet, T.S. Brugha, K. Demyttenaere, G. de Girolamo, J.M. Haro, R. Jin, E.G. Karam, V. Kovess-Masfety, D. Levinson, M.E. Medina Mora, Y. Ono, J. Ormel, B.E. Pennell, J. Posada-Villa, N.A. Sampson, D. Williams, and R.C. Kessler**, *Cross-national associations between gender and mental disorders in the World Health Organization World Mental Health Surveys.* Arch Gen Psychiatry, 2009. **66**(7): p. 785-95.
143. **Bromet, E., L.H. Andrade, I. Hwang, N.A. Sampson, J. Alonso, G. de Girolamo, R. de Graaf, K. Demyttenaere, C. Hu, N. Iwata, A.N. Karam, J. Kaur, S. Kostyuchenko, J.P. Lepine, D. Levinson, H. Matschinger, M.E. Mora, M.O. Browne, J. Posada-Villa, M.C. Viana, D.R. Williams, and R.C. Kessler**, *Cross-national epidemiology of DSM-IV major depressive episode.* BMC Med, 2011. **9**: p. 90.
144. **Kessler, R.C. and E.J. Bromet**, *The epidemiology of depression across cultures.* Annu Rev Public Health, 2013. **34**: p. 119-38.
145. **Hovens, J.G., E.J. Giltay, J.E. Wiersma, P. Spinhoven, B.W. Penninx, and F.G. Zitman**, *Impact of childhood life events and trauma on the course of depressive and anxiety disorders.* Acta Psychiatr Scand, 2012. **126**(3): p. 198-207.
146. **Spijker, J., R. de Graaf, R.V. Bijl, A.T. Beekman, J. Ormel, and W.A. Nolen**, *Duration of major depressive episodes in the general population: results from The Netherlands Mental Health Survey and Incidence Study (NEMESIS).* Br J Psychiatry, 2002. **181**: p. 208-13.
147. **Keller, M.B., P.W. Lavori, T.I. Mueller, J. Endicott, W. Coryell, R.M. Hirschfeld, and T. Shea**, *Time to recovery, chronicity, and levels of psychopathology in major depression. A 5-year prospective follow-up of 431 subjects.* Arch Gen Psychiatry, 1992. **49**(10): p. 809-16.

148. **Boschloo, L., R.A. Schoevers, A.T. Beekman, J.H. Smit, A.M. van Hemert, and B.W. Penninx**, *The four-year course of major depressive disorder: the role of staging and risk factor determination.* Psychother Psychosom, 2014. **83**(5): p. 279-88.
149. **Wells, K.B., M.A. Burnam, W. Rogers, R. Hays, and P. Camp**, *The course of depression in adult outpatients. Results from the Medical Outcomes Study.* Arch Gen Psychiatry, 1992. **49**(10): p. 788-94.
150. **Vos, T., M.M. Haby, J.J. Barendregt, M. Kruijshaar, J. Corry, and G. Andrews**, *The burden of major depression avoidable by longer-term treatment strategies.* Arch Gen Psychiatry, 2004. **61**(11): p. 1097-103.
151. **Cuijpers, P., N. Vogelzangs, J. Twisk, A. Kleiboer, J. Li, and B.W. Penninx**, *Comprehensive meta-analysis of excess mortality in depression in the general community versus patients with specific illnesses.* Am J Psychiatry, 2014. **171**(4): p. 453-62.
152. **Walker, E.R., R.E. McGee, and B.G. Druss**, *Mortality in mental disorders and global disease burden implications: a systematic review and meta-analysis.* JAMA Psychiatry, 2015. **72**(4): p. 334-41.
153. **Geschwind, D.H. and J. Flint**, *Genetics and genomics of psychiatric disease.* Science, 2015. **349**(6255): p. 1489-94.
154. **Kessler, R.C.**, *The effects of stressful life events on depression.* Annu Rev Psychol, 1997. **48**: p. 191-214.
155. **Li, M., C. D'Arcy, and X. Meng**, *Maltreatment in childhood substantially increases the risk of adult depression and anxiety in prospective cohort studies: systematic review, meta-analysis, and proportional attributable fractions.* Psychol Med, 2016. **46**(4): p. 717-30.
156. **Quan, N. and W.A. Banks**, *Brain-immune communication pathways.* Brain Behav Immun, 2007. **21**(6): p. 727-35.
157. **Pralong, E., P. Magistretti, and R. Stoop**, *Cellular perspectives on the glutamate-monoamine interactions in limbic lobe structures and their relevance for some psychiatric disorders.* Prog Neurobiol, 2002. **67**(3): p. 173-202.
158. **Meaney, M.J.**, *Maternal care, gene expression, and the transmission of individual differences in stress reactivity across generations.* Annu Rev Neurosci, 2001. **24**: p. 1161-92.
159. **Stetler, C. and G.E. Miller**, *Depression and hypothalamic-pituitary-adrenal activation: a quantitative summary of four decades of research.* Psychosom Med, 2011. **73**(2): p. 114-26.

160. **Goodyer, I.M., J. Herbert, A. Tamplin, and P.M. Altham**, *Recent life events, cortisol, dehydroepiandrosterone and the onset of major depression in high-risk adolescents.* Br J Psychiatry, 2000. **177**: p. 499-504.
161. **Harris, T.O., S. Borsanyi, S. Messari, K. Stanford, S.E. Cleary, H.M. Shiers, G.W. Brown, and J. Herbert**, *Morning cortisol as a risk factor for subsequent major depressive disorder in adult women.* Br J Psychiatry, 2000. **177**: p. 505-10.
162. **Myint, A.M., M.J. Schwarz, H.W. Steinbusch, and B.E. Leonard**, *Neuropsychiatric disorders related to interferon and interleukins treatment.* Metab Brain Dis, 2009. **24**(1): p. 55-68.
163. **Haapakoski, R., J. Mathieu, K.P. Ebmeier, H. Alenius, and M. Kivimaki**, *Cumulative meta-analysis of interleukins 6 and 1beta, tumour necrosis factor alpha and C-reactive protein in patients with major depressive disorder.* Brain Behav Immun, 2015. **49**: p. 206-15.
164. **Dowlati, Y., N. Herrmann, W. Swardfager, H. Liu, L. Sham, E.K. Reim, and K.L. Lanctot**, *A meta-analysis of cytokines in major depression.* Biol Psychiatry, 2010. **67**(5): p. 446-57.
165. **Oglodek, E., A. Szota, M. Just, D. Mos, and A. Araszkiewicz**, *The role of the neuroendocrine and immune systems in the pathogenesis of depression.* Pharmacol Rep, 2014. **66**(5): p. 776-81.
166. **Luppino, F.S., L.M. de Wit, P.F. Bouvy, T. Stijnen, P. Cuijpers, B.W. Penninx, and F.G. Zitman**, *Overweight, obesity, and depression: a systematic review and meta-analysis of longitudinal studies.* Arch Gen Psychiatry, 2010. **67**(3): p. 220-9.
167. **Vogelzangs, N., S.B. Kritchevsky, A.T. Beekman, A.B. Newman, S. Satterfield, E.M. Simonsick, K. Yaffe, T.B. Harris, and B.W. Penninx**, *Depressive symptoms and change in abdominal obesity in older persons.* Arch Gen Psychiatry, 2008. **65**(12): p. 1386-93.
168. **Faith, M.S., M. Butryn, T.A. Wadden, A. Fabricatore, A.M. Nguyen, and S.B. Heymsfield**, *Evidence for prospective associations among depression and obesity in population-based studies.* Obes Rev, 2011. **12**(5): p. e438-53.
169. **Williams, L.M.**, *Hypothalamic dysfunction in obesity.* Proc Nutr Soc, 2012. **71**(4): p. 521-33.
170. **Shin, A.C., H. Zheng, and H.R. Berthoud**, *An expanded view of energy homeostasis: neural integration of metabolic, cognitive, and emotional drives to eat.* Physiol Behav, 2009. **97**(5): p. 572-80.

171. **Lutter, M. and J. Elmquist**, *Depression and metabolism: linking changes in leptin and ghrelin to mood.* F1000 Biol Rep, 2009. **1**: p. 63.
172. **Schellekens, H., B.C. Finger, T.G. Dinan, and J.F. Cryan**, *Ghrelin signalling and obesity: at the interface of stress, mood and food reward.* Pharmacol Ther, 2012. **135**(3): p. 316-26.
173. **Lu, X.Y.**, *The leptin hypothesis of depression: a potential link between mood disorders and obesity?* Curr Opin Pharmacol, 2007. **7**(6): p. 648-52.
174. **Jow, G.M., T.T. Yang, and C.L. Chen**, *Leptin and cholesterol levels are low in major depressive disorder, but high in schizophrenia.* J Affect Disord, 2006. **90**(1): p. 21-7.
175. **Lu, X.Y., C.S. Kim, A. Frazer, and W. Zhang**, *Leptin: a potential novel antidepressant.* Proc Natl Acad Sci U S A, 2006. **103**(5): p. 1593-8.
176. **Kraus, T., M. Haack, A. Schuld, D. Hinze-Selch, and T. Pollmacher**, *Low leptin levels but normal body mass indices in patients with depression or schizophrenia.* Neuroendocrinology, 2001. **73**(4): p. 243-7.
177. **Maes, M., M. Kubera, and J.C. Leunis**, *The gut-brain barrier in major depression: intestinal mucosal dysfunction with an increased translocation of LPS from gram negative enterobacteria (leaky gut) plays a role in the inflammatory pathophysiology of depression.* Neuro Endocrinol Lett, 2008. **29**(1): p. 117-24.
178. **Maes, M., I. Mihaylova, and J.C. Leunis**, *Increased serum IgA and IgM against LPS of enterobacteria in chronic fatigue syndrome (CFS): indication for the involvement of gram-negative enterobacteria in the etiology of CFS and for the presence of an increased gut-intestinal permeability.* J Affect Disord, 2007. **99**(1-3): p. 237-40.
179. **Dantzer, R., J.C. O'Connor, G.G. Freund, R.W. Johnson, and K.W. Kelley**, *From inflammation to sickness and depression: when the immune system subjugates the brain.* Nat Rev Neurosci, 2008. **9**(1): p. 46-56.
180. **Wright, C.E., P.C. Strike, L. Brydon, and A. Steptoe**, *Acute inflammation and negative mood: mediation by cytokine activation.* Brain Behav Immun, 2005. **19**(4): p. 345-50.
181. **Lyte, M.**, *Probiotics function mechanistically as delivery vehicles for neuroactive compounds: Microbial endocrinology in the design and use of probiotics.* Bioessays, 2011. **33**(8): p. 574-81.

182. **Bercik, P., E. Denou, J. Collins, W. Jackson, J. Lu, J. Jury, Y. Deng, P. Blennerhassett, J. Macri, K.D. McCoy, E.F. Verdu, and S.M. Collins**, *The intestinal microbiota affect central levels of brain-derived neurotropic factor and behavior in mice.* Gastroenterology, 2011. **141**(2): p. 599-609, 609 e1-3.
183. **van Zoonen, K., C. Buntrock, D.D. Ebert, F. Smit, C.F. Reynolds, 3rd, A.T. Beekman, and P. Cuijpers**, *Preventing the onset of major depressive disorder: a meta-analytic review of psychological interventions.* Int J Epidemiol, 2014. **43**(2): p. 318-29.
184. **Härter, M., C. Klesse, I. Bermejo, F. Schneider, and M. Berger**, *Unipolar depression: diagnostic and therapeutic recommendations from the current S3/National Clinical Practice Guideline.* Deutsches Ärzteblatt International, 2010. **107**(40): p. 700.
185. **Cuijpers, P., A. van Straten, G. Andersson, and P. van Oppen**, *Psychotherapy for depression in adults: a meta-analysis of comparative outcome studies.* J Consult Clin Psychol, 2008. **76**(6): p. 909-22.
186. **Cuijpers, P., M. Berking, G. Andersson, L. Quigley, A. Kleiboer, and K.S. Dobson**, *A meta-analysis of cognitive-behavioural therapy for adult depression, alone and in comparison with other treatments.* Can J Psychiatry, 2013. **58**(7): p. 376-85.
187. **Linde, K., G. Rucker, K. Sigterman, S. Jamil, K. Meissner, A. Schneider, and L. Kriston**, *Comparative effectiveness of psychological treatments for depressive disorders in primary care: network meta-analysis.* BMC Fam Pract, 2015. **16**: p. 103.
188. **Cassano, P. and M. Fava**, *Tolerability issues during long-term treatment with antidepressants.* Ann Clin Psychiatry, 2004. **16**(1): p. 15-25.
189. **Bailey, K., J. Crawley, and J. Buccafusco**, *Methods of behavior analysis in neuroscience.* Anxiety-Related Behaviors in Mice, 2nd ed.(Buccafusco, JJ ed.), CRC Press/Taylor & Francis LCC, Boca Raton, 2009: p. 77-101.
190. **Crawley, J.N.**, *Designing mouse behavioral tasks relevant to autistic-like behaviors.* Ment Retard Dev Disabil Res Rev, 2004. **10**(4): p. 248-58.
191. **Moy, S.S., J.J. Nadler, M.D. Poe, R.J. Nonneman, N.B. Young, B.H. Koller, J.N. Crawley, G.E. Duncan, and J.W. Bodfish**, *Development of a mouse test for repetitive, restricted behaviors: relevance to autism.* Behav Brain Res, 2008. **188**(1): p. 178-94.

192. **McFarlane, H.G., G.K. Kusek, M. Yang, J.L. Phoenix, V.J. Bolivar, and J.N. Crawley**, *Autism-like behavioral phenotypes in BTBR T+tf/J mice.* Genes Brain Behav, 2008. **7**(2): p. 152-63.
193. **Cani, P.D., S. Possemiers, T. Van de Wiele, Y. Guiot, A. Everard, O. Rottier, L. Geurts, D. Naslain, A. Neyrinck, D.M. Lambert, G.G. Muccioli, and N.M. Delzenne**, *Changes in gut microbiota control inflammation in obese mice through a mechanism involving GLP-2-driven improvement of gut permeability.* Gut, 2009. **58**(8): p. 1091-103.
194. **Zhang, J., K. Kobert, T. Flouri, and A. Stamatakis**, *PEAR: a fast and accurate Illumina Paired-End reAd mergeR.* Bioinformatics, 2014. **30**(5): p. 614-20.
195. **Schmieder, R. and R. Edwards**, *Quality control and preprocessing of metagenomic datasets.* Bioinformatics, 2011. **27**(6): p. 863-4.
196. **Caporaso, J.G., J. Kuczynski, J. Stombaugh, K. Bittinger, F.D. Bushman, E.K. Costello, N. Fierer, A.G. Pena, J.K. Goodrich, J.I. Gordon, G.A. Huttley, S.T. Kelley, D. Knights, J.E. Koenig, R.E. Ley, C.A. Lozupone, D. McDonald, B.D. Muegge, M. Pirrung, J. Reeder, J.R. Sevinsky, P.J. Turnbaugh, W.A. Walters, J. Widmann, T. Yatsunenko, J. Zaneveld, and R. Knight**, *QIIME allows analysis of high-throughput community sequencing data.* Nat Methods, 2010. **7**(5): p. 335-6.
197. **DeSantis, T.Z., P. Hugenholtz, N. Larsen, M. Rojas, E.L. Brodie, K. Keller, T. Huber, D. Dalevi, P. Hu, and G.L. Andersen**, *Greengenes, a chimera-checked 16S rRNA gene database and workbench compatible with ARB.* Appl Environ Microbiol, 2006. **72**(7): p. 5069-72.
198. **Clarke, K.R.**, *Non-parametric multivariate analyses of changes in community structure.* Australian journal of ecology, 1993. **18**(1): p. 117-143.
199. **White, J.R., N. Nagarajan, and M. Pop**, *Statistical methods for detecting differentially abundant features in clinical metagenomic samples.* PLoS computational biology, 2009. **5**(4): p. e1000352.
200. **Segata, N., J. Izard, L. Waldron, D. Gevers, L. Miropolsky, W.S. Garrett, and C. Huttenhower**, *Metagenomic biomarker discovery and explanation.* Genome biology, 2011. **12**(6): p. R60.
201. **Paylor, R., C.M. Spencer, L.A. Yuva-Paylor, and S. Pieke-Dahl**, *The use of behavioral test batteries, II: effect of test interval.* Physiol Behav, 2006. **87**(1): p. 95-102.
202. **Stanford, S.C.**, *The Open Field Test: reinventing the wheel.* J Psychopharmacol, 2007. **21**(2): p. 134-5.

203. **Hartree, E.F.**, *Determination of protein: a modification of the Lowry method that gives a linear photometric response.* Anal Biochem, 1972. **48**(2): p. 422-7.
204. **Cairns, C.B., J. Walther, A.H. Harken, and A. Banerjee**, *Mitochondrial oxidative phosphorylation thermodynamic efficiencies reflect physiological organ roles.* Am J Physiol, 1998. **274**(5 Pt 2): p. R1376-83.
205. **Alexson, S.E. and J. Nedergaard**, *A novel type of short- and medium-chain acyl-CoA hydrolases in brown adipose tissue mitochondria.* J Biol Chem, 1988. **263**(27): p. 13564-71.
206. **Hausladen, A. and I. Fridovich**, *Measuring nitric oxide and superoxide: rate constants for aconitase reactivity.* Methods Enzymol, 1996. **269**: p. 37-41.
207. **Flohe, L. and F. Otting**, *Superoxide dismutase assays.* Methods Enzymol, 1984. **105**: p. 93-104.
208. **Montoliu, C., S. Valles, J. Renau-Piqueras, and C. Guerri**, *Ethanol-induced oxygen radical formation and lipid peroxidation in rat brain: effect of chronic alcohol consumption.* J Neurochem, 1994. **63**(5): p. 1855-62.
209. **Porsolt, R.D., M. Le Pichon, and M. Jalfre**, *Depression: a new animal model sensitive to antidepressant treatments.* Nature, 1977. **266**(5604): p. 730-2.
210. **Porsolt, R.D., A. Bertin, N. Blavet, M. Deniel, and M. Jalfre**, *Immobility induced by forced swimming in rats: effects of agents which modify central catecholamine and serotonin activity.* Eur J Pharmacol, 1979. **57**(2-3): p. 201-10.
211. **Lin, S.H., W.C. Chen, K.H. Lu, P.J. Chen, S.C. Hsieh, T.M. Pan, S.T. Chen, and L.Y. Sheen**, *Down-regulation of Slit-Robo pathway mediating neuronal cytoskeletal remodeling processes facilitates the antidepressive-like activity of Gastrodia elata Blume.* J Agric Food Chem, 2014. **62**(43): p. 10493-503.
212. **Borsini, F., A. Lecci, A. Sessarego, R. Frassine, and A. Meli**, *Discovery of antidepressant activity by forced swimming test may depend on pre-exposure of rats to a stressful situation.* Psychopharmacology (Berl), 1989. **97**(2): p. 183-8.
213. **Matsuno, K., T. Kobayashi, M.K. Tanaka, and S. Mita**, *Sigma 1 receptor subtype is involved in the relief of behavioral despair in the mouse forced swimming test.* Eur J Pharmacol, 1996. **312**(3): p. 267-71.
214. **Can, A., D.T. Dao, C.E. Terrillion, S.C. Piantadosi, S. Bhat, and T.D. Gould**, *The tail suspension test.* J Vis Exp, 2012(59): p. e3769.

215. **Zhu, W., Y. Gao, C.F. Chang, J.R. Wan, S.S. Zhu, and J. Wang**, *Mouse models of intracerebral hemorrhage in ventricle, cortex, and hippocampus by injections of autologous blood or collagenase.* PLoS One, 2014. **9**(5): p. e97423.
216. **Li, S., Y.X. Fan, W. Wang, and Y.Y. Tang**, *Effects of acute restraint stress on different components of memory as assessed by object-recognition and object-location tasks in mice.* Behavioural Brain Research, 2012. **227**(1): p. 199-207.
217. **Bevins, R.A. and J. Besheer**, *Object recognition in rats and mice: a one-trial non-matching-to-sample learning task to study 'recognition memory'.* Nat Protoc, 2006. **1**(3): p. 1306-11.
218. **Estes, M.L. and A.K. McAllister**, *Immune mediators in the brain and peripheral tissues in autism spectrum disorder.* Nat Rev Neurosci, 2015. **16**(8): p. 469-86.
219. **Scattoni, M.L., A. Martire, G. Cartocci, A. Ferrante, and L. Ricceri**, *Reduced social interaction, behavioural flexibility and BDNF signalling in the BTBR T+ tf/J strain, a mouse model of autism.* Behav Brain Res, 2013. **251**: p. 35-40.
220. **Heo, Y., Y. Zhang, D. Gao, V.M. Miller, and D.A. Lawrence**, *Aberrant immune responses in a mouse with behavioral disorders.* PLoS One, 2011. **6**(7): p. e20912.
221. **Theoharides, T.C., I. Tsilioni, A.B. Patel, and R. Doyle**, *Atopic diseases and inflammation of the brain in the pathogenesis of autism spectrum disorders.* Transl Psychiatry, 2016. **6**(6): p. e844.
222. **Bjorkholm, C. and L.M. Monteggia**, *BDNF - a key transducer of antidepressant effects.* Neuropharmacology, 2016. **102**: p. 72-9.
223. **Bell, R.D. and B.V. Zlokovic**, *Neurovascular mechanisms and blood-brain barrier disorder in Alzheimer's disease.* Acta Neuropathol, 2009. **118**(1): p. 103-13.
224. **Waye, M.M.Y. and H.Y. Cheng**, *Genetics and epigenetics of autism: A Review.* Psychiatry Clin Neurosci, 2018. **72**(4): p. 228-244.
225. **Kohane, I.S., A. McMurry, G. Weber, D. MacFadden, L. Rappaport, L. Kunkel, J. Bickel, N. Wattanasin, S. Spence, S. Murphy, and S. Churchill**, *The co-morbidity burden of children and young adults with autism spectrum disorders.* PLoS One, 2012. **7**(4): p. e33224.
226. **Antshel, K.M., Y. Zhang-James, K.E. Wagner, A. Ledesma, and S.V. Faraone**, *An update on the comorbidity of ADHD and ASD: a focus on clinical management.* Expert Rev Neurother, 2016. **16**(3): p. 279-93.

227. **Adams, J.B., L.J. Johansen, L.D. Powell, D. Quig, and R.A. Rubin**, *Gastrointestinal flora and gastrointestinal status in children with autism--comparisons to typical children and correlation with autism severity.* BMC Gastroenterol, 2011. **11**: p. 22.
228. **Fulceri, F., M. Morelli, E. Santocchi, H. Cena, T. Del Bianco, A. Narzisi, S. Calderoni, and F. Muratori**, *Gastrointestinal symptoms and behavioral problems in preschoolers with Autism Spectrum Disorder.* Dig Liver Dis, 2016. **48**(3): p. 248-54.
229. **Wasilewska, J. and M. Klukowski**, *Gastrointestinal symptoms and autism spectrum disorder: links and risks - a possible new overlap syndrome.* Pediatric Health Med Ther, 2015. **6**: p. 153-166.
230. **Sandler, R.H., S.M. Finegold, E.R. Bolte, C.P. Buchanan, A.P. Maxwell, M.L. Vaisanen, M.N. Nelson, and H.M. Wexler**, *Short-term benefit from oral vancomycin treatment of regressive-onset autism.* J Child Neurol, 2000. **15**(7): p. 429-35.
231. **Parracho, H.M., G.R. Gibson, F. Knott, D. Bosscher, M. Kleerebezem, and A.L. McCartney**, *A double-blind, placebo-controlled, crossover-designed probiotic feeding study in children diagnosed with autistic spectrum disorders.* International Journal of Probiotics & Prebiotics, 2010. **5**(2): p. 69.
232. **Emanuele, E., P. Orsi, M. Boso, D. Broglia, N. Brondino, F. Barale, S.U. di Nemi, and P. Politi**, *Low-grade endotoxemia in patients with severe autism.* Neurosci Lett, 2010. **471**(3): p. 162-5.
233. **Finegold, S.M., S.E. Dowd, V. Gontcharova, C. Liu, K.E. Henley, R.D. Wolcott, E. Youn, P.H. Summanen, D. Granpeesheh, D. Dixon, M. Liu, D.R. Molitoris, and J.A. Green, 3rd**, *Pyrosequencing study of fecal microflora of autistic and control children.* Anaerobe, 2010. **16**(4): p. 444-53.
234. **Williams, B.L., M. Hornig, T. Buie, M.L. Bauman, M. Cho Paik, I. Wick, A. Bennett, O. Jabado, D.L. Hirschberg, and W.I. Lipkin**, *Impaired carbohydrate digestion and transport and mucosal dysbiosis in the intestines of children with autism and gastrointestinal disturbances.* PLoS One, 2011. **6**(9): p. e24585.
235. **Wang, L., C.T. Christophersen, M.J. Sorich, J.P. Gerber, M.T. Angley, and M.A. Conlon**, *Increased abundance of Sutterella spp. and Ruminococcus torques in feces of children with autism spectrum disorder.* Mol Autism, 2013. **4**(1): p. 42.
236. **Williams, B.L., M. Hornig, T. Parekh, and W.I. Lipkin**, *Application of novel PCR-based methods for detection, quantitation, and phylogenetic characterization of Sutterella species in intestinal*

biopsy samples from children with autism and gastrointestinal disturbances. MBio, 2012. **3**(1).

237. **Onore, C.E., M. Careaga, B.A. Babineau, J.J. Schwartzer, R.F. Berman, and P. Ashwood**, *Inflammatory macrophage phenotype in BTBR T+tf/J mice.* Front Neurosci, 2013. **7**: p. 158.
238. **Antonucci, N., A. Cirillo, and D. Siniscalco**, *Beneficial Effects of Palmitoylethanolamide on Expressive Language, Cognition, and Behaviors in Autism: A Report of Two Cases.* Case Rep Psychiatry, 2015. **2015**: p. 325061.
239. **D'Agostino, G., C. Cristiano, D.J. Lyons, R. Citraro, E. Russo, C. Avagliano, R. Russo, G.M. Raso, R. Meli, G. De Sarro, L.K. Heisler, and A. Calignano**, *Peroxisome proliferator-activated receptor alpha plays a crucial role in behavioral repetition and cognitive flexibility in mice.* Mol Metab, 2015. **4**(7): p. 528-36.
240. **Greene-Schloesser, D., V. Payne, A.M. Peiffer, F.C. Hsu, D.R. Riddle, W. Zhao, M.D. Chan, L. Metheny-Barlow, and M.E. Robbins**, *The peroxisomal proliferator-activated receptor (PPAR) alpha agonist, fenofibrate, prevents fractionated whole-brain irradiation-induced cognitive impairment.* Radiat Res, 2014. **181**(1): p. 33-44.
241. **Xuan, A.G., Y. Chen, D.H. Long, M. Zhang, W.D. Ji, W.J. Zhang, J.H. Liu, L.P. Hong, X.S. He, and W.L. Chen**, *PPARalpha Agonist Fenofibrate Ameliorates Learning and Memory Deficits in Rats Following Global Cerebral Ischemia.* Mol Neurobiol, 2015. **52**(1): p. 601-9.
242. **Daimon, C.M., J.M. Jasien, W.H. Wood, 3rd, Y. Zhang, K.G. Becker, J.L. Silverman, J.N. Crawley, B. Martin, and S. Maudsley**, *Hippocampal Transcriptomic and Proteomic Alterations in the BTBR Mouse Model of Autism Spectrum Disorder.* Front Physiol, 2015. **6**: p. 324.
243. **Stephenson, D.T., S.M. O'Neill, S. Narayan, A. Tiwari, E. Arnold, H.D. Samaroo, F. Du, R.H. Ring, B. Campbell, M. Pletcher, V.A. Vaidya, and D. Morton**, *Histopathologic characterization of the BTBR mouse model of autistic-like behavior reveals selective changes in neurodevelopmental proteins and adult hippocampal neurogenesis.* Mol Autism, 2011. **2**(1): p. 7.
244. **Duman, R.S.**, *Synaptic plasticity and mood disorders.* Mol Psychiatry, 2002. **7 Suppl 1**: p. S29-34.
245. **Liu, H., P. Talalay, and J.W. Fahey**, *Biomarker-Guided Strategy for Treatment of Autism Spectrum Disorder (ASD).* CNS Neurol Disord Drug Targets, 2016. **15**(5): p. 602-13.

246. **Pei, L. and D.C. Wallace**, *Mitochondrial Etiology of Neuropsychiatric Disorders.* Biol Psychiatry, 2018. **83**(9): p. 722-730.
247. **Anitha, A., K. Nakamura, I. Thanseem, H. Matsuzaki, T. Miyachi, M. Tsujii, Y. Iwata, K. Suzuki, T. Sugiyama, and N. Mori**, *Downregulation of the expression of mitochondrial electron transport complex genes in autism brains.* Brain Pathol, 2013. **23**(3): p. 294-302.
248. **Ohja, K., E. Gozal, M. Fahnestock, L. Cai, J. Cai, J.H. Freedman, A. Switala, A. El-Baz, and G.N. Barnes**, *Neuroimmunologic and Neurotrophic Interactions in Autism Spectrum Disorders: Relationship to Neuroinflammation.* Neuromolecular Med, 2018. **20**(2): p. 161-173.
249. **Cipriani, C., L. Ricceri, C. Matteucci, A. De Felice, A.M. Tartaglione, A. Argaw-Denboba, F. Pica, S. Grelli, G. Calamandrei, P. Sinibaldi Vallebona, and E. Balestrieri**, *High expression of Endogenous Retroviruses from intrauterine life to adulthood in two mouse models of Autism Spectrum Disorders.* Sci Rep, 2018. **8**(1): p. 629.
250. **Canani, R.B., M.D. Costanzo, L. Leone, M. Pedata, R. Meli, and A. Calignano**, *Potential beneficial effects of butyrate in intestinal and extraintestinal diseases.* World J Gastroenterol, 2011. **17**(12): p. 1519-28.
251. **Patist, C.M., N.J.C. Stapelberg, E.F. Du Toit, and J.P. Headrick**, *The brain-adipocyte-gut network: Linking obesity and depression subtypes.* Cogn Affect Behav Neurosci, 2018.
252. **Wu, H., Q. Liu, P.K. Kalavagunta, Q. Huang, W. Lv, X. An, H. Chen, T. Wang, R.M. Heriniaina, T. Qiao, and J. Shang**, *Normal diet Vs High fat diet - A comparative study: Behavioral and neuroimmunological changes in adolescent male mice.* Metab Brain Dis, 2018. **33**(1): p. 177-190.
253. **Mollica, M.P., G. Mattace Raso, G. Cavaliere, G. Trinchese, C. De Filippo, S. Aceto, M. Prisco, C. Pirozzi, F. Di Guida, A. Lama, M. Crispino, D. Tronino, P. Di Vaio, R. Berni Canani, A. Calignano, and R. Meli**, *Butyrate Regulates Liver Mitochondrial Function, Efficiency, and Dynamics in Insulin-Resistant Obese Mice.* Diabetes, 2017. **66**(5): p. 1405-1418.
254. **Miller, A.A. and S.J. Spencer**, *Obesity and neuroinflammation: a pathway to cognitive impairment.* Brain Behav Immun, 2014. **42**: p. 10-21.

255. **Souza, G.F., C. Solon, L.F. Nascimento, J.C. De-Lima-Junior, G. Nogueira, R. Moura, G.Z. Rocha, M. Fioravante, V. Bobbo, J. Morari, D. Razolli, E.P. Araujo, and L.A. Velloso**, *Defective regulation of POMC precedes hypothalamic inflammation in diet-induced obesity.* Sci Rep, 2016. **6**: p. 29290.
256. **Park, J.H., Y. Yoo, J. Han, and Y.J. Park**, *Altered expression of inflammation-associated genes in the hypothalamus of obesity mouse models.* Nutr Res, 2018.
257. **Thaler, J.P., S.J. Guyenet, M.D. Dorfman, B.E. Wisse, and M.W. Schwartz**, *Hypothalamic inflammation: marker or mechanism of obesity pathogenesis?* Diabetes, 2013. **62**(8): p. 2629-34.
258. **Valdearcos, M., M.M. Robblee, D.I. Benjamin, D.K. Nomura, A.W. Xu, and S.K. Koliwad**, *Microglia dictate the impact of saturated fat consumption on hypothalamic inflammation and neuronal function.* Cell Rep, 2014. **9**(6): p. 2124-38.
259. **Gao, Y., N. Ottaway, S.C. Schriever, B. Legutko, C. Garcia-Caceres, E. de la Fuente, C. Mergen, S. Bour, J.P. Thaler, R.J. Seeley, J. Filosa, J.E. Stern, D. Perez-Tilve, M.W. Schwartz, M.H. Tschop, and C.X. Yi**, *Hormones and diet, but not body weight, control hypothalamic microglial activity.* Glia, 2014. **62**(1): p. 17-25.
260. **Eisch, A.J. and D. Petrik**, *Depression and hippocampal neurogenesis: a road to remission?* Science, 2012. **338**(6103): p. 72-5.
261. **Lu, J., D.M. Wu, Y.L. Zheng, B. Hu, W. Cheng, Z.F. Zhang, and Q. Shan**, *Ursolic acid improves high fat diet-induced cognitive impairments by blocking endoplasmic reticulum stress and IkappaB kinase beta/nuclear factor-kappaB-mediated inflammatory pathways in mice.* Brain Behav Immun, 2011. **25**(8): p. 1658-67.
262. **Guillemot-Legris, O. and G.G. Muccioli**, *Obesity-Induced Neuroinflammation: Beyond the Hypothalamus.* Trends Neurosci, 2017. **40**(4): p. 237-253.
263. **Preston, A.R. and H. Eichenbaum**, *Interplay of hippocampus and prefrontal cortex in memory.* Curr Biol, 2013. **23**(17): p. R764-73.
264. **Dingess, P.M., R.A. Darling, E. Kurt Dolence, B.W. Culver, and T.E. Brown**, *Exposure to a diet high in fat attenuates dendritic spine density in the medial prefrontal cortex.* Brain Struct Funct, 2017. **222**(2): p. 1077-1085.
265. **Roy, A., M. Jana, M. Kundu, G.T. Corbett, S.B. Rangaswamy, R.K. Mishra, C.H. Luan, F.J. Gonzalez, and K. Pahan**, *HMG-CoA Reductase Inhibitors Bind to PPARalpha to Upregulate*

Neurotrophin Expression in the Brain and Improve Memory in Mice. Cell Metab, 2015. **22**(2): p. 253-65.

266. **Yang, R., P. Wang, Z. Chen, W. Hu, Y. Gong, W. Zhang, and C. Huang**, *WY-14643, a selective agonist of peroxisome proliferator-activated receptor-alpha, ameliorates lipopolysaccharide-induced depressive-like behaviors by preventing neuroinflammation and oxido-nitrosative stress in mice.* Pharmacol Biochem Behav, 2017. **153**: p. 97-104.
267. **Zhang, C., M. Zhang, S. Wang, R. Han, Y. Cao, W. Hua, Y. Mao, X. Zhang, X. Pang, C. Wei, G. Zhao, Y. Chen, and L. Zhao**, *Interactions between gut microbiota, host genetics and diet relevant to development of metabolic syndromes in mice.* ISME J, 2010. **4**(2): p. 232-41.
268. **Xiao, S., N. Fei, X. Pang, J. Shen, L. Wang, B. Zhang, M. Zhang, X. Zhang, C. Zhang, M. Li, L. Sun, Z. Xue, J. Wang, J. Feng, F. Yan, N. Zhao, J. Liu, W. Long, and L. Zhao**, *A gut microbiota-targeted dietary intervention for amelioration of chronic inflammation underlying metabolic syndrome.* FEMS Microbiol Ecol, 2014. **87**(2): p. 357-67.
269. **Hildebrandt, M.A., C. Hoffmann, S.A. Sherrill-Mix, S.A. Keilbaugh, M. Hamady, Y.Y. Chen, R. Knight, R.S. Ahima, F. Bushman, and G.D. Wu**, *High-fat diet determines the composition of the murine gut microbiome independently of obesity.* Gastroenterology, 2009. **137**(5): p. 1716-24 e1-2.
270. **Yamawaki, Y., N. Yoshioka, K. Nozaki, H. Ito, K. Oda, K. Harada, S. Shirawachi, S. Asano, H. Aizawa, S. Yamawaki, T. Kanematsu, and H. Akagi**, *Sodium butyrate abolishes lipopolysaccharide-induced depression-like behaviors and hippocampal microglial activation in mice.* Brain Res, 2018. **1680**: p. 13-38.
271. **Javurek, A.B., D. Suresh, W.G. Spollen, M.L. Hart, S.A. Hansen, M.R. Ellersieck, N.J. Bivens, S.A. Givan, A. Upendran, R. Kannan, and C.S. Rosenfeld**, *Gut Dysbiosis and Neurobehavioral Alterations in Rats Exposed to Silver Nanoparticles.* Sci Rep, 2017. **7**(1): p. 2822.